Dissertation

Fully Massive Tadpoles at 5-loop: Reduction and Difference Equations

Jan Möller

In Attainment of the Academic Degree

Doctor rerum naturalium

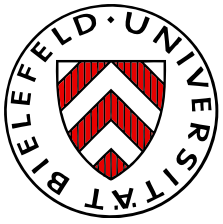

Bielefeld
2012

Fully Massive Tadpoles at 5-loop: Reduction and Difference Equations

Abstract

Loop integrals are essential for the computation of predictions in quantum field theories like the Standard Model of elementary particle physics. For instance, in the case of anomalous dimensions of QCD or the pressure in thermal QCD we face so-called tadpole loop integrals. In this thesis we study an important subset of these integrals, the fully massive vacuum (bubble) integrals. For the first time, we consider fully massive tadpoles at the 5-loop level pioneering the way for future high-precision calculations. We have implemented a Laporta algorithm in the algebraic manipulator `FORM` using generalized recurrence relations, a combination of integration-by-parts and space-time dimensional identities. This enabled us to perform the reduction of fully massive tadpoles up to the 5-loop level to a basis of master integrals. We modified the implementation in such a way that difference equations are obtained for a large number of the yet unknown master integrals. We started to solve the system of difference equations by means of factorial series expansions.

Dissertation in Theoretical Physics

Presented to: University of Bielefeld,
Department of Physics,
Theoretical Physics (E6/D6),
Universitätsstraße 25,
D-33615 Bielefeld,
Germany

Date: 11th of June 2012[1]

Supervisor & 1st Corrector: Prof. Dr. York Schröder
2nd Corrector: PD Dr. Markos Maniatis

Author: Jan Möller
Place of Birth: Bielefeld, Germany
E-Mail Address: jmoeller@physik.uni-bielefeld.de

[1] first revised version, including minor corrections

Contents

Preface

In recent years high-precision calculations of observables became more and more important because of the increasing precision provided by experiments. This holds true for many areas in physics. The physics of elementary particles are described by quantum field theories (QFT) with the Standard Model of particle physics given by quantum chromodynamics (QCD) and the electroweak interactions, with quantum electrodynamics (QED) a part of the electroweak interactions. A powerful tool to study and calculate measurable observables of quantum field theories is the perturbative expansion in a small parameter.

High-order perturbative computations with an increasing number of loops and/or external legs necessitate the use of computer algebra in order to deal with the growing complexity of these computations. As a consequence, a new field in theoretical physics evolved working on how the different steps in a perturbative calculation via Feynman diagrams [1] can be done as efficient as possible or developing alternative approaches as the very important scattering amplitude techniques, see e. g. the reviews [2, 3].

In the traditional approach based on the evaluation of Feynman diagrams, any perturbative computation can be basically divided into four different steps. The first one, the combinatorial part, consists of the complete generation of all relevant Feynman diagrams including its symmetry factors. After specifying appropriate Feynman rules, the second step is translating the diagrammatic objects (Feynman graphs) to actual mathematical expressions. At this point, one is usually confronted with a large number of Feynman integrals. The integrals are, in general, unknown and the calculation very difficult. Therefore, in a third step, the Feynman integrals are algebraically reduced to a small set of so-called master integrals by employing linear relations between different Feynman integrals. The last step, evaluating the remaining master integrals, is done either fully analytically, or if not possible, numerically in an expansion [4] for instance in dimensional regularization around the desired space-time dimension d.

In this thesis we focus on the last two steps for a particular class of integrals, the so-called fully massive vacuum (bubble) integrals also called tadpoles. This integrals occur in many perturbative calculations such as asymptotic expansions [5] with applications like the QCD β-function and anomalous dimensions [6, 7, 8] or the ρ-parameter [9, 10]. They also appear in lower space-time dimensions in the dimensionally reduced effective theory framework of QCD at high temperature T [11, 12]. Up to now, the fully massive $m_i = m$ and QED-type ones $m_i \in \{0, m\}$ are known up to the four-loop level [13, 14, 15]. We will, for the first time, study fully massive vacuum integrals at the five-loop level pioneering the way for future high-precision calculations.

The thesis is organized as follows. In Chapter 1 we give a brief introduction to QCD and describe the applications of fully massive tadpoles in zero- and finite-temperature QCD. In Chapter 2 we review reduction methods for Feynman integrals such as the integration-by-parts identities [16, 17] and the Laporta algorithm [18]. In Chapter 3 the methods are applied to fully massive tadpoles up to the five-loop level. This means, we perform a reduction to master integrals and determine for the first time the basis of master integrals at five-loop. Also, we adapt our implementation in `FORM` [19, 20, 21] in such a way that difference equations [18, 22] are obtained and determined for a large number of master integrals the corresponding difference equations. We start and solve these difference equations numerically by means of factorial series expansions in Chapter 4. A summary and concluding remarks are given in Chapter 5.

1 Introduction and Motivation

The following discussion is intended to motivate the study of massive vacuum integrals (tadpoles) rather than to give a detailed introduction to perturbative quantum field theory. For the latter we refer to e. g. [23, 24, 25].

Although there are many applications of massive tadpoles, we review here two specific applications. The first is the beta-function of quantum chromodynamics (QCD) which is, up to now, known at the 4-loop level. The knowledge of this function allows, in combination with the anomalous dimensions of fields, the reconstruction of all renormalization constants (RC) which are necessary to renormalize the theory. The second application is the study of equilibrium thermodynamics of hot QCD. We consider finite-temperature QCD at high temperature T and vanishing chemical potential μ. In this regime, perturbation theory is applicable and the observable of interest will be the free energy F or, equivalently, the thermodynamic pressure P. We will show that the specific subset of Feynman integrals, the massive vacuum integrals or tadpoles, play a crucial role in the computation of the corresponding perturbative corrections.

In this chapter we start and show what is exactly meant by saying "a massive tadpole integral". Then we proceed and give in Section 1.2 the basic facts of the theory of strong interactions described by the non-Abelian $SU(3)$ gauge theory by Yang-Mills [26]. This is followed in Section 1.2.1 by the renormalization group equation and the definition of the beta-function and anomalous dimensions of fields. In Section 1.2.2 we outline a procedure [27] which simplifies the computation of beta-functions and anomalous dimensions to massive tadpole integrals. Then we consider as another application, the thermodynamic pressure of QCD at high temperature. In Section 1.3.1 we introduce the basics of thermal field theory and outline the imaginary time formalism. In Section 1.3.2 we show, on the basis of scalar field theory, the complications of a weak-coupling expansion in that approach. Finally, in Section 1.3.3 we review the concept of dimensional reduction [28, 29] as a solution to the infrared problem of hot non-Abelian gauge theories [30]. The solution turns out out to be a sequence of two 3-dimensional effective field theories [31, 32] and calculations therein require the knowledge of massive tadpole integrals.

1.1 In a Nutshell: Massive Tadpoles, Recurrence Relations and Difference Equations

A vacuum integral or tadpole is a Feynman integrals with no external legs or lines. For example, let us consider the 1-loop massive tadpole in d-dimensional Euclidean space-time

$$J(n) = \int \frac{d^d k}{\pi^{d/2}} \frac{1}{(k^2 + m^2)^n} \,, \tag{1.1}$$

with massive propagator $1/(k^2 + m^2)$ to power n. From the diagrammatical point of view, the vacuum integral in Eq. (1.1) is represented by the following diagrams

$$J(1) = \quad , \qquad J(2) = \quad , \qquad \ldots \qquad , \tag{1.2}$$

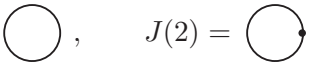

where a 'dot' indicates that the corresponding propagator carries an additional power. In order to avoid any misunderstandings, we point out that the diagrams in Eq. (1.2) represent single Feynman

integrals not to be confused with a Feynman diagram which, in general, results in a large number of Feynman integrals. The massive tadpole in Eq. (1.1) can be explicitly written in terms of Γ-functions and reads

$$J(n) = \frac{\Gamma(n - d/2)}{\Gamma(n)} (m^2)^{d/2-n} \,, \tag{1.3}$$

where we made use of the d-dimensional unit sphere

$$\int d\Omega_d = \frac{2\pi^{d/2}}{\Gamma(d/2)} \,, \tag{1.4}$$

and the definition of the beta function

$$\int_0^1 dx x^{\alpha-1}(1-x)^{\beta-1} = B(\alpha, \beta) = \frac{\Gamma(\alpha)\Gamma(\beta)}{\Gamma(\alpha+\beta)} \,. \tag{1.5}$$

The massive vacuum integral in Eq. (1.1) and Feynman integrals in general are divergent and need to be regularized. There is a large variety of regularization prescriptions, the most prominent ones are cutoff (Pauli-Villars [33]) and dimensional regularization [4]. In this work we use, if not otherwise indicated, dimensional regularization. However, let us inspect the massive tadpole $J(2)$ in both regularizations, with an integral momentum cutoff Λ and in dimensional regularization in $d = 4 - 2\epsilon$ space-time dimensions

$$\begin{aligned} &\text{cutoff } \Lambda: && J(2) \underset{\Lambda\to\infty}{\longrightarrow} \log\left(\frac{\Lambda}{m^2}\right) + \mathcal{O}(\Lambda^{-1}) \,, \\ &\text{dimensional}: && J(2) \underset{d\to 4}{\longrightarrow} \frac{1}{\epsilon} - \log\left(m^2\right) - \gamma + \mathcal{O}(\epsilon) \,, \end{aligned} \tag{1.6}$$

where γ is the Euler-Mascheroni constant. In cutoff regularization we recognize that $J(2)$ has a logarithmic divergence which corresponds to the $1/\epsilon$ pole in dimensional regularization.

In the following we try to find a relation between $J(n+1)$ and $J(n)$, by shifting $n \to n+1$ in Eq. (1.3) we get

$$J(n+1) = \frac{\Gamma(n - d/2 + 1)}{\Gamma(n+1)} (m^2)^{d/2-n-1} = \frac{n - d/2}{nm^2} \cdot \frac{\Gamma(n - d/2)}{\Gamma(n)} (m^2)^{d/2-n} = -\frac{d - 2n}{2nm^2} J(n) \,, \tag{1.7}$$

where we made use of the property $\Gamma(x)x = \Gamma(x+1)$. The iterative use of the relation in Eq. (1.7) allows us to relate $J(n)$ with arbitrary power n to $J(1)$. In Chapter 2 we will refer to $J(1)$ as a master integral and to the relation in Eq. (1.7) as a recurrence relation. Of course, the recurrence relation has been derived from the explicit solution in Eq. (1.3) which is usually not known. However, as we will see later, relations such as in Eq. (1.7) can be directly computed from the definition, here Eq. (1.1), by employing e. g. the integration-by-parts method [16, 17].

Looking from a different point of view on Eq. (1.7), we realize that it is a so-called linear difference equation [22],

$$p_1(n)J(n+1) + p_0(n)J(n) = 0 \,, \tag{1.8}$$

with polynomial coefficients $p_0(n) = d - 2n$, $p_1(n) = 2nm^2$. This can be solved in order to get an expression for the unknown function $J(n)$, e. g. in terms of an ϵ-expansion cf. Eq. (1.6). This issue will be discussed in Chapter 4.

Beyond 1-loop, we encounter a large number of different massive vacuum integrals, see Chapter 3. Some examples are shown in Figure 1.1.

Figure 1.1: Some of the massive tadpoles occuring at the 2-, 3-, 4- and 5-loop level.

1.2 Quantum Chromodynamics and Yang-Mills Theory

The development of a theory of strong interactions dates back to the mid 1950s where it was by far not clear whether the non-Abelian $SU(3)$ Yang-Mills gauge theory [26] really describes the strong interactions. This changed after it was shown that Yang-Mills theories are, in fact, renormalizable [34] and share the property of asymptotic freedom [35, 36]. The theory of strong interactions is described by the non-Abelian gauge theory with gauge group $SU(3)$ acting in color space with quarks in the fundamental representation. The famous Yang-Mills Lagrangian reads

$$\mathcal{L} = -\frac{1}{4}F^a_{\mu\nu}F^{a\mu\nu} + \sum_{f=1}^{N_f} \bar{\psi}^f_i \left[i\not{D} - m_f\right]_{ij} \psi^f_j \,, \tag{1.9}$$

with field strenght tensor $F^a_{\mu\nu}$ and covariant derivative D_μ,

$$F^a_{\mu\nu} = \partial_\mu A^a_\nu - \partial_\nu A^a_\mu + g f^{abc} A^a_\mu A^b_\nu, \qquad [D_\mu]_{ij} = \delta_{ij}\partial_\mu - ig A^a_\mu t^a_{ij} \,. \tag{1.10}$$

The fields A^a_μ denote the gluon fields with adjoint index $a = 1, \ldots, 8$ and ψ^f_j the quark spinors with flavor index f and color index $j = 1, 2, 3$. The generators of the symmetry group can be represented by Hermitian matrices t^a satisfying the commutation relations

$$[t^a, t^b] = i f^{abc} t^c \,, \tag{1.11}$$

where f^{abc} are the so-called structure functions. The basis of the matrices t^a is usually chosen in such a way that the functions f^{abc} are completely antisymmetric. From the Lagrangian in Eq. (1.9) and the covariant derivative D_μ in Eq. (1.10) we see that the matrices t^a connect the adjoint gluon representation to the fundamental and anti-fundamental quark spinors.

1.2.1 Renormalization, Beta-function and Anomalous Dimensions

In the following discussion we use the modified minimal substraction scheme $\overline{\text{MS}}$ [34]. In covariant gauge the QCD Lagrangian (1.9) becomes

$$\mathcal{L} = -\frac{1}{4}F^a_{\mu\nu}F^{a\mu\nu} + \sum_{f=1}^{N_f} \bar{\psi}^f \left[i\not{D} - m_f\right] \psi^f - \frac{1}{2\xi}\left(\partial^\mu A^a_\mu\right)^2 + \partial^\mu \bar{c}^a \left(\partial_\mu c^a - g f^{abc} c^b A^c_\mu\right) , \tag{1.12}$$

where the color indices of quark fields ψ^f are suppressed and c^a denote the ghost fields. The parameter ξ is the gauge parameter of the covariant gauge and $\xi = 0$ corresponds to Landau gauge. From the Lagrangian (1.12), Greens functions can be computed and need to be renormalized. Let us therefore write the bare Lagrangian of Eq. (1.12) in terms of renormalized fields

$$\begin{aligned}\mathcal{L} = &-\frac{1}{4}Z_3\left(\partial_\mu A_\nu - \partial_\nu A_\mu\right)^2 - \frac{1}{2}g Z_1^{3g}\left(\partial_\mu A_\nu - \partial_\nu A_\mu\right) f^{abc} A^b_\mu A^c_\nu - \frac{1}{4}g^2 Z_1^{4g} f^{abc} f^{ade} A^b_\mu A^c_\nu A^{\mu d} A^{\nu d} \\ &- Z_\xi^{2g}\frac{1}{2\xi}\left(\partial_\nu A_\mu\right)^2 + Z_3^c \partial_\nu \bar{c}\left(\partial^\nu c\right) + g Z_1^{ccg} \partial^\mu \bar{c}^a f^{abc} A^b_\mu c^c + Z_2 \bar{\psi}^f \left(i\partial\!\!\!/ + g Z_1^{\psi\psi g} Z_2^{-1} A\!\!\!/ - Z_m m_f\right) \psi^f \,,\end{aligned} \tag{1.13}$$

where we have omitted the sum over quark flavors f in the last term. The wave-function renormalization constants (RC) are

$$A_0^{a\mu} = \sqrt{Z_3} A^{a\mu}\,, \qquad \psi_0^f = \sqrt{Z_2}\psi^f\,, \qquad c_0^a = \sqrt{Z_3^c} c^a\,, \tag{1.14}$$

and mass, coupling and gauge parameter are renormalized by

$$g_0 = Z_g g\,, \qquad m_{0,f} = Z_m m_f\,, \qquad \xi_0 = Z_\xi \xi\,, \qquad Z_\xi^{2g} = \frac{Z_3}{Z_\xi}\,, \tag{1.15}$$

where Z_ξ^{2g} is expressed in terms of Z_ξ and Z_3. The four vertex renormalization constants Z_1^{3g}, Z_1^{4g}, Z_1^{ccg}, $Z_1^{\psi\psi g}$ renormalize the 3-gluon, 4-gluon, ghost-ghost-gluon and quark-quark-gluon vertex, respectively. The Slavnov-Taylor identities impose certain relations among the counterterms. As it turns out, we can write all vertex renormalization constants in terms of Z_g and the wave-function RCs in Eq. (1.14),

$$Z_g = \sqrt{Z_1^{4g}}(Z_3)^{-1} = Z_1^{3g}(Z_3)^{-3/2} = Z_1^{ccg}(Z_3)^{-1/2}(Z_3^c)^{-1} = Z_1^{\psi\psi g}(Z_3)^{-1/2}(Z_2)^{-1}\,, \tag{1.16}$$

and $Z_\xi = Z_3$. Since we are working in the modified minimal substraction scheme $\overline{\text{MS}}$, all renormalization constants are independent of momenta and masses. This means we can, right from the beginning, work with massless quarks. In this framework, the renormalization constants can be written as

$$Z(h) = 1 + \sum_{n=1}^{\infty} \frac{z^{(n)}(h)}{\epsilon^n}\,, \tag{1.17}$$

where $h \equiv g^2/(16\pi^2)$. The corresponding anomalous dimensions are defined by

$$\gamma(h) \equiv -\mu^2 \frac{d\log Z(h)}{d\mu^2} = h\frac{\partial z^{(1)}(h)}{\partial h} = -\sum_{n=0}^{\infty}(\gamma)_n h^{(n+1)}\,, \tag{1.18}$$

and, in particular, for $Z_h = Z_g^2$ the associated anomalous dimension is called beta function

$$\beta(h) \equiv -\mu^2 \frac{d\log Z_h(h)}{d\mu^2} = 2\gamma_g(h) = 2h\frac{\partial z_g^{(1)}(h)}{\partial h} = -\sum_{n=0}^{\infty}\beta_n h^{(n+1)}\,, \tag{1.19}$$

where $z^{(1)}(h)$ is the coefficient of the first pole in ϵ, cf. Eq. (1.17). Let us briefly show where this formula comes from and recall the gauge coupling renormalization in Eq. (1.15), keeping the mass scale μ, we have

$$h_0 = Z_h \mu^{2\epsilon} h\,. \tag{1.20}$$

The mass scale is arbitrarily chosen and the bare quantity does not depend on μ, consequently

$$\mu^{-2\epsilon}\mu^2\frac{\partial h_0}{\partial \mu^2} = 0 = \frac{\partial Z_h}{\partial \mu^2}h\mu^2 + Z_h\frac{\partial h}{\partial \mu^2}\mu^2 + Z_h\, h\,\epsilon\,, \tag{1.21}$$

dividing the equation by $1/Z_h$, using the chain rule and identifying the resulting terms with $\beta(h)$ we get

$$[-\epsilon + \beta(h)]\, h\frac{\partial \log Z_h}{\partial h} = -\beta(h)\,, \tag{1.22}$$

with the formal solution

$$Z_h(h) = \exp\left(\int_0^h \frac{dh'}{h'}\frac{\beta(h')}{\epsilon - \beta(h')}\right). \tag{1.23}$$

Solving Eq. (1.23) for small h we obtain the desired expansion

$$Z_h = 1 + \frac{\beta_0}{\epsilon}h + \frac{\beta_1}{2\epsilon}h^2 + \left[\frac{\beta_2}{3\epsilon} - \frac{\beta_0\beta_1}{6\epsilon^2}\right]h^3 + \left[\frac{\beta_3}{4\epsilon} - \frac{3\beta_1^2+4\beta_0\beta_2}{24\epsilon^2} + \frac{\beta_0^2\beta_1}{12\epsilon^3}\right]h^4 + \left[\frac{\beta_4}{5\epsilon} - \frac{14\beta_1\beta_2+9\beta_0\beta_3}{60\epsilon^2} + \frac{17\beta_0\beta_1^2+12\beta_0^2\beta_2}{120\epsilon^3} - \frac{\beta_0^3\beta_1}{20\epsilon^4}\right]h^5 + \mathcal{O}(h^6)\,. \quad (1.24)$$

Let us again consider Eq. (1.18), with help of Eq. (1.16) we find the following relations between anomalous dimensions and the beta function

$$\beta = \gamma_1^{4g} - 2\gamma_3 = 2\gamma_1^{3g} - 3\gamma_3 = 2\gamma_1^{ccg} - 2\gamma_3^c - \gamma_3 = 2\gamma_1^{\psi\psi g} - 2\gamma_2 - \gamma_3\,. \quad (1.25)$$

As we already mentioned, the renormalization constants can be reconstructed from anomalous dimensions γ and beta function β, for an arbitrary Z we have the general form

$$[-\epsilon + \beta(h)]\,h\frac{\partial \log Z}{\partial h} + \gamma_3(h)\xi\frac{\partial \log Z}{\partial \xi} = -\gamma(h)\,, \quad (1.26)$$

where the dependence on μ enters through the coupling h and gauge parameter ξ. In order to compute all renormalization constants of the QCD Lagrangian (1.13) we need, according to Eq. (1.16), at least the wave-function RCs Z_3, Z_2, Z_3^c and mass RC Z_m in addition to the gauge couling renormalization constant Z_g. Alternatively one can choose one of the vertex RCs Z_1^{3g}, Z_1^{4g}, Z_1^{ccg}, $Z_1^{\psi\psi g}$ in exchange for Z_g.

The QCD beta function has a long standing history starting with the discovery of asymptotic freedom [35, 36] in the early 1970s. Within 10 years, the 2-loop [37, 38] and 3-loop [39, 40] corrections have been computed. All the computations have in common that they determined the beta function in the same way by computing either the quark- and gluon-propagator and quark-quark-gluon vertex RCs Z_2, Z_3, $Z_1^{\psi\psi g}$ or the ghost- and gluon-propagator and ghost-ghost-gluon vertex RCs Z_3^c, Z_3, Z_1^{ccg}, cf. the last and second last equality sign in Eq. (1.25). Instead of performing three independent calculations, two 2-point and a 3-point computation, one can also calculate the three- or four-gluon vertex in addition to the gluon-propagator which is, however, by far more demanding because of the complex vertex structure [41]. The 4-loop beta function has been computed by Vermaseren et al. [6] via Z_3^c, Z_3, Z_1^{ccg} which was later independently checked in references [7, 8] through Z_2, Z_3, $Z_1^{\psi\psi g}$.

It is apparent, practical computations at the 3-loop level and beyond[1], necessitate the use of computer algebra. For the 3-loop and 4-loop computations, algebra programs like `SCHOONSHIP` [42] or `FORM` [19] were used. As we know from Eq. (1.24), the beta function is determined by the $1/\epsilon$-poles of the renormalization constant Z_h. We can take advantage of this fact and simplify the calculation considerably. This means, in practice, it is not necessary to compute the full vertex functions or propagators at the corresponding order. It turns out to be sufficient to consider fully massive tadpoles, exactly those we consider in this thesis.

1.2.2 Computation of Anomalous Dimensions: Infrared Rearrangement

In this section we demonstrate how the simplification to massive vacuum integrals works. There are basically two different approaches based on the general method of infrared rearrangement [43]. Both rely on the fact that within a mass-independent renormalization scheme, such as MS or $\overline{\text{MS}}$, the ultraviolet (UV) counterterms are polynomial in masses and momenta after all subdivergences

[1] The computations involve about $\mathcal{O}(1000)$ and $\mathcal{O}(50000)$ Feynman diagrams at the 3-loop and 4-loop level, respectively.

have been removed [44]. This allows to perform a certain expansion in masses or external momenta even before the loop momentum integrations are carried out. In case of a massless theory, an expansion in external momenta causes spurious infrared (IR) divergences which are, in dimensional regularization, indistinguishable from UV divergences if not regularized in an appropriate way. This is usually done by introducing artificial masses or external momenta in certain propagators of a given Feynman diagram such that no spurious IR divergences appear and the diagram remains computable. A disadvantage of this is, however, the limited applicability of methods we would then usually use for the reduction to simpler diagrams.

Basically two solutions are available, first the so-called R^*-operation [45], constructing the UV divergence of every l-loop Feynman integral out of the divergent and finite part of a carefully chosen l-loop massless propagator integral. The method is rather complicated and seems not to allow an algorithmical implementation. We will follow a different approach [5, 27], where the same artificial mass is introducted in all propagators of all Feynman integrals. As a consequence, no spurious IR divergences are present. The proof in [44] remains true and the UV divergence is still a polynomial in masses and momenta including the artificial mass after subdivergences are subtracted. In the end, the corresponding UV divergence is recovered by setting the artificial mass to zero.

The subtraction of subdivergences needs to be done within the same framework. This means, at 2-loop the corresponding subdivergences are subtracted by replacing the vertices and propagators of the 1-loop diagrams by effective vertices and propagators i. e. the counterterms are included, which cancels the subdivergences of the 2-loop diagrams. The counterterms are calculated in the same way, that is with massive propagators also for the gluon propagator. Of course, from the physical point, the theory is meaningless but it has, in a mass-independent renormalization scheme, the same counterterms as QCD except for the "gluon mass" renormalization [5]. It should be noted, that the various vertex and propagator renormalization constants necessary for the effective vertices and propagators are mass independent and therefore already known from massless calculations. Hence, only the UV divergence for the massive gluon propagator needs to be calculated.

Let us start and discuss the expansion which is performed in the external momentum p after the auxiliary (or artificial) mass m is introduced. All scalar propagators are replaced by the exact decomposition

$$\frac{1}{(k+p)^2+m^2} = \frac{1}{k^2+m^2} - \frac{2k\cdot p+p^2}{k^2+m^2}\frac{1}{(k+p)^2+m^2}\,, \tag{1.27}$$

where k and p are linear combinations of loop- and external momenta, respectively. The decomposition splits the original propagator into two parts, a part polynomial in the external momenta and a piece contributing with a lower degree of divergence. We apply the decomposition in Eq. (1.27) recursively as long as the last piece contributes only with a sufficiently low negative degree of divergence. Then we are allowed to drop the last term in the decomposition because it does not affect the UV-divergent part of the corresponding Greens function. The external momenta can be factorized out by applying suitable tensor decompositions and, as a consequence, we are left with integrals only depending on the loop momenta and the auxiliary mass m. In other words, fully massive tadpoles!

In order to show how this procedure works, we compute the 1-loop beta function in QCD using the decomposition from Eq. (1.27). For convenience, we choose background field gauge [46, 47], then the renormalization constant of coupling $h = g^2/(16\pi^2)$ is given by

$$Z_h = (Z_g)^2 = (Z_B)^{-1}\,, \tag{1.28}$$

where B denotes the background field. This means we only need to compute background field propagator corrections instead of various vertex and propagator corrections as outlined in Section 1.2.1. However, in this approach, the corresponding Feynman rules are slightly more complicated,

see e. g. [46]. At 1-loop only three diagrams contribute to the background field propagator, in Feynman gauge and d-dimensional Euclidean space-time we have


$$= -g_B^2 N_c\, \delta^{ab} \frac{\delta(p+q)}{(p^2)^2} \int_k \frac{1}{k^2(p-k)^2} \Big[(2k_\mu - p_\mu)(2k_\nu - p_\nu) \Big] \,,$$


$$= -\frac{g_B^2}{2} N_c \delta^{ab} \frac{\delta(p+q)}{(p^2)^2} \int_k \frac{1}{k^2(p-k)^2} \Big[-8\delta_{\mu\nu} p^2 + (8-d) p_\mu p_\nu + 2d(k_\nu p_\mu - 2k_\mu k_\nu + k_\mu p_\nu) \Big] \,,$$


$$= 2 g_B^2 N_f\, \delta^{ab} \frac{\delta(p+q)}{(p^2)^2} \int_k \frac{1}{k^2(p-k)^2} \Big[-8\delta_{\mu\nu}(k^2 - p\cdot k) + k_\nu p_\mu - 2k_\mu k_\nu + k_\mu p_\nu) \Big] \,, \tag{1.29}$$

where g_B is the bare coupling and measure $\int_k = \int d^dk/(2\pi)^d$. The quarks are drawn as solid lines, the ghost fields as dotted lines and gluons as wavy lines, respectively. External wavy lines are the background fields. In Eq. (1.29) we should have already written the auxiliary mass m in each of the propagators. We sum up all contributions and project out the transverse part

$$\Pi_B(p^2) = \frac{\delta^{ab}}{N_c^2 - 1} \frac{1}{d-1} \left[-g_{\mu\nu} + \frac{p_\mu p_\nu}{p^2} \frac{1}{p^2} \right] \times (\Pi_B)^{\mu\nu}_{ab}(p) \,, \tag{1.30}$$

which evaluates to

$$\Pi_B(p^2) = \frac{1}{d-1} \int_k \frac{1}{[k^2+m^2]\,[(p+k)^2+m^2]} \left[N_c \left(1 + \frac{7d-8}{2} \right) + N_f(2-d) \right] g_B^2 + \mathcal{O}(g_B^4) \,. \tag{1.31}$$

Now, the propagator decomposition from Eq. (1.27) is performed, we replace the second propagator and get

$$\int_k \frac{1}{[k^2+m^2]\,[(p+k)^2+m^2]} = \int_k \frac{1}{k^2+m^2} \left[\frac{1}{k^2+m^2} - \frac{2k\cdot p + p^2}{k^2+m^2} \frac{1}{(k+p)^2+m^2} \right] \,, \tag{1.32}$$

where the first integrand has an overall degree of divergence $\Delta D = -4$ and the second $\Delta D = -5$. Let us assume we compute the beta function in $d = 4 - 2\epsilon$ dimension, then we are allowed to drop the last term and obtain

$$\int_k \frac{1}{[k^2+m^2]\,[(p+k)^2+m^2]} \approx \int_k \frac{1}{(k^2+m^2)^2} \,, \tag{1.33}$$

where the approximation sign ($\approx$) indicates that only the divergence is properly reconstructed by the right-hand side. We have already derived the explicit solution for the 1-loop massive tadpole in Eq. (1.3), taking care of different normalizations we get

$$\int \frac{d^dk}{(2\pi)^d} \frac{1}{(k^2+m^2)^2} = \frac{1}{(4\pi)^{d/2}} J(2) = \frac{1}{(4\pi)^{d/2}} \frac{\Gamma(2-d/2)}{\Gamma(2)} (m^2)^{d/2-2} = \frac{1}{(4\pi)^2} \frac{1}{\epsilon} + \mathcal{O}(\epsilon^0) \,. \tag{1.34}$$

Combining all ingredients from Eqs. (1.32)-(1.34), plugging the result in Eq. (1.31) and expanding around $d = 4 - 2\epsilon$, we get the bare 2-point function Π_B for the background field,

$$\Pi_{B,bare}(p^2) = \frac{1}{(4\pi)^2} \frac{1}{\epsilon} \left[\frac{11}{3} N_c - \frac{2}{3} N_f \right] g_B^2 + \mathcal{O}(\epsilon^0, g_B^4) \,, \tag{1.35}$$

which is renormalized by $Z_B = 1 - \frac{1}{(4\pi)^2} \frac{1}{\epsilon} \left[\frac{11}{3} N_c - \frac{2}{3} N_f \right] g^2 + \mathcal{O}(g^4)$. With help of Eqs. (1.28) and (1.24) we recover the well-known result

$$\beta_0 = \frac{11}{3} N_c - \frac{2}{3} N_f \,. \tag{1.36}$$

The procedure outline above has been used to compute the beta function and anomalous dimensions at the 4-loop level [6, 7, 8]. A correction at the 5-loop level requires the corresponding fully massive tadpoles which we study in this thesis.

1.3 Thermal Field Theory: QCD at High Temperature

So far we only considered quantum field theories at zero temperature $T = 0$. Now we would like to study finite-temperature QCD and show that massive tadpoles do play an important role in equilibrium thermodynamics. We will focus on the bulk equilibrium properties of matter. They are described by the thermodynamic pressure P or, equivalently, its free energy F as functions of temperature T and chemical potential μ.

Hadronic matter undergoes a phase transition to a quark-gluon plasma if heated up to sufficient high temperature. This fact is predicted by quantum chromodynamics (QCD) and investigated in heavy-ion collisions at present collider experiments such as the Relativistic Heavy Ion Collider (RHIC) or the Large Hadron Collider (LHC). In order to study the quark-gluon plasma experimentally, it is, from the theoretical side, necessary to understand the properties as accurately as possible. There are basically two ways to study this regime, either by lattice simulations or in perturbative QCD. Both have its advantages and disadvantages. Lattice QCD can be, for instance, applied to the quark-gluon phase as well as the hadronic phase whereas perturbative QCD only works properly in the high temperature phase. On the other hand, lattice simulations have difficulties with chemical potentials which are straightforwardly implemented in the perturbative approach.

However, a perturbative approach is only applicable in the case of a small coupling g, see (1.10), which is, due to asymptotic freedom, guaranteed in the limit of very high temperatures or baryon densities. Such extreme conditions are usually not present in the above mentioned situations and therefore, at realistic temperatures, the expansion is expected to converge only very slowly. Consequently any further correction improves the expansion and might allow to get reliable insight even at rather low temperatures T of a few hundred MeV.

1.3.1 The Partition Function and Imaginary Time Formalism

We start by introducing a fundamental quantity in statistical mechanics, the partition function $\mathcal{Z}$. In the canonical ensemble with convention $k_B = 1$ we have

$$\mathcal{Z} \equiv \mathrm{Tr}[\exp(-\beta H)]\,, \tag{1.37}$$

where $\beta = 1/T$ and H is the Hamiltonian of our quantum mechanical system. Having the partition function at hand, observables like the free energy F, average energy E or entropy S can be obtained by taking the logarithm of $\mathcal{Z}$ or derivatives of F with respect to the temperature:

$$\begin{aligned} F &= -T \ln \mathcal{Z}\,, \\ E &= \frac{1}{\mathcal{Z}} \mathrm{Tr}[H \exp(-\beta H)]\,, \\ S &= \frac{\partial F}{\partial T}\,. \end{aligned} \tag{1.38}$$

Usually it is more convenient to consider the partition function in Eq. (1.37) in the path integral formalism. In order to rewrite the partition function $\mathcal{Z}$ in terms of a path integral, we basically employ the same techniques used in the derivation of the path integral at zero temperature [48]. For a better understanding, we consider scalar field theory with the Minkowskian Lagrangian

$$\mathcal{L}_M = \frac{1}{2}(\partial^\mu \phi)(\partial_\mu \phi) - V(\phi)\,. \tag{1.39}$$

In this case, the partition function from Eq. (1.37) becomes ($\hbar = 1$)

$$\mathcal{Z} = \int_{\phi(\beta,\mathbf{x})=\phi(0,\mathbf{x})} \prod_{\mathbf{x}} [C\mathcal{D}\phi(\tau,\mathbf{x})] \exp\left\{ -\int_0^\beta d\tau \int d^d\mathbf{x} \mathcal{L}_E \right\}, \tag{1.40}$$

where $d = 3$ and with Euclidean Lagrangian

$$\mathcal{L}_E = -\mathcal{L}_M(t = -i\tau) = \frac{1}{2}\left(\partial_\mu\phi\right)\left(\partial_\mu\phi\right) + V(\phi)\,, \tag{1.41}$$

with periodic boundary conditions $\phi(x, \tau = 0) = \phi(x, \tau = \beta)$ in imaginary time τ. For the derivation we refer to references [49, 50]. In case of an interacting field theory, we split the Euclidean action

$$S_E = \int_0^\beta d\tau \int d^d\mathbf{x}\mathcal{L}_E\,, \tag{1.42}$$

in two parts $S_E = S_0 + S_I$, S_0 quadratically in the fields and the interaction part S_I containing at least terms cubic in the fields. A naive expansion of the exponential in Eq. (1.40) yields

$$\mathcal{Z} = C' \int [\mathcal{D}\phi] e^{-S_0} \sum_{l=0}^{\infty} \frac{(-S_I)^l}{l!}\,, \tag{1.43}$$

where we have used the short cut $\int[\mathcal{D}\phi]$ for the integration measure. Taking the logarithm leads to

$$\ln \mathcal{Z} = \ln\left(C' \int [\mathcal{D}\phi] e^{-S_0}\right) + \ln\left(1 + \sum_{l=1}^{\infty} \frac{(-1)^l}{l!} \frac{\int[\mathcal{D}\phi] e^{-S_0} S_I^l}{\int[\mathcal{D}\phi] e^{-S_0}}\right) \equiv \ln \mathcal{Z}_0 + \ln \mathcal{Z}_I\,. \tag{1.44}$$

The first term is simply the ideal gas contribution to the free energy and the second gives perturbative corrections. By using the notation

$$\langle \dots \rangle_0 \equiv \frac{\int[d\phi](\dots) e^{-S_0}}{\int[d\phi] e^{-S_0}}\,, \tag{1.45}$$

we are able to write the interacting part of Eq. (1.44) in the following short form

$$\ln \mathcal{Z}_I = \ln\left(1 + \sum_{l=1}^{\infty} \frac{(-1)^l}{l!} \langle S_I^l \rangle_0\right). \tag{1.46}$$

The relevant quantity is Eq. (1.46), expanding the logarithm in a power series we get

$$\begin{aligned} \ln \mathcal{Z}_I &= \sum_{k=0}^{\infty} \frac{(-1)^k}{k+1} \left(\sum_{l=1}^{\infty} \frac{(-1)^l}{l!} \langle S_I^l \rangle_0\right)^{k+1} \\ &= \sum_{k=0}^{\infty} \frac{(-1)^k}{k+1} \left(-\langle S_I^1 \rangle_0 + \frac{1}{2}\langle S_I^2 \rangle_0 - \frac{1}{6}\langle S_I^3 \rangle_0 + \dots\right)^{k+1} \\ &= -\langle S_I \rangle_0 + \frac{1}{2}\left[\langle S_I^2 \rangle_0 - \langle S_I \rangle_0^2\right] - \frac{1}{6}\left[\langle S_I^3 \rangle_0 - 3\langle S_I \rangle_0 \langle S_I^2 \rangle_0 + 2\langle S_I \rangle_0^3\right] + \dots, \end{aligned} \tag{1.47}$$

by assuming λ to be the coupling constant, the first term is of order λ, the second and third of order $\mathcal{O}(\lambda^2)$ and $\mathcal{O}(\lambda^3)$, respectively. The corrections can be computed by evaluating the corresponding connected diagrams in finite-temperature perturbation theory using the Matsubara formalism, see e. g. [50]. However, a naive expansion as in Eq. (1.47) breaks down beyond leading order due to infrared divergencies caused by the so-called Matsubara zero-modes [49],

$$I(T, m) = T \sum_{n=-\infty}^{\infty} \int \frac{d^dk}{(2\pi)^d} \frac{1}{\omega_n^2 + E_k^2} = T \sum_{n\neq 0} \int \frac{d^dk}{(2\pi)^d} \frac{1}{\omega_n^2 + E_k^2} + T \int \frac{d^dk}{(2\pi)^d} \frac{1}{E_k^2}\,, \tag{1.48}$$

where $E_k = \sqrt{k^2 + m^2}$ and $\omega_n = 2\pi n T$ the bosonic Matsubara frequencies. This can either be cured by resumming an infinite number of so-called ring diagrams or, in a more systematic way, by using an effective field theory approach [51, 52] which disentangles the different scales contributing to the free energy or pressure. This effective field theory is, in fact, three dimensional and computations therein require the calculation of massive tadpoles.

1.3.2 Scalar Field Theory

Before focussing on full QCD, we would like to see on the basis of scalar field theory from where these complications arise. We consider scalar field theory with $\lambda\phi^4$ interaction, the Euclidean Lagrangian reads

$$\mathcal{L} = \frac{1}{2}\left(\partial_\mu\phi\right)\left(\partial_\mu\phi\right) + \frac{1}{2}m_B^2\phi^2 + \frac{1}{4}\lambda_B\phi^4\,. \tag{1.49}$$

According to Eqs. (1.44) and (1.47), the free energy density is given by

$$\frac{F(T,V)}{V} = -\frac{T}{V}\ln\mathcal{Z} = \frac{F^{(0)}}{V} - \frac{T}{V}\Big\{ - \langle S_I\rangle_0 + \frac{1}{2}\left[\langle S_I^2\rangle_0 - \langle S_I\rangle_0^2\right] - \\ - \frac{1}{6}\left[\langle S_I^3\rangle_0 - 3\langle S_I\rangle_0\langle S_I^2\rangle_0 + 2\langle S_I\rangle_0^3\right] + \ldots\Big\}\,. \tag{1.50}$$

Defining $f(T) \equiv \lim_{V\to\infty} F(T,V)/V$ and performing the usual steps in finite temperature perturbation theory (Wick contraction, Feynman calculus, solving sum-integrals) we obtain, in the limit $m_{phys} \to 0$, the known expression

$$f(T) = -\frac{\pi^2 T^4}{90}\left[1 - \frac{15}{32}\frac{\lambda_R}{\pi^2} + \frac{15}{16}\left(\frac{\lambda_R}{\pi^2}\right)^{3/2} + \mathcal{O}(\lambda_R^2)\right]\,, \tag{1.51}$$

where $\lambda_B = \lambda_R + \mathcal{O}(\lambda_R^2)$, $m_B^2 = m_R^2 + \mathcal{O}(\lambda_R)$ relates the bare and renormalized coupling and mass, respectively. For the detailed computation we refer to [49] or [50]. Let us inspect the weak coupling expansion in Eq. (1.51) in more detail. The first term is the contribution of a noninteracting gas of massless scalar particles followed by a correction of order λ_R which corresponds to $\langle S_I\rangle_0$ in Eq. (1.50). Then we would naively expect a contribution of order λ_R^2 originating from the second term in Eq. (1.50). This contribution, denoted by $f_{(2)}(T)$, and expanded in small m_B is given by

$$f_{(2)}(T) = -\frac{9}{4}\lambda_B^2\frac{T^4}{144}\frac{T}{8\pi m_B} + \mathcal{O}(m_B^0)\,. \tag{1.52}$$

We can easily see, in the limit $m_B \to 0$ a infrared divergence appears and the naive loop expansion from Eq. (1.50) breaks down. One can try and sum the divergent terms to all orders to get a finite result in the limit of vanishing m_B. The correction in Eq. (1.51) with an odd power in λ_R originates from that resumming procedure. Let us, in short, illustrate how this odd power is obtained by resumming an infinite number of so-called ring-diagrams. Similarly to Eq. (1.52) the contributions $f_{(0)}$ and $f_{(1)}$ are given by

$$\begin{aligned} f_{(0)}(T) &= -\frac{\pi^2 T^4}{90} + \frac{m_B^2 T^2}{24} - \frac{m_B^3 T}{12\pi} + \mathcal{O}(m_B^4)\,, \\ f_{(1)}(T) &= \frac{3}{4}\lambda_B\left[\frac{T^4}{144} - \frac{m_B T^3}{24\pi} + \mathcal{O}(m_B^2 T^2)\right]\,, \end{aligned} \tag{1.53}$$

again in small m_B expansion. We note the odd powers in m_B in Eqs. (1.52) and (1.53) are associated with Matsubara zero-mode contributions, cf. the second term in Eq. (1.48). The problem becomes increasingly severe as we go to higher orders $f_{(3)}, f_{(4)}, \ldots$. At order N in λ_B, one can show that these problematic terms are caused by diagrams with N non-zero mode contributions $I'(0,T)$ and one zero-mode contribution $I^{(n=0)}$,

$$I'(0,T) = T\sum_{n\neq 0}\int\frac{d^dk}{(2\pi)^d}\frac{1}{\omega_n^2 + E_k^2}\,, \qquad I^{(n=0)} = T\int\frac{d^dk}{(2\pi)^d}\frac{1}{E_k^2}\,. \tag{1.54}$$

From the diagrammatical point of view, the diagrams are those with one zero-mode loop dressed with N non-zero mode bubbles, also called daisy diagrams:

$$= \frac{(-1)^{N+1}}{N!}\left(\frac{\lambda_B}{4}\right)^N \Big\langle \phi\,\phi\,\overset{6}{\overbrace{\phi\,\phi}}\underbrace{\phi\quad\phi}_{2(N-1)}\,\phi\,\overset{6}{\overbrace{\phi\,\phi}}\underbrace{\phi\quad\phi}_{2(N-2)}\,\phi\,\overset{6}{\overbrace{\phi\,\phi}}\,\phi \quad \dots \quad \phi\,\overset{6}{\overbrace{\phi\,\phi}}\,\phi\,\phi \Big\rangle_{0,c}$$

$$= \frac{(-1)^{N+1}}{N!}\left(\frac{\lambda_B}{4}\right)^N 6^N 2(N-1)2(N-2)\dots 2\left[I'(0,T)\right]^N T\int\frac{d^dk}{(2\pi)^d}\left(\frac{1}{k^2+m_B^2}\right)^N, \tag{1.55}$$

where the subscript $\langle\dots\rangle_{0,c}$ indicates that only the connected contribution is considered. The product of combinatorial factors becomes $6^N 2^{N-1}(N-1)!$, $I'(0,T) = T^2/12$ and the zero-mode ring can be written as

$$\int\frac{d^{3-2\epsilon}k}{(2\pi)^{3-2\epsilon}}\frac{1}{(k^2+m_B^2)^N} = \frac{(-1)^N}{(N-1)!}\left(\frac{d}{dm_B^2}\right)^N\left(\frac{m_B^3}{6\pi}\right). \tag{1.56}$$

Putting all the ingredients together, we observe that the odd terms in m_B at λ_B^N are given by

$$\delta_{odd}f_{(N)} = -\frac{T}{2}\frac{1}{N!}\left(\frac{\lambda_B T^2}{4}\right)^N\left(\frac{d}{dm_B^2}\right)^N\left(\frac{m_B^3}{6\pi}\right), \tag{1.57}$$

which can be summed to all orders by recognizing that the structure in Eq. (1.57) equals a Taylor expansion

$$\sum_{N=0}^{\infty}\frac{1}{N!}\left(\frac{\lambda_B T^2}{4}\right)^N\left(\frac{d}{dm_B^2}\right)^N\left(-\frac{m_B^3 T}{12\pi}\right) = -\frac{T}{12\pi}\left(m_B^2+\frac{\lambda_B T^2}{4}\right)^{3/2}. \tag{1.58}$$

Surprisingly, the limit $m_B^2 \to 0$ can be taken and no divergencies arise. As it can be seen from the resummation in Eq. (1.58), the contribution we get is of order $\lambda_B^{3/2}$ rather than $\mathcal{O}(\lambda_B^2)$ which is exactly what is shown in Eq. (1.51). This means, infrared divergencies do substantially modify the weak-coupling expansion at finite-temperature. We can complete the calculation at $\mathcal{O}(\lambda_B^2)$ by including the terms we have neglected in Eq. (1.52).

At higher orders in the weak-coupling expansion it gets more and more involved to perform the resummations. However, as we have already mentioned, one can address this issue more systematically and efficient by constructing an effective field theory which takes care of the contributions from bosonic zero-modes. Before we discuss this issue, we want to summarize the current status of the weak-coupling expansion of the free energy density (or minus the pressure) in scalar field theory. The calculation has been performed for $\mathcal{O}(\lambda_R^2)$ [53], $\mathcal{O}(\lambda_R^{5/2})$ [54], $\mathcal{O}(\lambda_R^{5/2}\ln\lambda_R)$ [32], $\mathcal{O}(\lambda_R^3\ln\lambda_R)$ [32] and $\mathcal{O}(\lambda_R^3)$ [55] either by using similar resummation techniques or completely within the effective theory framework.

1.3.3 Dimensionally Reduced QCD Framework: Electro- and Magnetostatic QCD

Following we would like to discuss the framework on the basis of QCD rather than the scalar field theory considered in the previous section. Let us start and point out that the path integral formulation of the partition function $\mathcal{Z}$ in Eqs. (1.40) and (1.41) looks quite similar in case of gauge

fields. Before gauge fixing, the Euclidean Lagrangian and action of QCD with N_f massless[2] flavors of quarks reads

$$\begin{aligned} S_{QCD} &= \int_0^\beta d\tau \int d^d x \mathcal{L}_{QCD}\,, \\ \mathcal{L}_{QCD} &= \frac{1}{4} F^a_{\mu\nu} F^a_{\mu\nu} + \bar{\psi}\gamma_\mu D_\mu \psi\,, \end{aligned} \tag{1.59}$$

where $\beta = 1/T$, $d = 3 - 2\epsilon$, $\mu, \nu = 0, \ldots, 3$ and

$$F^a_{\mu\nu} = \partial_\mu A^a_\nu - \partial_\nu A^a_\mu + g f^{abc} A^b_\mu A^c_\nu\,, \qquad D_\mu = \partial_\mu - igA_\mu\,, \tag{1.60}$$

with $A_\mu = A^a_\mu T^a$, $\mathrm{Tr}[T^a T^b] = \delta^{ab}/2$, $\gamma^\dagger_\mu = \gamma_\mu$, $\{\gamma_\mu, \gamma_\nu\} = 2\delta_{\mu\nu}$. The coupling g is the bare gauge coupling and ψ carries Dirac, color and flavor indices. In analogy to Eq. (1.40), the partition function $\mathcal{Z}_{QCD}$ becomes

$$\mathcal{Z}_{QCD} = C \int \mathcal{D}A^a_\mu \int \mathcal{D}\bar{\psi}\mathcal{D}\psi \exp\left(-S_{QCD}\right), \tag{1.61}$$

where the gluon fields A^a_μ and quark fields ψ obey periodic and anti-periodic boundary conditions in imaginary space-time τ, respectively. The thermodynamic pressure of QCD is than given by

$$P_{\mathrm{QCD}}(T) \equiv \lim_{V\to\infty} \frac{T}{V} \ln \mathcal{Z}_{QCD}(T) = \lim_{V\to\infty} \frac{T}{V} \ln \int \mathcal{D}A^a_\mu \int \mathcal{D}\psi\mathcal{D}\bar{\psi} \exp\left(-S_{\mathrm{QCD}}\right), \tag{1.62}$$

where V denotes the d-dimensional volume. After we have chosen a convenient gauge, e. g. covariant gauge, we can proceed in the same way as in Section 1.3.1 and compute perturbative corrections in a weak-coupling expansion. The pressure of QCD up to next-to-leading order reads

$$P_{QCD}(T) = \frac{\pi^2 T^4}{90}\left[2(N_c^2-1) + \frac{7}{2}N_f N_c - \frac{5}{8}\frac{g^2}{\pi^2}\left(N_c^2-1\right)\left(N_c + \frac{5}{4}N_f\right) + \mathcal{O}(g^3)\right]. \tag{1.63}$$

The leading term can be seen as the QCD-version of the Stefan-Boltzmann law. The first correction can be obtained by computing the corresponding 1-loop vacuum diagrams in thermal QCD. Beyond that order, the weak-coupling expansion breaks down similar to the case of scalar field theory in Eq. (1.52). This can either be cured by performing a resummation of so-called plasmon diagrams or, as we will outline in the following, by using a sequence of two effective field theories known as electrostatic and magnetostatic QCD [32, 31]. Before discussing the idea we would like to summarize the perturbative corrections already known. It turns out the pressure in Eq. (1.62) has the following expansion

$$\frac{P(T)}{P_{\mathrm{SB}}} = 1 + c_2 g^2 + c_3 g^3 + \left(c_4' \ln g + c_4\right) g^4 + c_5 g^5 + \left(c_6' \ln g + c_6\right) g^6 + \mathcal{O}(g^7)\,, \tag{1.64}$$

normalized to the Stefan-Boltzmann pressure P_{SB} mentioned above. The weak-coupling expansion has again a nontrivial structure with odd powers in the coupling g. All coefficients, except c_6, can be found in references [56, 57, 58, 59, 60, 61].

The key observation is that QCD exhibits three different momentum scales, the hard scale T, soft scale gT and the so-called ultrasoft scale g^2T. At high temperatures T ($g \ll 1$), all momentum scales are clearly separated. The hard scale T, or $2\pi T$, is the typical momentum of a particle in the plasma whereas the soft and ultrasoft scales gT and g^2T are associated with the exchange of static

[2] At very high temperatures, particle masses can be neglected and the functions we are interested in are solely functions of temperature T.

(zero-mode) gluons. This effect, the exchange of electrostatic and magnetostatic gluons, causes the breakdown of the weak-coupling expansion. From the physical point of view, these effects are screened by plasma effects and can be taken into account, in the case of scale gT, by a resumming an infinite number of diagrams which eventually leads to the odd power correction starting at $\mathcal{O}(g^3)$. The contribution from the scale g^2T, starting to contribute at $\mathcal{O}(g^6)$, is of complete non-perturbative nature [30] and can only be taken into account via lattice simulations. At this point, we note that the scale $k \sim g^2T$ is not present in scalar field theory and therefore it is possible to compute all orders perturbatively [55].

Let us now move on and study the effective field theories. Because of the periodic and anti-periodic boundary conditions of gauge and fermion fields in imaginary time τ,

$$A^a_\mu(x, \tau = \beta) = A^a_\mu(x, \tau = 0)\,, \qquad \psi^f_j(x, \tau = \beta) = -\psi^f_j(x, \tau = 0)\,, \tag{1.65}$$

we can expand them into Fourier modes with Matsubara frequencies

$$\omega_{b,n} = 2\pi nT\,, \qquad \omega_{f,n} = (2n+1)\pi T\,, \tag{1.66}$$

where subscript b, f stands for bosonic and fermionic fields, respectively. The only modes which do not fall off exponentially at large distances $R > 1/T$ are the bosonic zero-modes $\omega_{b,n=0}$. They are responsible for the infrared divergencies and lead to the breakdown of the weak-coupling expansion. Thus the idea is to construct an effective field theory only containing the zero-modes by integrating out all non-static ($n \neq 0$) bosonic modes and fermionic modes. This resulting field theory reproduces full QCD at high temperatures T for distances $R \gg 1/T$ and reads

$$\begin{aligned} \mathcal{L}_{\rm E} &= \frac{1}{2}{\rm Tr}F^2_{kl} + {\rm Tr}\,[D_k, A_0]^2 + m^2_{\rm E}{\rm Tr}A^2_0 + \lambda^{(1)}_{\rm E}\left({\rm Tr}A^2_0\right)^2 + \lambda^{(2)}_{\rm E}{\rm Tr}A^4_0 + \dots\,, \\ S_{\rm E} &= \int d^dx \mathcal{L}_{\rm E}\,, \end{aligned} \tag{1.67}$$

where k, $l = 1, \dots, 3$ and

$$F_{kl} = i/g_{\rm E}\,[D_k, D_l]\,, \qquad D_k = \partial_k - ig_{\rm E}A_k\,. \tag{1.68}$$

The effective field theory in Eq. (1.67) is a 3-dimensional $SU(N_c)$ gauge theory coupled to an adjoint scalar A^a_0. The electrostatic gauge field A^a_0 and magnetostatic gauge field A^a_i can be related (up to normalization) to the zero modes of A^a_μ in thermal QCD, Eqs. (1.59). The effective field theory shown above is known as electrostatic QCD (EQCD) and contains four effective parameters

$$m^2_{\rm E},\, g^2_{\rm E},\, \lambda^{(1)}_{\rm E},\, \lambda^{(2)}_{\rm E}\,, \tag{1.69}$$

which can be determined by performing a matching computation, this is requiring the same result on the QCD and EQCD side within the domain of validity, for a concise review see [62]. The effective gauge coupling $g_{\rm E}$ and mass $m_{\rm E}$ are known up to 2-loop accuracy [63] and will be available soon at 3-loop [64, 65]. This specific matching computation involves the computation of 3-loop 2-point functions in finite temperature QCD. A serious problem turned out to be the evaluation of 3-loop sum-integrals [66].

In the Lagrangian in Eq. (1.67), operators of dimension 3 and higher [67] are neglected and need to be included as soon as they start to contribute at the order one is working at. The general structure of higher order operators is obtained from those in Eq. (1.67) by adding at least two D_μ or gA_0. It can be shown that they start to contribute, in case of the thermodynamic pressure, at order g^7 [61]. Let us again consider Eq. (1.62), the pressure is decomposed in two pieces

$$P_{\rm QCD} = P_{\rm E}(T) + \lim_{V\to\infty}\frac{T}{V}\ln\int \mathcal{D}A_k\mathcal{D}A_0\exp\left(-S_{\rm E}\right). \tag{1.70}$$

Now, $P_{\rm E}(T)$ contains the contribution from scale T and can be obtained in full QCD in an unresummed expansion in coupling g^2. The second term in Eq. (1.70) can either be calculated using lattice simulations or in a perturbative expansion in the small coupling $g_{\rm E}$. Unfortunately, the expansion is afflicted with infrared divergencies and breaks down. This is, because EQCD still contains two dynamical scales gT and g^2T. Integrating out the color electric field A_0 separates both scales and leads to a pure 3-dimensional $SU(N_c)$ gauge theory called magnetostatic QCD (MQCD) only containing the magnetostatic gauge field A_k ,

$$\begin{aligned} S_{\rm M} &= \int d^dx \mathcal{L}_{\rm M} \,, \\ \mathcal{L}_{\rm M} &= \frac{1}{2}{\rm Tr}F_{kl}^2 + \dots \,, \end{aligned} \tag{1.71}$$

where again k, $l = 1, \dots, 3$ and

$$F_{kl} = i/g_{\rm M} \left[D_k, D_l\right] \,, \qquad D_k = \partial_k - ig_{\rm M}A_k \,. \tag{1.72}$$

The effective field theory in Eq. (1.71) describes the contribution of scale g^2T and reproduces thermal QCD at distances $R \gg 1/gT$. Again, the parameter $g_{\rm M}$ can be obtained by a matching computation in EQCD and MQCD and differs from $g_{\rm E}$ by perturbative corrections, see [62] and references therein. The second term of Eq. (1.70) splits into two parts and reads

$$\lim_{V\to\infty} \frac{T}{V} \ln \int \mathcal{D}A_k \mathcal{D}A_0 \exp\left(-S_{\rm E}\right) \equiv P_{\rm M}(T) + \lim_{V\to\infty} \frac{T}{V} \ln \int \mathcal{D}A_k \exp\left(-S_{\rm M}\right) , \tag{1.73}$$

where $P_{\rm M}(T)$ contains the contribution of scale gT and is computed in EQCD. The second piece denoted by

$$P_{\rm G}(T) \equiv \lim_{V\to\infty} \frac{T}{V} \ln \int \mathcal{D}A_k \exp\left(-S_{\rm M}\right) , \tag{1.74}$$

is the contribution of scale g^2T associated with the screening of magnetostatic gluons. The theory in Eq. (1.71) is afflicted with infrared divergencies and only accessible via lattice simulations. Surprisingly, the contribution $P_{\rm G}(T)$ can be expanded in $g_{\rm M}$ with leading term proportional to $g_{\rm M}^6$. The MQCD Lagrangian in Eq. (1.71) has only one dimensionful parameter and consequently the leading contribution is of the following form

$$P_{\rm G}(T) \sim T g_{\rm M}^6 \,, \tag{1.75}$$

with nonperturbative coefficient determined in references [68, 69]. Putting all the ingredients together we obtain the decomposition

$$P_{\rm QCD}(T) = P_{\rm E}(T) + P_{\rm M}(T) + P_{\rm G}(T) \,. \tag{1.76}$$

where $P_{\rm E}(T)$ starts to contribute at g^2, $P_{\rm M}(T)$ at g^3 and $P_{\rm G}(T)$ finally at g^6 which is the first order where all physical scales contribute. From this point of view, the order g^6 can be seen as leading order of the pressure of hot QCD.

We have already mentioned, the contribution $P_{\rm M}(T)$ from physical scale gT can be computed in EQCD which involves massive tadpoles in $d = 3 - 2\epsilon$ space-time dimensions. Five loop massive tadpoles are necessary to compute the order g^7 to $P_{\rm M}(T)$. Although the g^6 correction is still unknown, which is mainly due to the fact that a 4-loop calculation within thermal QCD is involved, it would be, for example, interesting to see whether the odd g^7 contribution turns out to be again big in the same way as the g^3 and g^5 corrections. For more details we refer to [61], Section VII.

2 Reduction Methods for Feynman Integrals

In this chapter we introduce the most important techniques for the algebraic reduction of a typically large number of Feynman integrals to a small set of so-called master integrals. The methods are playing a crucial role in the following work. Throughout the chapter most of the concepts are illustrated on the basis of simple examples.

The plan of the chapter is as follows. We start in Section 2.1 with basic definitions and useful notations. Then in Section 2.2 we proceed and review the well-known integration-by-parts and Lorentz-invariance identities [16, 17, 70]. This is followed by an introduction of Feynman graph polynomials [71] in Section 2.3. The Feynman graph polynomials are necessary for the discussion of the so-called space-time dimensional relations [72, 73, 74] in Section 2.4. In Section 2.5 we combine the integration-by-parts and space-time dimensional relations and obtain generalized recurrence relations. Section 2.6 is devoted to the question how these relations can be incorporated in an algorithmic approach, the Laporta algorithm [18]. In order to discuss the reduction problem of Feynman integrals systematically, we introduce the concept of an auxiliary topology, a sector relation and sector symmetry in Sections 2.6.1 and 2.6.2, respectively. In Section 2.6.3 we discuss the general structure of how integration-by-parts identities are relating Feynman integrals among each other. This knowledge helps us to understand one of the key building blocks of the Laporta algorithm, the unique ordering of Feynman integrals in Section 2.6.4. In Section 2.7 we discuss the benefit of using generalized recurrence relations instead of the traditional integration-by-parts relations.

2.1 Definitions and Notations

A generic Feynman integral with N_k loops, N_e external and N_d internal lines is defined by

$$F(p_1, \ldots, p_{N_e}) \equiv \int_{k_1,\ldots,k_{N_k}} V_{ab}\,, \tag{2.1}$$

with the integrand

$$V_{ab} = \frac{\prod_{i=1}^{N_p}\prod_{j=1}^{N_k}(p_i\cdot k_j)^{a_{ij1}}\prod_{i=1}^{N_k}\prod_{j=i}^{N_k}(k_i\cdot k_j)^{a_{ij2}}}{\prod_{i=1}^{N_d} D_i^{b_i}}\,, \quad a_{ijl}\geq 0,\ b_i\geq 0\,, \tag{2.2}$$

where the propagators are of the form $D_i = \pm q_i^2 + m_i^2$ and $N_p = N_e - 1$ the number of independent external momenta. The upper $(+)$ and lower $(-)$ sign corresponds to Euclidean and Minkowski space-time, respectively. In the latter case we have suppressed the usual prescription with $i\epsilon$. The momenta q_i are, in general, linear combinations of loop- and external momenta $\{k_i\}, \{p_i\}$ and can be written as

$$q_i = \sum_{j=1}^{N_k}\lambda_{ij}k_j + \sum_{j=1}^{N_e}\sigma_{ij}p_j\,, \tag{2.3}$$

where $\lambda_{ij}, \sigma_{ij} \in \{-1, 0, 1\}$. The numerator in Eq. (2.2) is composed out of all possible scalar products of loop- and external momenta and the number of such scalar products is given by

$$N_{sp} = N_p N_k + N_k(N_k+1)/2\,. \tag{2.4}$$

The integrand given in Eq. (2.2) can be further simplified by rewriting scalar products involving loop momentum in terms of inverse propagators using

$$\frac{(p\cdot k)_j}{D_j} = \frac{1}{C_j}\left(1 - \frac{D_j - C_j(p\cdot k)_j}{D_j}\right), \quad j = 1,\ldots,N_d\,, \tag{2.5}$$

where the scalar product denoted by $(p\cdot k)_j$ appears in the expression for D_j with coefficient C_j. Applying subsequently the identity in Eq. (2.5) to V_{ab} and terms generated in this procedure we end up with a sum of terms with the general structure

$$V'_{ni\alpha\beta} = \frac{\prod_{j=1}^{N_{sp}-n}(p\cdot k \text{ irred.})_j^{\beta_j}}{\prod_{j=1}^{n} D_{i_j}^{\alpha_i}}, \quad n \le N_d\,, \quad \alpha_j,\beta_j \ge 0\,, \tag{2.6}$$

where we have $j = 1,\ldots,N_{sp}-n$ irreducible scalar products and n denominators $D_{i_1},\ldots,D_{i_n}$, $\{i_1,\ldots,i_n\} \subset \{1,\ldots,N_d\}$ with exponents $\alpha = \{\alpha_1,\ldots,\alpha_n\}$ and $\beta = \{\beta_1,\ldots,\beta_{N_{sp}-n}\}$, respectively. Irreducible means we are not able to reduce the number of scalar products further with one of the denominators $D_{i_1},\ldots,D_{i_n}$ by using Eq. (2.5).

2.2 The Integration-by-Parts and Lorentz-invariance Identities

The so-called integration-by-parts (IBP) relations [16, 17] of Feynman integrals are generated by the fact that

$$\int_{k_1,\ldots,k_{N_k}} \frac{\partial}{\partial k_j^\mu}\left[p_l^\mu V'_{ni\alpha\beta}\right] = 0\,, \quad \int_{k_1,\ldots,k_{N_k}} \frac{\partial}{\partial k_j^\mu}\left[k_l^\mu V'_{ni\alpha\beta}\right] = 0\,, \tag{2.7}$$

vanishes identically in dimensional regularization [34] with $j = 1,\ldots,N_k$, $l = 1,\ldots,N_e-1$ and $j,l = 1,\ldots,N_k$, respectively. From Eqs. (2.7) we can construct a total number of $N_k(N_p+N_k)$ identities for each $V'_{ni\alpha\beta}$. The integration measure used above and throughout this work (if not otherwise indicated) is given by

$$\int_{k_1,\ldots,k_{N_k}} = \int \frac{d^dk_1\ldots d^dk_{N_k}}{\left(\pi^{d/2}\right)^{N_k}}\,. \tag{2.8}$$

Calculating of IBP relations in Eq. (2.7) requires two operations, performing the derivatives and contracting the μ index. This can produce reducible scalar products and those can be reduced to irreducible ones by applying the identity in Eq. (2.5) as before. The integration by parts relations obtained from Eq. (2.7) are linear relations among integrals with polynomial coefficients in the space-time dimension d. Depending on the specific problem additional invariants can be involved. The linear relations are made out of two kinds of integrals, integrals containing all denominators $D_{i_1},\ldots,D_{i_n}$ and those with one denominator cancelled.

The IBP identities obey very interesting properties, for instance, they form a closed Lie algebra. Let us define, in complete analogy to Ref. [75], the following operators

$$\begin{aligned}(A_\alpha f)(n_1,\ldots,n_M) &= n_\alpha f(n_1,\ldots,n_\alpha+1,\ldots,n_M)\,,\\ (B_\alpha f)(n_1,\ldots,n_M) &= f(n_1,\ldots,n_\alpha-1,\ldots,n_M)\,.\end{aligned} \tag{2.9}$$

The arguments $n_1,\ldots,n_M$ can be understood as the exponents α,β of irreducible scalar products and denominators cf. Eq. (2.6), respectively. By means of these operators, we can write the IBP identities as

$$-PJ = 0\,, \qquad \text{with} \qquad P = a^{\alpha\beta}A_\alpha B_\beta + b^\alpha A_\alpha + c\,, \tag{2.10}$$

where $a^{\alpha\beta}, b^{\alpha}$ and c are coefficients. The function J is the original Feynman integral in Eq. (2.1) as a function of its exponents

$$J(\mathbf{n}) = J(n_1, \ldots, n_M) = \int_{k_1,\ldots,k_{N_k}} V_{ab}\,, \tag{2.11}$$

and

$$-(P_{ik}J)(\mathbf{n}) = \int_{k_1,\ldots,k_{N_k}} O_{ik}V(\mathbf{n})\,, \quad O_{ik} = \frac{\partial}{\partial k_i}\cdot q_k\,. \tag{2.12}$$

where $q_{1,\ldots,N_k} = k_{1,\ldots,N_k}, q_{N_{k+1},\ldots,N_k+N_e} = p_1, \ldots, p_{N_e}$ The operators O and therefore also the P operators follow the commutations relations

$$[P_{ik}, P_{jl}] = \delta_{il}P_{jk} - \delta_{jk}P_{il}\,. \tag{2.13}$$

As a consequence, it is sufficient to consider a smaller set of IBP identities

$$\begin{aligned} &\frac{\partial}{\partial k_i}\cdot k_{i+1}, \qquad i = 1,\ldots,N_k, \quad k_{N_{k+1}} \equiv k_1\,, \\ &\frac{\partial}{\partial k_1}\cdot p_j, \qquad j = 1,\ldots,N_e, \quad \sum_{i=1}^{N_k}\frac{\partial}{\partial k_i}\cdot k_i\,, \end{aligned} \tag{2.14}$$

and in fact, these operators form a multiplicative basis of the Lie-algebra in Eq. (2.13). Counting the number of identities in Eqs. (2.14) we find $N_k + N_e + 1$. This is not only interesting from the theoretical point of view, as we will see, the system generated by IBP identities is highly overdetermined and therefore any attempt to reduce the number of identities in each point $\mathbf{n} \in \mathbb{Z}^M$ is important. We will discuss this issue, and others, such as the question how to combine the IBP identities to reduce a given integral, later on in Section 2.6.

As an example we consider the 1-loop massive tadpole from Section 1.1 denoted by

$$J(n) = \int_k \frac{1}{(k^2+m^2)^n}\,. \tag{2.15}$$

Comparing the 1-loop tadpole above with Eq. (2.1) and applying Eq. (2.7) we get

$$\begin{aligned} 0 &= \int_k \partial_k\left[k\frac{1}{(k^2+m^2)^n}\right] = \int_k\left[\frac{d}{(k^2+m^2)^n} - 2n\frac{k^2}{(k^2+m^2)^{n+1}}\right] \\ &= J(n)(d-2n) + 2nm^2J(n+1)\,, \end{aligned} \tag{2.16}$$

and this leads immediately to the simple recursion relation we already encountered in Eq. (1.7),

$$J(n+1) = -\frac{d-2n}{2nm^2}J(n)\,, \quad n \geq 1\,. \tag{2.17}$$

In other words we can express 1-loop massive tadpoles with arbitrary power n in terms of $J(1)$ times a rational function of space-time dimension d and mass squared m^2. The 1-loop tadpole is a very illustrative example how IBP relations can be used to relate all possible integrals to a single one called master integral.

Moreover, there are additional relations, the so-called Lorentz-invariance identities (LI) [70]. These relations are based on the fact that the Feynman integral in Eq. (2.1) is invariant under

a Lorentz transformation in the external momenta $p_1, \ldots, p_{N_e}$. Let us consider the infinitesimal Lorentz transformation

$$p^\mu \longrightarrow p^\mu + \delta p^\mu = p^\mu + \delta\epsilon^\mu_\nu p^\nu \,, \tag{2.18}$$

where $\delta\epsilon^\mu_\nu = -\delta\epsilon^\nu_\mu$. The Feynman integral in Eq. (2.1) is invariant under this transformation

$$F(p_1 + \delta p_1, \ldots, p_{N_e} + \delta p_{N_e}) = F(p_1, \ldots, p_{N_e}) \,, \tag{2.19}$$

and an expansion of the left-hand side yields

$$F(p_1 + \delta p_1, \ldots, p_{N_e} + \delta p_{N_e}) = \left[1 + \delta p_1^\mu \frac{\partial}{\partial p_1^\mu} + \cdots + \delta p_{N_e}^\mu \frac{\partial}{\partial p_{N_e}^\mu}\right] F(p_1, \ldots, p_{N_e}) \,. \tag{2.20}$$

From Eqs. (2.19) and (2.20) we immediately get the desired identities

$$p_{i\mu} p_{j\nu} \left(\sum_k p_k^\nu \frac{\partial}{\partial p_{k\mu}}\right) F(p_1, \ldots, p_{N_e}) = 0 \,, \tag{2.21}$$

where we have contracted the equation with all possible antisymmetric combinations of pairs of external momenta $p_{i\mu} p_{j\nu}$. The differential operator $\sum_k p_k^\nu \partial/\partial p_{k\mu}$ acts directly on the integrand of the corresponding Feynman integral $F(p_1, \ldots, p_{N_e})$. In some cases these identities can be quite useful, but as it turns out, they are all expressible in terms of linear combinations of IBP identities [75] and therefore we do not consider these relations in the following work.

2.3 Feynman Graph Polynomials

In the following sections we are using certain Feynman integral representations where the so-called graph polynomials are going to show up. This section is devoted to summarize some of the most important properties of these polynomials [71].

For loop calculations it is sometimes advantageous to rewrite the d-dimensional loop integrals in Eq. (2.1) in terms of integrals over Feynman parameters. After Feynman parametrization the integrand $V'_{ni\alpha\beta}$ in Eq. (2.6) is characterized by two polynomials called the first and second Symanzik polynomial. These polynomials can be deduced from the specific combination of propagators and irreducible scalar product of the integral under consideration. Let us, for convenience, assume that all irreducible scalar products are expressed in terms of additional propagators with negative powers, then Eq. (2.1) becomes

$$F(p_1, \ldots, p_{N_e}) = \int_{k_1, \ldots, k_{N_k}} \prod_{i=1}^{N_d} \frac{1}{(-q_i^2 + m_i^2)^{b_i}} \,, \tag{2.22}$$

where the minus in front of the momentum flow q_i indicates Minkowski space-time and the usual prescription with $i\epsilon$ is suppressed. The internal momenta q_i are fixed by the matrices of incidences λ and σ in Eq. (2.3). Using the Feynman parameter technique [25] we can rewrite the product of propagators as a sum

$$\prod_{i=1}^{N_d} \frac{1}{D_i^{b_i}} = \frac{\Gamma(b)}{\prod_{i=1}^{N_d} \Gamma(b_i)} \int_{\alpha_i \geq 0} d\alpha_1 \ldots d\alpha_{N_d}\, \delta\left(1 - \sum_{i=1}^{N_d} \alpha_i\right) \frac{\prod_{i=1}^{N_d} \alpha_i^{b_i - 1}}{\left(\sum_{i=1}^{N_d} \alpha_i D_i\right)^b} \,, \qquad b = \sum_{i=1}^{N_d} b_i \,, \tag{2.23}$$

where $D_i = -q_i^2 + m_i^2$. Plugging this formula into Eq. (2.22) and using translational invariance of the d-dimensional loop integrals leads to the nice simplification that the integrand becomes only

a function of squares of k_i. Consequently, all loop integrations can be performed and we finally arrive at

$$F(p_1,\dots,p_{N_e}) = \frac{\Gamma(b-N_k\,d/2)}{\prod_{i=1}^{N_d}\Gamma(b_i)}\int_{\alpha_i\geq 0} d\alpha_1\dots d\alpha_{N_d}\,\delta\left(1-\sum_{i=1}^{N_d}\alpha_i\right)\left(\prod_{i=1}^{N_d}\alpha_i^{b_i-1}\right)\frac{\mathcal{U}^{b-(N_k+1)d/2}}{\mathcal{F}^{b-N_k d/2}}\,, \quad (2.24)$$

where $\mathcal{U}$ and $\mathcal{F}$ are functions of Feynman parameters α_i. Having this formula at hand, we can rewrite all d-dimensional loop integrals in Eq. (2.22) as integrals over Feynman parameters in Eq. (2.24). Introducing the scalar $N_k \times N_k$ matrix M and N_k-vector Q, carrying four-vectors as elements, and rewriting the denominator in Eq. (2.23) as

$$\sum_{i=1}^{N_d}\alpha_i\left(-q_i^2+m_i^2\right) = -\sum_{r=1}^{N_k}\sum_{s=1}^{N_k}k_r M_{rs}k_s + \sum_{r=1}^{N_k}2k_r\cdot Q_r + J\,, \quad (2.25)$$

we obtain the following expressions for $\mathcal{U}$ and $\mathcal{F}$

$$\mathcal{U} = \det(M)\,, \qquad \mathcal{F} = \det(M)(J+QM^{-1}Q)\,. \quad (2.26)$$

The functions $\mathcal{U}$ and $\mathcal{F}$ are polynomials in Feynman parameters α_i and can be, as previously mentioned, deduced from the topology[1] of the corresponding Feynman integral. They are therefore also called graph polynomials. We would like to summarize briefly some important properties at this point.

The graph polynomials $\mathcal{U}$ and $\mathcal{F}$ are homogeneous in α_i with degree N_k and degree N_k+1, respectively. On top of this, the polynomial $\mathcal{U}$ is linear in each α_i and in expanded form each monomial has coefficient $+1$.

As an example, let us consider the 1-loop massive tadpole of Eq. (2.15) in Minkowski space-time and determine the corresponding polynomials $\mathcal{U}$ and $\mathcal{F}$. Starting from Eq. (2.25) we immediately get $M = M_{11} = \alpha_1, Q = 0$ and $J = \alpha_1 m_1^2$ and therefore

$$\mathcal{U} = \alpha_1\,, \qquad \mathcal{F} = \alpha_1^2 m_1^2\,. \quad (2.27)$$

In the literature $\mathcal{U}$ and $\mathcal{F}$ are often called the first and second Symanzik polynomials. There are several ways to determined these polynomials from the underlying graph. For instance, it can be shown that the polynomials $\mathcal{U}$ and $\mathcal{F}$ are closely related to the spanning tree and spanning 2-forest of the underlying graph [71, 24]. This method is quite illustrative but not well suited for automatization. On the other hand, introducing the Laplacian of a graph and using the matrix-tree theorem leads to a third method only involving the computation of a matrix determinant [71]. However, for our purposes it is enough to have Eqs. (2.25) and (2.26) at hand.

2.4 Space-time Dimensional Relations

In Section 2.2 we have reviewed the important IBP relations. But there are additional relations [72, 73, 74] complementary to the former ones relating integrals with dimension d to integrals with space-time dimension $d-2$. Furthermore, it can be shown that integrals with irreducible numerators such as the irreducible scalar products of Eq. (2.6) in Section 2.1 are expressible in terms of integrals without these scalar products but with shifted space-time dimension d. In this

[1] So far we have not defined what exactly is meant by saying topology. This question is postponed to Section 2.6.1 where the concept of an auxiliary topology is introduced. By saying topology of a graph we refer to a specific combination of propagators in Eq. (2.22).

section, we are using a slightly different notation to keep in touch with the corresponding literature. Defining an arbitrary scalar N_k-loop Feynman integral as

$$G^{(d)}(\{s_i\}),\{m_s^2\}) = \prod_{i=1}^{N_k} \int d^d k_i \prod_{j=1}^{N_d} P_{q_j,m_j}^{\nu_j}\,, \tag{2.28}$$

with

$$P_{k,m}^{\nu} = \frac{1}{\left(k^2-m^2+i\epsilon\right)^{\nu}}\,, \quad q_j^{\mu} = \sum_{n=1}^{N_k} \lambda_{jn} k_n^{\mu} + \sum_{m=1}^{N_e} \sigma_{jm} p_m^{\mu}\,, \tag{2.29}$$

where N_d and N_e are the numbers of internal and external lines, respectively. The p_m are external momenta, λ and σ the matrices of incidences from Eq. (2.3) and $\{s_i\}$ represents a set of scalar invariants formed out of external momenta.

Starting from the α-parametric representation (see e. g. [24]) for the propagator

$$\frac{1}{\left(k^2-m^2+i\epsilon\right)^{\nu}} = \frac{i^{-\nu}}{\Gamma(\nu)} \int_0^{\infty} d\alpha\; \alpha^{\nu-1} e^{i\alpha\left[k^2-m^2+i\epsilon\right]}\,, \tag{2.30}$$

and using the Gaussian integration formula in d-dimensions

$$\int d^d k\; e^{i\left[Ak^2+2p\cdot k\right]} = i\left(\frac{\pi}{iA}\right)^{d/2} e^{-ip^2/A}\,, \tag{2.31}$$

enables us to perform the loop integrations in Eq. (2.28). We obtain the representation

$$G^{(d)}\left(\{s_i\},\{m_s^2\}\right) = i^{N_k}\left(\frac{\pi}{i}\right)^{\frac{dN_k}{2}} \prod_{j=1}^{N_d} \frac{i^{-\nu_j}}{\Gamma(\nu_j)} \int_0^{\infty} \cdots \int_0^{\infty} \frac{d\alpha_j \alpha_j^{\nu_j-1}}{[D(\alpha)]^{d/2}} e^{i\left[\frac{Q(\{s_i\},\alpha)}{D(\alpha)} - \sum_{l=1}^{N_d} \alpha_l (m_l^2 - i\epsilon)\right]}\,, \tag{2.32}$$

where $D(\alpha)$ and $Q(\{s_i\},\alpha)$ are the graph polynomials $\mathcal{U}$ and $\mathcal{F}$ discussed in Section 2.3. Having a closer look on Eq. (2.32) we observe that the integrand depends rather simple, only linearly in the exponent of $D(\alpha)$, on the space-time dimension d. As mentioned before, we are looking for relations connecting integrals with different space-time dimensions d. The first step is to assume that all scalar propagators in Eq. (2.28) have different masses. Then we construct the polynomial differential operator

$$D\left(\frac{\partial}{\partial m_j^2}\right)\,, \tag{2.33}$$

by replacing $\alpha_j \to \partial_j \equiv \partial/\partial m_j^2$ in $D(\alpha)$. Applying this operator to Eq. (2.32) gives

$$D(\partial) e^{-i\sum \alpha_l m_l^2} \to D(\alpha)(-i)^{N_k} e^{-i\sum \alpha_l m_l^2}\,, \tag{2.34}$$

and consequently $D(\partial)G^{(d)}$ is directly proportional to $G^{(d-2)}$. More explicitly, we have

$$\begin{aligned} D(\partial)G^{(d)}\left(\{s_i\},\{m_s^2\}\right) &= \left(\frac{\pi}{i}\right)^{\frac{dN_k}{2}} \prod_{j=1}^{N_d} \frac{i^{-\nu_j}}{\Gamma(\nu_j)} \int_0^{\infty} \cdots \int_0^{\infty} \frac{d\alpha_j \alpha_j^{\nu_j-1}}{[D(\alpha)]^{(d-2)/2}} e^{i\left[\frac{Q(\{s_i\},\alpha)}{D(\alpha)} - \ldots\right]} \\ &= (-\pi)^{N_k} G^{(d-2)}(\{s_j\},\{m_s^2\})\,, \end{aligned} \tag{2.35}$$

and finally

$$G^{(d-2)}(\{s_j\},\{m_s^2\}) = \left(-\frac{1}{\pi}\right)^{N_k} D(\partial) G^{(d)}(\{s_j\},\{m_s^2\})\,. \tag{2.36}$$

The masses that we initially assigned all different can be identified right after performing the differentiation with the physical ones.

We want to extend this to tensor integrals in the following and it turns out we can use similar ideas to accomplish this issue. First we associate to each internal line an auxiliary vector a_j and then we take derivatives with respect to these vectors

$$\prod_{l=1}^{n_1} q_{1\mu_l} \cdots \prod_{s=1}^{n_{N_d}} q_{N_d\lambda_s} = \frac{1}{i^{n_1} \dots i^{n_{N_d}}} \prod_{r=1}^{n_1} \frac{\partial}{\partial_{a_{1\mu_r}}} \cdots \prod_{s=1}^{n_{N_d}} \frac{\partial}{\partial_{a_{N_d\lambda_s}}} e^{i\left[a_1 q_1 + \cdots + a_{N_d} q_{N_d}\right]} \Big|_{a_j=0} . \tag{2.37}$$

In this manner we can reconstruct all possible tensors which might be present in the numerator of a given tensor integral. Having this in mind, the parametric representation in Eq. (2.32) for the scalar case can be easily generalized to the tensor case [72] and reads

$$\begin{aligned} \prod_{i=1}^{N_k} \int d^d k_i \prod_{j=1}^{N_d} P_{q_j,m_j}^{\nu_j} \prod_{l=1}^{n_1} q_{1\mu_l} \cdots \prod_{s=1}^{n_{N_d}} q_{N_d\lambda_s} &= i^{N_k} \left(\frac{\pi}{i}\right)^{\frac{dN_k}{2}} \prod_{j=1}^{N_d} \frac{i^{-\nu_j - n_j}}{\Gamma(\nu_j)} \\ &\times \prod_{r=1}^{n_1} \frac{\partial}{\partial_{a_{1\mu_r}}} \cdots \prod_{s=1}^{n_{N_d}} \frac{\partial}{\partial_{a_{N_d\lambda_s}}} \int_0^\infty \cdots \int_0^\infty \frac{d\alpha_j \alpha_j^{\nu_j - 1}}{[D(\alpha)]^{d/2}} e^{i\left[\frac{Q(\{\overline{s}_i\},\alpha)}{D(\alpha)} - \sum_{l=1}^{N} \alpha_l (\overline{m}_l^2 - i\epsilon)\right]} \Big|_{a_j=0} , \end{aligned} \tag{2.38}$$

with mass $\overline{m}_l^2 = m_l^2 + a_l^2/(4\alpha_l^2)$ and new scalar invariants $\overline{s}_i$ made out of vectors $\overline{p}_i = p_i + \sum_j \epsilon_{ij} a_j/(2\alpha_j)$ where p_i represents the external momentum incoming at vertex i. The matrix ϵ is the incidence matrix [25, 72] of the underlying topology defined as

$$\epsilon_{ij} = \begin{cases} +1 & : \quad \text{if the vertex } i \text{ is the starting point of line } j \\ -1 & : \quad \text{if the vertex } i \text{ is the endpoint of line } j \\ 0 & : \quad \text{if line } j \text{ is not incident on vertex } i\,. \end{cases} \tag{2.39}$$

Performing the derivatives in Eq. (2.38) results in a factor in front of the exponential containing external momenta and metric tensors $g_{\mu\nu}$ multiplied by some polynomials $R_s(\alpha)$ over $D(\alpha)$ with some exponent. As before, the polynomials are replaced by the operators $R_s(\partial)$ and the $D(\alpha)$ can be absorbed by redefining the space-time dimension d.

We would like to write the right-hand side of Eq. (2.38) in terms of an operator acting on the scalar Feynman integral $G^{(d)}$

$$\prod_{i=1}^{N_k} \int d^d k_i \prod_{j=1}^{N_d} P_{q_j,m_j}^{\nu_j} \prod_{l=1}^{n_1} q_{1\mu_l} \cdots \prod_{s=1}^{n_{N_d}} q_{N_d\lambda_s} = T_{\mu_1,\dots,\lambda_s}(q, \partial, \mathbf{d}^+)\, G^{(d)}\left(\{s_i\}, \{m_s^2\}\right) , \tag{2.40}$$

where the tensor operator $T_{\mu_1,\dots,\lambda_s}$ turns out to be of the following form [72],

$$T_{\mu_1,\dots,\lambda_s}(q, \partial, \mathbf{d}^+) = \frac{e^{-iQ(\{\overline{s}_i,\alpha\})\rho}}{i^{n_1} \dots i^{n_{N_d}}} \prod_{r=1}^{n_1} \frac{\partial}{\partial_{a_{1\mu_r}}} \cdots \prod_{s=1}^{n_{N_d}} \frac{\partial}{\partial_{a_{N\lambda_s}}} e^{i\left[Q(\{\overline{s}_i,\alpha\}) - \sum_{l=1}^{N_d} a_l^2/(4\alpha_l) D(\alpha)\right]\rho} \Big|_{\substack{a_j=0 \\ \alpha_j = i\partial_j \\ \rho=(-\pi)^{-N_k}\mathbf{d}^+}} , \tag{2.41}$$

with the operator $\mathbf{d}^+$ shifting the space-time dimension by two $\mathbf{d}^+ G^{(d)} = G^{(d+2)}$. As in the case of the D operator in Eq. (2.35) we assume that all propagators have different masses and finally, after applying the T operator, we set all to physical values.

An alternative to the auxiliary vectors a_j introduced in Eq. (2.37) for tensor integrals are scalar parameters b_j in case we are only interested in rewriting irreducible scalar products

$$(q_i \cdot q_j)^{n_1} \dots (q_k \cdot q_l)^{n_{N_i}} = \frac{1}{i^{n_1} \dots i^{n_{N_i}}} \frac{\partial^{n_1}}{\partial b_1^{n_1}} \cdots \frac{\partial^{n_{N_i}}}{\partial b_{N_i}^{n_{N_i}}} e^{i\left[b_1 (q_i \cdot q_j) + \cdots + b_{N_i} (q_k \cdot q_l)\right]} \Big|_{b_i=0} , \tag{2.42}$$

where N_i is the number of irreducible scalar products cf. Eq. (2.6). Similar to Eq. (2.40) we have [74],

$$\prod_{i=1}^{N_k} \int d^d k_i \prod_{j=1}^{N_d} P_{q_j,m_j}^{\nu_j} (q_m \cdot q_n)^{n_1} \ldots (q_o \cdot q_p)^{n_{N_i}} = T_{n_1,\ldots,n_{N_i}}(q, \partial, \mathbf{d}^+)\, G^{(d)}\left(\{s_i\}, \{m_s^2\}\right) . \tag{2.43}$$

A few remarks should be made at this point. Employing Eq. (2.40) or Eq. (2.43) enables us to express any Feynman integral with tensors or irreducible scalar products in the numerator in terms of scalar integrals without numerators but shifted space-time dimension d. In the case of irreducible scalar products we can either go through Eq. (2.40) by contracting the momenta to construct appropriate scalar products or start right from the beginning with Eq. (2.43). The latter approach is more favorable because each scalar product only induces a single $\mathbf{d}^+$ instead of two (two derivatives) in Eq. (2.40).

For an actual reduction of Feynman integrals to a small set of master integrals one should combine those with the IBP relations introduced in Section 2.2. As we have seen, irreducible scalar products cannot be further reduced by using a strategy as in Eq. (2.5). Having the picture in mind that every Feynman integral can be expressed as a list of powers of propagators cf. Eq. (2.15) we could always introduce additional propagators to express such scalar products in terms of these propagators raised to some negative power. However, this would enlarge the number of indices and consequently we would have a more complicated class of integrals at hand.

The benefit of this method is that we are staying in the class of integrals we have started with. Or in other words, we are effectively reducing the number of indices for a given problem. A more detailed discussion will follow in Sections 2.5 and 2.7.

2.5 Generalized Recurrence Relations

In order to compute the generalized recurrence relations we are starting from the same point as for the IBP relations in Section 2.2. From Eqs. (2.7) we have

$$\prod_{i=1}^{N_k} \int d^d k_i \frac{\partial}{\partial k_{r\mu}} \left[\left(\sum_l x_l q_{l\mu} \right) \prod_{j=1}^{N_d} P_{q_j,m_j}^{\nu_j} \right] = 0 , \tag{2.44}$$

where $r = 1, \ldots, N_k$ and constants x_l which are arbitrary chosen. The differentiation will in general produce scalar products involving loop- and external momenta. These scalar products are usually expressed in terms of inverse propagators e. g.

$$k_1^2 = P_{k_1,m_1}^{-1} + m_1^2 , \tag{2.45}$$

and if not possible count as an irreducible scalar product. However, from here on we are following a different way and write all scalar products containing loop momenta in terms of integrals with different space-time dimension according to Eq. (2.43). The result is a system of equations relating integrals with changed space-time dimension d and different combinations of powers of propagators.

In other words, the well-known integration-by-parts (IBP) method is just a special case of relations obtained from Eq. (2.44) for a particular way of rewriting the emerging scalar products

$$\begin{aligned} k_1^2 &\longrightarrow P_{k_1,m_1}^{-1} + m_1^2 \quad : \quad \text{integration-by-parts}, \\ k_1^2 &\longrightarrow T(q, \partial, \mathbf{d}^+) \quad : \quad T\text{-Operator}. \end{aligned}$$

For completeness it should be pointed out that the minimal change of space-time dimension d is ± 2. Changing the dimension only by ± 1 would result in functions that are not part of the class

of continuous functions. This can be easily seen in cases where the analytic result in terms of hypergeometric functions is explicitly known.

As an example we would like to discuss the generalized recurrence relations for the 1-loop massive tadpole

$$I_{\nu_1}^{(d)}(m_1^2) \equiv \int \frac{d^d k_1}{i\pi^{d/2}} P_{k_1,m_1}^{\nu_1} \,. \tag{2.46}$$

According to Eq. (2.27) the first and second Symanzik polynomials are

$$D(\alpha) = \alpha_1 \,, \quad Q\left(\{s\},\alpha\right) = \alpha_1^2 m_1^2 \,,$$

and therefore the D-operator relation from Eq. (2.36) becomes

$$G^{(d-2)}(m_1^2) = -\frac{1}{\pi} D(\partial) G^{(d)}(m_1^2) = -\frac{1}{\pi} \partial_{m_1^2} \int d^d k_1 P_{k_1,m_1}^{\nu_1} = -\frac{\nu_1}{\pi} \int d^d k_1 P_{k_1,m_1}^{\nu_1+1} \,, \tag{2.47}$$

rescaling $d \to d+2$ and rewriting of $G^{(d-2)}$ in terms of $I_{\nu_1}^{(d-2)}$ finally yields

$$I_{\nu_1}^{(d)} + \nu_1 I_{\nu_1+1}^{(d+2)} = 0 \,. \tag{2.48}$$

For the T-operator relation we are starting from Eq. (2.44) and have

$$0 = \int d^d k_1 \frac{\partial}{\partial k_{1\mu}} \left[k_{1\mu} P_{k_1,m_1}^{v_1} \right] = \int d^d k_1 \left[d P_{k_1,m_1}^{v_1} - 2\nu_1 k_1^2 P_{k_1,m_1}^{v_1+1} \right] \,, \tag{2.49}$$

where the very last term on the right-hand side is rewritten in terms of the tensor integral

$$-2\nu_1 g^{\mu\nu} \int d^d k_1 k_{1\mu} k_{1\nu} P_{k_1,m_1}^{v_1+1} \,. \tag{2.50}$$

Comparing the integral above with Eq. (2.40) and calculating the T-operator according to Eq. (2.41) we obtain $T(q,\partial,\mathbf{d}^+) = -\frac{g_{\mu\nu}}{2\pi}\,\mathbf{d}^+$ and therefore

$$-2\nu_1 g^{\mu\nu} \int d^d k_1 k_{1\mu} k_{1\nu} P_{k_1,m_1}^{v_1+1} = \frac{\nu_1}{\pi} g^{\mu\nu} g_{\mu\nu}\, \mathbf{d}^+ G^{(d)} = \frac{\nu_1}{\pi}\, d\, G^{(d+2)} \,. \tag{2.51}$$

Plugging this result into Eq. (2.49) and rewriting again $G^{(d+2)}$ in terms of $I_{\nu_1+1}^{(d+2)}$ we finally arrive at

$$I_{\nu_1}^{(d)} + \nu_1 I_{\nu_1+1}^{(d+2)} = 0 \,, \tag{2.52}$$

which is in fact the same as for the D-operator in Eq. (2.48). This means we only have two generalized recurrence relations instead of three (D or T-operator + IBP) at the one loop level. The corresponding integration-by-parts relation can be deduced from Eq. (2.15) via Wick-rotation [23] back to Minkowski space-time or directly from Eq. (2.49) by rewriting the scalar product k_1^2 in terms of the inverse propagator. In the end we have

$$(d-2\nu_1) I_{v_1}^{(d)} - 2\nu_1 m_1^2 I_{v_1+1}^{(d)} = 0 \,. \tag{2.53}$$

In general, the set of T,D-operators and IBP relations for a given problem are not linearly independent. It turns out there are as many independent identities as possible scalar products in the numerator cf. Eq. (2.4). Instead of using Eq. (2.44) to generate generalized recurrence relations we use the following prescription

$$\prod_{i=1}^{N_k} \int d^d k_i \prod_{j=1}^{N_d} P_{q_j,m_j}^{\nu_j} \left[q_m \cdot q_n - q_m \cdot q_n \right] = 0 \,, \tag{2.54}$$

where one scalar product is replaced by an appropriate combination of inverse propagators and the other by the T-operator according to Eq. (2.43)

$$\begin{aligned}(q_m \cdot q_n) &\longrightarrow \sum_u a_u \left(P^{-1}_{q_u,m_u} + m_u^2\right) , \\ (q_m \cdot q_n) &\longrightarrow T(q, \partial, \mathbf{d}^+) .\end{aligned} \tag{2.55}$$

The recurrence relations of Eq. (2.54) combined with the D-operator relation from Eq. (2.36) are forming the set of $N_{sp} + 1$ generalized recurrence relations. For the 1-loop massive tadpole of Eq. (2.48) we get

$$\int d^d k_1 \left[k_1 \cdot k_1 - k_1 \cdot k_1\right] P^{\nu_1+1}_{k_1,m_1} = I^{(d)}_{\nu_1} + m_1^2 I^{(d)}_{\nu_1+1} - \frac{d}{2} I^{(d+2)}_{\nu_1+1} = 0 , \tag{2.56}$$

where we made use of Eq. (2.51).

As we will see in Chapter 3, the usage of generalized recurrence relations is an essential building block of the work described in this thesis.

2.6 Solving the System of Identities: The Laporta Algorithm

So far we only discussed the identities relating Feynman integrals among each other. However, without knowing a definite prescription which of the identities should be used for a reduction of a given Feynman integral, they are useless at this point. That is, in a sense, contrary to the experience we have gained from the 1-loop massive tadpole in Eq. (2.15). In general, a simple recurrence relations as in Eq. (2.17) is more exception than the rule. In order to discuss this issue more in detail, we start introducing some useful notation first.

2.6.1 Propagators, Sectors and Integrals

Let us recall the Eqs. (2.1) and (2.11). Once the propagators are specified, any Feynman integral can be expressed in terms of powers n_i and masses m_i of the corresponding propagators

$$J(\mathbf{n}) = J(n_1, \ldots, n_M) = \int_{k_1,\ldots,k_{N_k}} \frac{1}{D_1^{n_1} \ldots D_M^{n_M}} , \qquad \mathbf{n} \in \mathbb{Z}^M , \tag{2.57}$$

where we assumed that all irreducible scalar products are expressed by introducing additional inverse propagators. The integrals in Eq. (2.57) are classified in the following sense

- The topology (total number of propagators with positive powers): $t \equiv \sum_{i=1}^{M} \theta(n_i - 1)$,
- The sum of powers of propagators with positive n_i: $r \equiv \sum_{i=1}^{M} n_i \cdot \theta(n_i - 1)$,
- The absolute sum of powers of propagators with negative n_i: $s \equiv \sum_{i=1}^{M} |n_i| \cdot \theta(-n_i)$,

where θ is the Heaviside-function. For practical reasons, we introduce the shortcut $I_{t,r,s}$ to merge a certain class of integrals together

$$I_{t,r,s} \equiv \left\{ J(n_1, \ldots, n_M) \,|\, \text{with } (t, r, s) \text{ according to the definitions above} \right\} . \tag{2.58}$$

We define, in analogy to Refs. [76, 77], an auxiliary topology (or integral family) A_M to be an ordered set of propagators $A_M = \{D_1, \ldots, D_M\}$ constructed to cover all possible scalar products (cf. Eq. (2.4)) $k_i \cdot k_j$ and $k_i \cdot p_j$ as linear combinations of the propagators $D_i \in A_M$. We consider

subsets of A_M with exactly t propagators $D_{j_1}, \ldots, D_{j_t}$ where $\{j_1, \ldots, j_t\} \subset \{1, \ldots, M\}$ resulting in so-called sectors T_t each associated with an unique identification number

$$ID = \sum_{k=1}^{t} 2^{j_k - 1} \,. \tag{2.59}$$

The total number of t-propagator sectors T_t is given by the binomial coefficient $\binom{M}{t}$ and therefore we can construct

$$\sum_{t=0}^{M} \binom{M}{t} = 2^M \,, \tag{2.60}$$

sectors out of the auxiliary topology A_M. We can consider subsectors T_{t-1} of the sector T_t by removing one of the t propagators of T_t and, in general, there are t different subsectors of T_t. The sectors T_t representing actual Feynman integrals are called topologies. A tree (or subsector tree) of T_t is the set of all subsectors of T_t and subsectors thereof in a recursive manner. The subsector tree of A_M contains all sectors and is called main sector. The total number of integrals in a given t propagator sector T_t of the auxiliary topology A_M for fixed r, s can be derived from simple combinatorics and reads

$$\mathcal{N}(I_{t,r,s}) = \underbrace{\binom{r-1}{t-1}}_{\text{\# Positive Powers}} \cdot \underbrace{\binom{s+M-t-1}{M-t-1}}_{\text{\# Negative Powers}} , \tag{2.61}$$

with $\binom{-1}{-1} = 1$. For a given sector T_t the integral with $r = t$ and $s = 0$ is called corner integral of that sector. Any topology has a certain number of necessary propagators in order to write the corresponding integrals in the form of Eq. (2.57). If one starts from the most complicated topology (let us say for the moment the one with the largest number of different propagators $t = t_{max}$) and uses this set of propagators as the auxiliary topology, all topologies are consequently expressible as subsectors of this auxiliary topology. On the other hand, in cases where more than one most complicated topology exists, we need to introduce additional so-called auxiliary propagators $t_{max} \leq M$ to express those topologies and its physical subsectors within the auxiliary topology.

In addition, there is always some freedom in choosing the momenta flowing in the propagators. This and the choice of introducing additional auxiliary propagators can be used to maximize the number of symmetry relations (cf. Sec. 2.6.2) in a given auxiliary topology. That is important, because, at first glance, different subsectors turn out to describe the same topology and one wants to reduce these equivalences as much as possible right from the beginning. In the end it depends on the actual problem whether it is more advantageous to use more than one auxiliary topology, each more symmetric, or stick to a single auxiliary topology which is presumably less symmetric. In this work we will always consider a single auxiliary topology.

As an example, let us consider the 2-loop massive tadpole. We define the following auxiliary topology

$$A_3 = \left\{ k_1^2 + m^2, k_2^2 + m^2, (k_1 - k_2)^2 + m^2 \right\} , \tag{2.62}$$

where we have a maximal number of three different propagators. From the auxiliary topology in Eq. (2.62) we immediately get the representation for any 2-loop massive tadpole in terms of powers of its propagators

$$J(n_1, n_2, n_3) = \int_{k_1,k_2} \frac{1}{(k_1^2 + m^2)^{n_1}} \frac{1}{(k_2^2 + m^2)^{n_2}} \frac{1}{((k_1 - k_2)^2 + m^2)^{n_3}} \,. \tag{2.63}$$

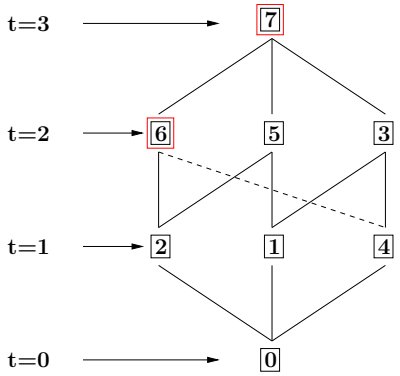

Figure 2.1: The subsector tree of auxiliary topology A_3 displaying all possible subsectors and its identification numbers. Also unphysical subsectors with $t = 1, 0$ are shown. These subsectors are consisting of integrals which are identically zero in dimensional regularization. The subsectors indicated in red represents our choice of the two physical subsectors or topologies diagramed in Eq. (2.64). The subsectors 3 and 5 can be shifted to subsector 6 employing the linear shift relations discussed in Section 2.6.2.

At 2-loop we have only two different non-vanishing topologies[2], namely

$$\begin{aligned} I(1,1,1) &= \quad _{3,7}\,, \\ I(1,1,0) &= \quad _{2,6}\,, \end{aligned} \tag{2.64}$$

where the function arguments 1 or 0 on the left-hand side are indicating a positive or negative/zero power of the corresponding propagator (ordering relative to auxiliary topology), respectively. This binary representation turns out to be quite useful and will be encountered in the following work intensively. Furthermore, the first subscript on the right-hand side in Eq. (2.64) stands for the number of positive lines (number of different propagators with positive power: t) and the second is, according to Eq. (2.59), the binary representation translated into the decimal number system

$$\begin{aligned} I(1,1,1) &\longrightarrow ID = 1 \cdot 2^2 + 1 \cdot 2^1 + 1 \cdot 2^0 = 7\,, \\ I(1,1,0) &\longrightarrow ID = 1 \cdot 2^2 + 1 \cdot 2^1 + 0 \cdot 2^0 = 6\,. \end{aligned} \tag{2.65}$$

In Figure 2.1 we have summarized all subsectors of auxiliary topology A_3. Starting from a certain sector and going downwards corresponds to shrinking lines or removing propagators in the associated Feynman diagrams or integrals as illustrated in Figure 2.2.

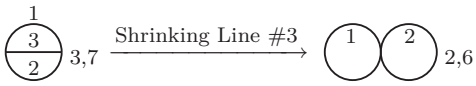

Figure 2.2: Shrinking of lines corresponds to removing propagators from the subset T_3 of the auxiliary topology A_3.

On top of this, we classify the 2^M sectors from Eq. (2.59) in the following categories. Let T_t be a t-propagator sector with identification number ID. The sector T_t

1. is called physical sector (or topology) if one can draw a graph with the specified momenta.

[2]All graphs shown in this work are drawn using the Axodraw package [78].

2. is called trivial zero if the number of propagators t is less then N_k. In dimensional regularization that sector is identically zero.

3. is called nontrivial zero if the number of propagators t is larger or equal N_k but turns out to vanish after a suitable momentum shift is performed (see Section 2.6.2).

4. is called trivial antisector if the number of positive propagators t is larger than t_{max}.

5. is called nontrivial antisector if the number of positive propagators t is smaller or equal t_{max} but not possible to draw a graph with the specified momenta.

We have already encountered the first two cases in the 2-loop example given above. According to Figure 2.1, sectors $7, 6, 5$ and 3 are physical sectors whereas $4, 2$ and 1 are trivial zeros. The cases $3, 4$ and 5 are not present in the 1- and 2-loop example. Those categories are discussed in Chapter 3.

2.6.2 Linear Shifting of Internal Momenta: Sector Relations and Symmetries

In the previous section we have encountered the fact that, at first glance, different sectors turn out to describe the same topology. One of the questions we would like to answer in this section is how can we find out whether sectors are equivalent or not. For this purpose we consider linear transformations of integration variables of the form

$$k_i \longrightarrow \sum_{j=1}^{N_k} M_{ij} k_j + \sum_{j=1}^{N_e} N_{ij} p_j \,, \qquad i = 1, \ldots, N_k \,, \tag{2.66}$$

where $i = 1, \ldots, N_k$ and $|\det M| = 1$. Let T_t and T_t' be t-propagator sectors ($T_t \neq T_t'$) of auxiliary topology A_M. The transformation in Eq. (2.66) applied to the corner integral of sector T_t leads, in general, to the following situations:

1. Each of the M independent propagators of auxiliary topology A_M is mapped to a propagator belonging to auxiliary A_M.

2. The propagators of sector T_t are mapped to propagators of auxiliary topology A_M, but the remaining $M - t$ propagators are not all or none part of auxiliary topology A_M.

3. The propagators $D_1, \ldots, D_{j_t}$ of sector T_t are mapped to the same set of propagators whereas the remaining $M - t$ propagators are, as in 2. , not all or none part of auxiliary topology A_M.

Having this in mind we can define a sector relation of sectors T_t and T_t' as the transformation (case 1. and 2.) that maps the set of propagators of T_t into the set of T_t'. If two sectors are related by a sector relation they are considered to be equivalent and consequently one sector can be excluded from reduction. In general, there are $\binom{M}{t}$ t-propagator sectors and the ones we are left with after finding all sector relations among them are called representatives of the corresponding topologies, see Figure 2.3. In case of auxiliary topology A_3, we have chosen the sector with identification number 6, cf. Figure 2.1, to be the representative of all sectors T_t with $t = 2$ as we can immediately see from Eq. (2.64) by shifting the integration variable k_1

$$\begin{aligned} I(0,1,1) &\xrightarrow[k_1 \to k_1 + k_2]{} I(1,1,0) \,, \\ I(1,0,1) &\xrightarrow[k_2 \to k_1 + k_2]{} I(1,1,0) \,. \end{aligned} \tag{2.67}$$

In case we have a sector relation of type 1, any integral of sector T_t can be expressed in terms of exactly one integral of sector T'_t. Let us further assume a sector relation, for two given sectors T_t and T'_t, turns out to be only available as in case 2, we find that any integral of T_t can be written as a linear combination of integrals of T'_t and its subsectors. Usually there is some freedom in choosing sector relations between sectors and it is preferable, if possible, to chose sector relations of type 1. So far we have only considered transformations leading to the first two situations. However,

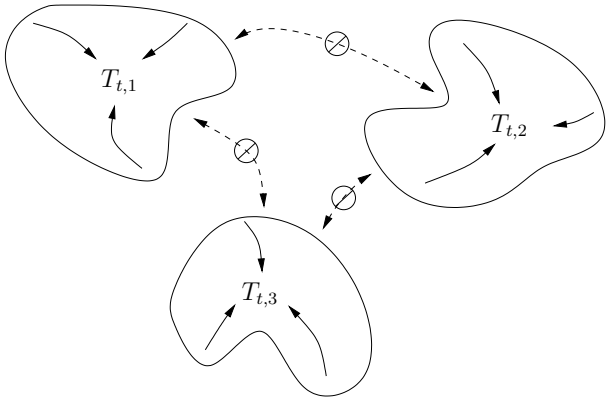

Figure 2.3: We consider the set of all t-propagator sectors of a given auxiliary topology A_M. Let us assume that there are three representatives $T_{t,1}$, $T_{t,2}$ and $T_{t,3}$. Each representative is surrounded with equivalent sectors which are related to the representative by a sector relation indicated with a solid arrow (subsectors are not considered). Sectors from different sets are not related among each other which is indicated by a crossed dashed arrow.

linear transformations as in Eq. (2.66) can be used to derive additional identities, the so-called sectors symmetries. Sector symmetries are generated by particular linear transformations leaving a given t-propagator sector T_t invariant (case 3.). Also transformations of type 1, restricted to those where all t propagators of T_t are mapped to itself, lead to sector symmetries. In the latter case a given integral is expressed in terms of itself only differing by permutations of its propagator powers, whereas in case 3, integrals of T_t are written as linear combinations of integrals in T_t and subsectors thereof. For example let us consider the 2-loop massive tadpole from Eq. (2.63) again

$$\begin{aligned} &\text{case 1}: J(n_1,n_2,n_3) = J(n_2,n_1,n_3) = J(n_3,n_2,n_1) = J(n_1,n_3,n_2)\,, \qquad n_i \text{ arbitrary}\,, \\ &\text{case 3}: J(n_1,n_2,n_3) = J(n_1,n_2,0) \times \left[2D_1 + 2D_2 - D_3 - 2m^2\right]^{-n_3}\,, \qquad n_3 \leq 0\,, \end{aligned} \tag{2.68}$$

where the latter equation ($k_2 \to -k_2$) is rewritten in terms of functions $J(n_1,n_2,n_3)$ after expanding the right-hand side for a given n_3. The methods to find appropriate sector relations and symmetries range from straightforward (brute-force) approaches to more elegant ones using graph and matroid theory. For more details and practical implementations on the latter approach we refer to [71, 77] and references therein.

In conclusion, sector relations are used to reduce equivalences and to determine the number of physical sectors to be reduced. Sector symmetries are usually combined with IBP relations to reduce a given sector more efficiently as well as to minimize the number of master integrals one is left with.

2.6.3 Different Point of View: Identities among Feynman Integrals in *r*-*s* Space

We resume the discussion postponed in Section 2.2. As already mentioned, in general, the system of identities we obtain for a given problem is not easy to solve. The simple recurrence relation for

the 1-loop massive tadpole in Eq. (2.17) was an exceptional case. Starting from the integral class $I_{t,r,s}$, the integration-by-parts identities contain integrals[3] of the following types:

1. $I_{t,r,s}$: The integral initially started with.

2. $I_{t,r+1,s}, I_{t,r+1,s+1}$: Integrals with one propagator raised $(r+1)$ or propagator and inverse propagator raised $(r+1, s+1)$.

3. $I_{t,r,s-1}, I_{t,r-1,s-1}$: Integrals with one inverse propagator lowered $(s-1)$ or propagator and inverse propagator lowered $(r-1, s-1)$.

4. $I_{t-1,r+1,s}, I_{t-1,r,s-1}$: Integrals belonging to the class of integrals with $t-1$ different propagators and one raised propagator $(r+1)$ or lowered inverse propagator $(s-1)$, respectively.

The integrals in 2. can be considered to be more difficult, whereas the integrals in 3. and 4. are simpler than the initial integral $I_{t,r,s}$. At this point, we are not introducing a prescription to categorize different integrals according to their complexity. However, such an ordering will be discussed in Section 2.6.4. Here we only want to illustrate which integral class is more complicated than others and vice versa.

By considering only single IBP relations we are, in general, not able to deduce simple recursion relations such as in Eq. (2.17). Integration-by-parts relations applied to the class of integrals $I_{t,r,s}$

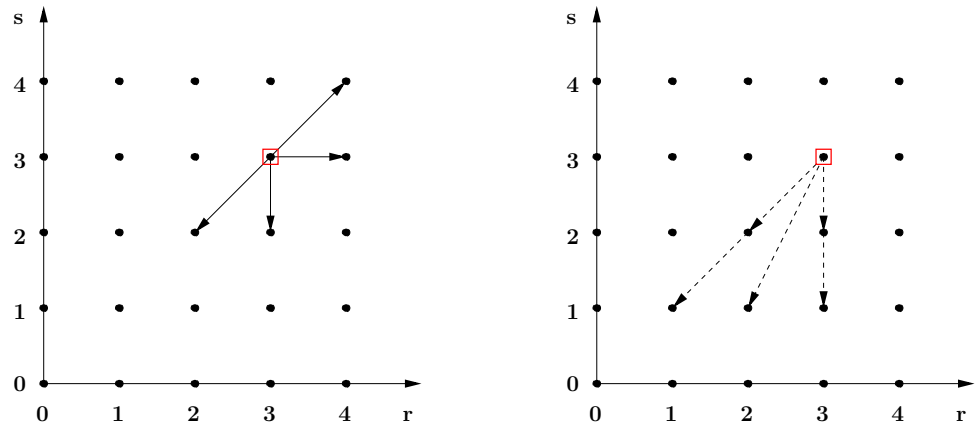

(a) Integration-by-parts relates integrals always in the same way.

(b) A sector symmetry relates integrals to those with smaller values of (r, s).

Figure 2.4: The integration-by-parts identities (a) and sector symmetries (b) applied to the set of integrals $I_{t,r,s}$ with $(r, s) = (3, 3)$ shown in the (r, s)-plane. The solid arrows in (a) pointing away from the point $(3, 3)$ are indicating all possible (r, s)-values for integrals which might be present in the identities. On the other hand, the (r, s) values of integrals related by sector symmetries do depend on the specific sector symmetry considered as well as the value s the symmetry is applied to. This behavior is indicated by using dashed arrows (b) and can be easily seen from Eq. (2.68).

can be used to reduce $I_{t,r+1,s}$ or $I_{t,r+1,s+1}$ in terms of $I_{t,r,s}$ and simpler ones but not to get suitable information about $I_{t,r,s}$ itself. There are in principle two different approaches. First, one can try to derive explicit reduction formulae (not fixed to some integer) by studying carefully the IBP relations for a given integral with arbitrary powers, or second, choosing some fixed integer values for $(n_1, \ldots, n_M)$ and generate all possible IBP relations and combine them with some deterministic

[3]By saying integrals we always referring to the integral class.

procedure to reduce integrals with large (r, s) in terms of simpler ones with small (r, s). The former approach is, at first glance, more desirable but demands a case-by-case analysis of every topology, see e. g. [79, 80]. On the other hand, the latter approach can be carried out almost automatically which is, in particular, interesting in cases with a large number of topologies. Since we are working in that regime the latter one is our method of choice.

In Figure 2.4 it is shown how the IBP identities are relating different integrals in the (r, s)-plane for some certain starting point. Each point in the (r, s)-plot generates $\mathcal{N}_{\text{IBP}} \cdot \mathcal{N}(I_{t,r,s})$ new relations with $\mathcal{N}_{\text{IBP}}$ denoting the number of IBP identities and $\mathcal{N}(I_{t,r,s})$ the total number of integrals belonging to the set $I_{t,r,s}$ as defined in Eq. (2.61). For increasing values r and s the number of new relations grows as the volume of $\mathbb{Z}^M$ times the number of IBP relations $\mathcal{N}_{\text{IBP}}$ in each point $(n_1, \ldots, n_M) \in \mathbb{Z}^M$, while the number of unknowns (integrals) only grows as the volume of $\mathbb{Z}^M$. At some point, we accumulate more relations than having unknowns and the system gets overdetermined. In fact, the set of equations obtained by generating all possible IBP relations with values $r \in [r_{min}, r_{max}]$ and $s \in [s_{min}, s_{max}]$ is not linearly independent and it is not known how many integrals will be undetermined after reduction. The integrals we are left with are called master integrals. They form a basis in such a way that all other integrals are expressible in terms of these master integrals. A more detailed discussion on this issue will follow in Section 2.6.4.

In the limit of large values r and s only one identity out of $\mathcal{N}_{\text{IBP}}$ identities produces a relation which gives new information. We have already started to tackle this problem by reducing the number of identities in each point using the Lie algebra structure of the IBP operator in Eq. (2.13). However, further investigation of this problem is necessary to minimize the number of linearly dependent relations right from the beginning. This will result in considerably less computing time for checking whether relations are linearly dependent or not as we will see later on.

2.6.4 The Laporta Algorithm and an Unique Ordering of Feynman integrals

This Section is devoted to the question how to combine the relations above in a systematic way to reduce a given Feynman integral in terms of simpler ones. To do so, we first introduce an unique ordering [18] which, in our context, classifies integrals according to their complexity. This is followed by an algorithm, known as as the Laporta algorithm [18], able to solve a given system of equations build out of identities such as the IBP relations or generalized recurrence relations discussed in Section 2.2 and 2.5, respectively.

Before Laporta's algorithm with the idea of an unique ordering of Feynman integrals was known, the finding of recurrence relations was merely guess work with respect to the constants in Eq. (2.44), see e. g. [81]. The approach allows to tackle more complicated problems with a larger numbers of loops and/or external legs which would otherwise not be possible. Moreover, the method does not depend on the specific problem and allows almost automatic calculations for all inherent topologies.

Let us assume that all identities are generated according to Eqs. (2.7) or Eqs. (2.36),(2.54) up to a certain level. We pick one identity which has, in general, the form

$$\sum_j c_j J_j = 0\,, \tag{2.69}$$

where J_j are integrals as functions of its powers[4] of propagators $(n_1, \ldots, n_M) \in \mathbb{Z}^M$ and c_j are polynomials in space-time dimensions d, masses m_i and, depending on the specific problem, other scales as coefficients. We choose one particular integral J_l out of the set $\{J_j\}$ according to a unique prescription classifying the integrals with respect to their complexity. The next step is to rewrite

[4] In case of generalized recurrence relations they also depend on the dimension shift caused by the $\mathbf{d}^+$ operator in Eq. (2.41).

the identity in Eq. (2.69) as

$$J_l = -\sum_{j \neq l} c'_j J_j \,, \qquad c'_j = \frac{c_j}{c_l} \,. \tag{2.70}$$

where the most complicated integral J_l is expressed in terms of simpler ones (according to the ordering we have chosen). It should be pointed out that each rewriting of identities as in Eq. (2.70) demands the computation of new coefficients c'_j involving time consuming polynomial algebra. From here we pick the next identity of the form of Eq. (2.69) and substitute Eq. (2.70) in that identity which immediately becomes

$$\sum_j c''_j J'_j = 0 \,, \tag{2.71}$$

and again after choosing the most complicated one, let us say J'_l out of the set $\{J'_j\}$, we have

$$J'_l = -\sum_{j \neq l} c'''_j J'_j \,, \qquad c'''_j = \frac{c''_j}{c''_l} \,. \tag{2.72}$$

It is guaranteed that $J'_l \neq J_l$ because J_l was not present in Eq. (2.71) either due to the substitution, or due to absence right from the beginning. Then we substitute the identity of Eq. (2.72) in Eq. (2.70). This procedure is now in turn applied to the next identity and can be summarized:

1. Let $\sum_j c_j J_j = 0$ be a new identity. Substitute already existing identities such as Eq.(2.72) in that identity, it becomes $\sum_j c'_j J'_j = 0$.

2. Choose one particular integral (according to the unique ordering) out of the identity from step 1. an rewrite that identity as $J'_l = -\sum_{j \neq l} c''_j J'_j$.

3. Add the identity from step 2. to the system and substitute this identity in all existing identities of the system.

After all identities have been processed, the system contains identities relating more difficult integrals in terms of simpler ones. Most of these integrals are expressed through a few master integrals. The set of master integral we are left with depends strongly on the choice of the ordering. More details on the unique ordering will follow below after a few addition remarks.

So far we only discussed the basic concept of the algorithm. A simple implementation can be deduced from Figure A.3 in Appendix A.1. However, some improvements should be mentioned at this point. The order of processing the identities turns out to significantly affect the computing time and needs to be optimized. This is because each new identity added to the system in step 3. can cause a large number of substitutions if the integral occurs in many of the already existing identities.

A rather good choice to minimize those substitutions is to start with the simplest possible integrals, i. e. those with the smallest (r, s) values, and increase successively the values of (r, s) which is, in fact, inverse to the order we are extracting integrals in step 2.. The order of processing the identities does not change the final solution of the system but can blow up the compution time if badly chosen. We have sketched the inverse processing of identities in Figure 2.5.

On top of this, it is quite useful to divide the system of identities into subsystems of the different physical sectors T_t (topologies). More precisely, the subsystems are built of identities originating from integrals

$$I_{t,r,s} \,, \qquad r \in [r_{min}, r_{max}] \quad \text{and} \quad s \in [s_{min}, s_{max}] \,, \tag{2.73}$$

with a certain combination of denominators $D_{j_1}, \ldots, D_{j_t}$ specified by the unique identification number in Eq. (2.59). As we have already seen in Section 2.6.3, those equations can not only

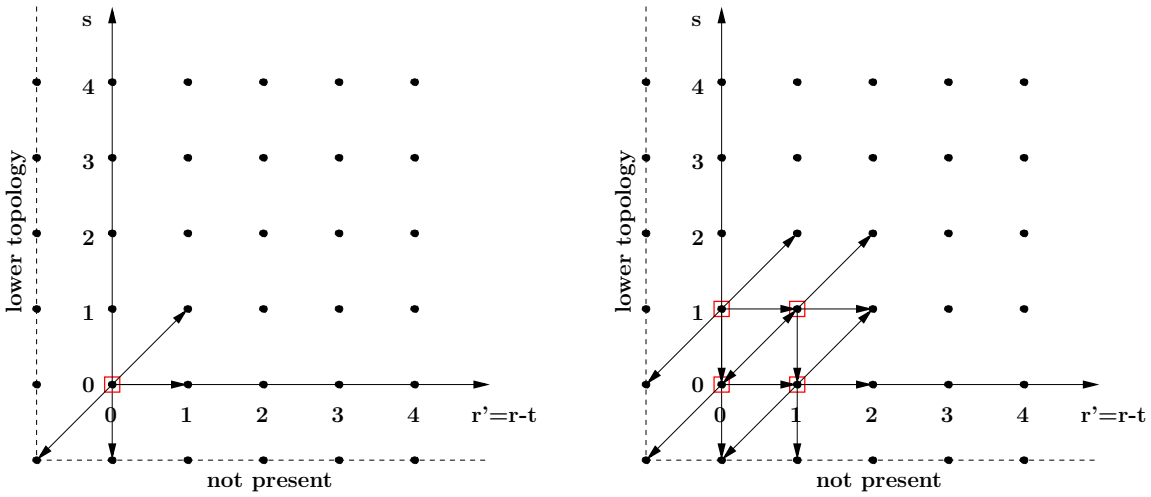

(a) The first identities generated and processed are those with $(r', s) = (0, 0)$.

(b) Followed by identities with $(r', s) = (0, 1), (1, 0)$ and $(1, 1)$.

Figure 2.5: The inverse ordering of identities processed in the Laporta algorithm shown in the (r', s)-plane with $r', s \in [0, 1]$. The r'-axis is associated with the original r shifted by $-t$ such that $r' = 0$ corresponds to integrals with all propagators having powers equal to one. In this context, a value $r' < 0$ would correspond to at least one propagator power being zero or negative and consequently represent a topology with a smaller number of different propagators t. In addition, starting from an integral with $(r', s = 0)$, the IBP identity does not contain integrals (not present) with negative powers of propagators.

contain t-propagator integrals but also those with $t - 1$ different ones. A reduction of sectors T_t would result in equations depending on many unreduced integrals of its subsectors. These integrals are again part of independent reductions in the corresponding subsystems. To this end, the reduction of any given sector T_t always starts with reducing the relevant subsectors with the smallest number of different propagators t'. The solutions are inserted in all physical sectors with $t' + 1$ propagators and are again reduced. This procedure will be continued until the reduction has reached the initial sector T_t. It can happen that the most complicated integral in Eq. (2.70) turns out to belong to a subsector of $T_{t'}$. Relations of that kind are not added to the system of equations of sector $T_{t'}$ because we do not want to blow up the system with relations that are already available in the corresponding subsystems.

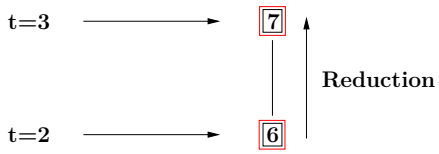

Figure 2.6: The subsector tree of physical subsectors of auxiliary topology A_3. The arrow pointing vertically indicates the order of reduction.

For example, in the case of the 2-loop massive tadpole we have exactly two subsystems associated to the two nontrivial topologies, cf. Figure 2.6, with identification numbers 7 and 6. If topology 7 needs to be reduced we first start reducing topology 6 and insert the solutions in subsystem 7 before the reduction is started.

All in all, starting a reduction from the bottom of a subsector tree one avoids lengthy expressions

and speeds up the reduction considerably. This is because intermediate integrals of subsectors with rather large powers of propagators do not occur since they are immediately replaced by an appropriate reduction to master integrals.

Let us now focus on the unique ordering of Feynman integrals we have mentioned before. As we already know, the ordering[5] must be unique in order to identify exactly one integral and designed to pick the most complicated (cf. Sec. 2.6.3) out of a set of integrals. For this purpose we assume to have an ordered set of propagators defined in an appropriate auxiliary topology $A_M = \{D_1, \ldots, D_M\}$ with powers $\mathbf{n} = (n_1, \ldots, n_M) \in \mathbb{Z}^M$. Considering a set of integrals $\{J_1, \ldots, J_n\}$ we have chosen the following order of priority for extracting integrals. Take the integral with

1. largest number of different propagators t. If more than one integral has the same value t proceed with 2..

2. largest $r + s$. If more than one integral has the same value $r + s$ proceed with 3..

3. largest number of negative propagators. If more than one integral has the same number of negative propagators proceed with 4..

4. greatest power n_M. If more than one integral has the same power n_M proceed with the greatest power $n_{M-1}, \ldots$, the greatest n_1.

The rules we have specified here can be basically divided into two categories. Rules 1, 2 and 3 are classifying the integrals according to their complexity and rule 4 guarantees uniqueness by means of an arbitrary choice. In Table 2.1 we have shown how the ordering is used to determine the most

Rule	$J(1,1,1)$	$J(2,1,0)$	$J(1,1,-1)$	$J(1,2,1)$	$J(2,1,1)$
1	3	2	2	3	3
2	3	3	3	4	4
3	0	0	1	0	0
4	-	-	-	$n_2\surd$	n_1

Table 2.1: Using our choice of an unique ordering to determine the most complicated integral out of a set of five integrals. The integrals $J(n_1, n_2, n_3)$ are 2-loop massive tadpoles as defined in Eq. (2.63). We have indicated which integral would be chosen to be the most complicated one.

complicated integral out of a set of 2-loop massive tadpoles, see the example of Section 2.6.1.

The ordering introduced above tends to express integrals with powers of propagators randomly distributed in terms of those where the powers of propagators are shifted towards some very few propagators. Propagators with negative powers (irreducible scalar products) are usually disappearing in exchange for higher powers on the initial t positive propagators.

For more details on integration-by-parts, reduction algorithms and related topics we refer to e. g. [82].

[5]It should be noted that the term 'lexicographic ordering' is commonly used in the corresponding literature, see e. g. [18]. This might be misleading because, strictly speaking, the prescription given there and referred to as 'lexicographic ordering' is nothing but an unique ordering.

2.7 Generalized Recurrence Relations: The Advantages and Consequences

The usage of generalized recurrence relations has a tremendous benefit in the reduction problem of Feynman integrals. The first thing to tackle a reduction problem is to find an appropriate auxiliary topology A_M such that all topologies are covered. Usually A_M contains more propagators than the most complicated topology (largest number of different propagators) we are faced with. This is because additional auxiliary propagators are introduced to cover all, if more than one, complicated topology is present. In other words, the space of powers of propagators $\mathbf{n} \in \mathbb{Z}^M$ in which we are considering the topologies is bigger than it should be.

On the other hand, a reduction only in terms of integration-by-parts identities works, but turns out to be very slow without sector symmetries. Using sector symmetries leads, in general, to a smaller set of master integrals and speeds up the reduction considerably due to the symmetrization of lengthy intermediate expressions. However, the number of sector symmetries increases with M and depends strongly on the symmetry properties of each topology. At higher loop order we observe numbers of sector symmetries, typically a few thousand for some certain sectors, making it difficult to perform a reduction simply by combining IBP identities and sector symmetries. For a given sector only very few sector symmetries produce new relations and it is a priori not clear which one. Since we are interested in a mechanical approach a carefully chosen set of sector symmetries for each sector is not an option.

We have decided to address this issue in a different way by using the generalized recurrence relations introduced in Section 2.5. By doing so, we effectively reduce the number of indices for a given t-propagator sector T_t from M to $t+1$ indices which is, in particular, advantageous for sectors with rather small t.

For this purpose, let us recall some basic facts from Section 2.4. The T operator in Eq. (2.43) can be used to get rid of the $M-t$ inverse propagators (or irreducible scalar products) in exchange for an additional index specifying the deviation from physical space-time dimensions d as well as higher powers for the remaining t propagators. In analogy to Eq. (2.57) we define

$$J'(\mathbf{n}) = J'(n_0, n_1, \ldots, n_M) = \int_{k_1,\ldots,k_{N_k}}^{(d')} \frac{1}{D_1^{n_1} \ldots D_M^{n_M}}\,, \qquad \mathbf{n} \in \mathbb{Z}^{M+1}\,, \tag{2.74}$$

with integration measure

$$\int_{k_1,\ldots,k_{N_k}}^{(d')} = \int \frac{d^{d'}k_1 \ldots d^{d'}k_n}{(\pi^{d'/2})^{N_k}}\,, \tag{2.75}$$

where $d' = d - 2n_0$ and $n_0 \leq 0$. In the case of $n_0 = 0$ we recover the integral $J(\mathbf{n})$ in Eq. (2.57) immediately

$$J(n_1, \ldots, n_M) = J'(n_0 = 0, n_1, \ldots, n_M)\,. \tag{2.76}$$

Let us again consider the 1-loop massive tadpole and rewrite the generalized recurrence relations in Eqs. (2.48) and (2.56) using the notation of Eq. (2.74)

$$\begin{aligned} 0 &= J'(n_0, n_1 - 1) + m_1^2 J'(n_0, n_1) - \left[\frac{d}{2} - n_0\right] J'(n_0 - 1, n_1)\,, \\ 0 &= J'(n_0, n_1) + n_1 J'(n_0 - 1, n_1 + 1)\,. \end{aligned} \tag{2.77}$$

Starting from the definition of T in Eq. (2.43), one can estimate that for each scalar product the values of r and d' are increasing as

$$s \to s - 1: \qquad r \to r + N_k - 1 \;\text{ and }\; d' \to d' + 2\,. \tag{2.78}$$

This behavior looks, at first glance, quite disappointing because for each scalar product less ($s \to s-1$) we are forced to consider integrals with $r \to r' = r + N_k - 1$ and it becomes worse as we go to higher loops. Nevertheless, the method turns out to be quite powerful for a reduction and especially for the problem of finding difference equations for master integrals as we will see in Section 3.4.1. In the same way as we merged certain integrals together in Eq. (2.58) we introduce

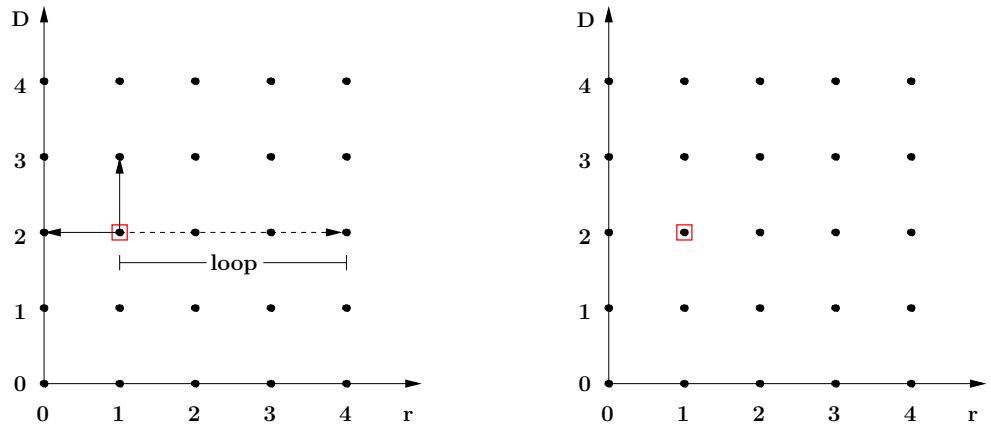

(a) Generalized recurrence relation applied to $(1, 2)$.

(b) Sector symmetries for $s = 0$ permutates powers of propagators.

Figure 2.7: The generalized recurrence relations (a) and sector symmetries (b) applied to the set of integrals with $(r, D) = (1, 2)$ shown in the (r, D)-plane. Solid lines show the values (r, D) of integrals present in the relations. In addition, also integrals with up to $r \to r + N_k$ will be part of the relation. The dependence on the number of loops N_k is indicated by the dashed arrow pointing to the right. A Sector symmetry for $s = 0$ does not change the values of r and D, it only permutates the powers of propagators.

a similar quantity here, namely

$$I_{t,r,D} \equiv \left\{ J'(n_0, n_1, \ldots, n_M) \,|\, \text{with } (t, r, s = 0) \text{ as usual and } n_0 = -D \right\}. \tag{2.79}$$

Assuming a t-propagator sector T_t specifying a set $\{j_1, \ldots, j_t\} \subset \{1, \ldots, M\}$ of propagators $D_{j_1}, \ldots, D_{j_t}$, the total number of integrals for fixed (r, D) is then given by

$$\mathcal{N}(I_{t,r,D}) = \binom{r-1}{t-1}. \tag{2.80}$$

This follows from Eq. (2.61) by omitting the binomial coefficient which takes into account permutations of inverse propagators. Since we got rid of the $M - t$ inverse propagators, also the number of sector symmetries for a given sector T_t is smaller and consequently it is not longer a serious problem to combine them with the generalized recurrence relations. To get an impression on how the numbers of sector symmetries reduces we have summarized the numbers for fully massive tadpoles in Tables A.3 and A.4 in Appendix A.1. We point out, it is not primarily the reduced number of sector symmetries which allows us to take them all into account rather the simplified structure of the remaining sector symmetries.

Figure 2.7 shows the generalized recurrence relations and sector symmetries in the (r, D)-space. The pattern shown in Figure 2.7a is directly related to the fact that only a single scalar product is replaced in Eq. (2.54) to obtain generalized recurrence relations. In contrast to the IBP identities in Figure 2.4, we can end up having relations containing integrals with nonvanishing s although we initially started with integrals belonging to the integral class $I_{t,r,D}$. Relations of that kind are

not added to the system of equations in the Laporta algorithm (see Section 2.6.4) and therefore, by construction, integrals with $s \neq 0$ will never show up.

At this point, a few words regarding sector symmetries should be mentioned. Since all powers of inverse propagators are zero ($s = 0$), the sector symmetries from Section 2.6.2 simplify to permutations of powers of the remaining t propagators. There are a lot of redundant sector symmetries because different linear transformations in Eq. (2.66) are leading to the same permutation of propagator powers $n_{j_1}, \ldots, n_{j_t}$ but different realizations of the remaining $M - t$ propagators.

For instance, let us consider the 2-loop massive tadpole with shifts $k_2 \to \pm k_2$, where $(+)$ is nothing but the identity and for $(-)$ we get

$$J'(n_0, n_1, n_2, n_3) = J'(n_0, n_1, n_2, 0) \times \left[2D_1 + 2D_2 - D_3 - 2m^2\right]^{-n_3} , \tag{2.81}$$

which is exactly the same in case $n_3 = 0$. In other words, different transformations are leading to different sector symmetries but coincide in the case of $s = 0$. We remove the redundant sector symmetries and use the rest for the symmetrization of intermediate integrals. More details on this issue will follow in the Chapter 3.

As mentioned above, an additional index is introduced to specify the dimension of the integral under consideration. We need to extend the ordering discussed in Section 2.6.4 for integrals in different dimensions. Since the physical dimension corresponds to $n_0 = 0$ and integrals with values of n_0 differing from zero are primarily introduced to rewrite the scalar products, the rule should be to extract integrals with smaller n_0 first and then those with $0 \geq n_0' > n_0$. We decided to give the ordering in dimension highest priority and place it even before the number of positive propagators t is compared:

0. Order the integrals with respect to their value n_0, with smaller values corresponding to a higher priority. In case of degenerate integrals with the same value n_0 proceed with 1. ,

followed by the rules given in Section 2.6.4. This ordering leads, in general, to relations expressing integrals in higher dimensions in terms of those with physical dimensions ($n_0 = 0$).

3 Massive Tadpoles up to the 5-loop Level: Reduction, Master Integrals and Difference Equations

The following chapter is devoted to a detailed description of fully massive tadpoles up to the 5-loop level. We have already encountered the 1- and 2-loop case in the previous chapter. From time to time the concepts were demonstrated on the basis of the 1- and 2-loop vacuum integrals (tadpoles). All concepts introduced so far are necessary to understand the following discussion.

The plan of this chapter is as follows. In Section 3.1, we define the class of tadpoles by specifying appropriate auxiliary topologies followed by introducing a convenient notation. In Section 3.2, we prepare the reduction by specifying all physical subsectors (topologies) and their representatives as well as necessary sector relations and symmetries. In Section 3.3.1 we give a review of the most frequently used computer algebra systems in particle physics and already existing implementations of reduction algorithms. In Section 3.3.2, we discuss the actual implementation of our approach in the algebraic manipulator `FORM` [19, 20, 21] which is used to perform the reduction to master integrals. On top of this, we adapt the algorithm to derive difference equations for the remaining master integrals in Section 3.3.3. The reduction to master integrals is discussed in Section 3.4. Finally, in Section 3.4.1 we present the difference equations we obtained. In addition to this, we discuss a basis transformation in order to guarantee that all master integrals are covered by the difference equations we derived.

3.1 Notations and Momenta Conventions

We consider the special class of fully massive tadpoles where all propagators have the same mass m. Following the notation outlined in Eq. (2.74) we have

$$J'(\mathbf{n}) = J'(n_0, n_1, \ldots, n_M) = \int_{k_1,\ldots,k_{N_k}}^{(d')} \frac{1}{D_1^{n_1} \ldots D_M^{n_M}}\,, \qquad \mathbf{n} \in \mathbb{Z}^{M+1}\,, \tag{3.1}$$

with propagators $D_i = q_i^2 + m^2$ to the power n_i. From now on, if not otherwise indicated, we use Euclidean space-time metric throughout the whole chapter. Since all propagators have the same mass m, we consider a more convenient representations of Eq. (3.1) by rescaling the integration momenta $k_i \to m k_i$. We obtain

$$J'(\mathbf{n}) = J'(n_0, n_1, \ldots, n_M) = \frac{(m^2)^{d' N_k/2}}{(m^2)^{n_1+\cdots+n_M}} \int_{k_1,\ldots,k_{N_k}}^{(d')} \frac{1}{D_1^{n_1} \ldots D_M^{n_M}}\,, \qquad \mathbf{n} \in \mathbb{Z}^{M+1}\,, \tag{3.2}$$

with propagators $D_i = q_i^2 + 1$ having mass squared $m^2 = 1$. The factor in front of the integral, carrying the mass dependence, is neglected. In the end the prefactor can be reconstructed simply by counting the dimension of each integral. This is advantageous because in a reduction such as in the Laporta approach (see Section 2.6.4, Eq. (2.70)) we are forced to compute quotients of multivariate polynomials which, in fact, turns out to consume most of the computing time. Therefore, from the computational point of view, it is always a benefit to remove those unnecessary scales right from the beginning.

Let us now focus on the momenta convention to write the tadpoles in the notation of Eq. (3.2). In Table 3.1 we have summarized the auxiliary topologies A_1, A_3, A_6, A_{10} and A_{15} corresponding to the one-, two-, three-, four- and five-loop massive tadpole. There are $N_{sp} = N_k(N_k+1)/2$ scalar products, cf. Eq. (2.4) and Section 2.6.1, and consequently we have an equal number of propagators M in the corresponding auxiliary topologies. The auxiliary topologies A_1, A_3, A_6, A_{10}

Propagator	A_1	A_3	A_6	A_{10}	A_{15}
1	k_1^2	k_1^2	k_1^2	k_1^2	k_1^2
2		k_2^2	k_2^2	k_2^2	k_2^2
3		$(k_1-k_2)^2$	k_3^2	k_3^2	k_3^2
4			$(k_1-k_2)^2$	k_4^2	k_4^2
5			$(k_1-k_3)^2$	$(k_1-k_4)^2$	k_5^2
6			$(k_2-k_3)^2$	$(k_2-k_4)^2$	$(k_1-k_3)^2$
7				$(k_3-k_4)^2$	$(k_1-k_4)^2$
8				$(k_1-k_2)^2$	$(k_1-k_5)^2$
9				$(k_1-k_3)^2$	$(k_2-k_3)^2$
10				$(k_1-k_2-k_3)^2$	$(k_2-k_4)^2$
11					$(k_2-k_5)^2$
12					$(k_3-k_5)^2$
13					$(k_4-k_5)^2$
14					$(k_1+k_2-k_4)^2$
15					$(k_3-k_4)^2$

Table 3.1: The auxiliary topologies A_1, A_3, A_6, A_{10} and A_{15} for fully massive tadpoles up to 5-loop. We have suppressed the mass $m^2 = 1$ in each propagator for legibility. As we already know from Eqs. (2.15) and (2.62), the 1- and 2-loop case have $M = 1$ and $M = 3$, respectively. Going beyond 2-loop we have $M = 6, M = 10$ and at 5-loop $M = 15$.

and A_{15} are ordered sets of $M = 1, 3, 6, 10$ and $M = 15$ propagators. As it turns out, the auxiliary topologies A_1, A_3 and A_6 corresponding to the 1-, 2- and 3-loop case have exactly the same number of propagators as their most complicated topology. At 4- and 5-loop we have more than one most complicated topology and additional auxiliary propagators are introduced to guarantee that all topologies are covered. In general, the most complicated vacuum topology one can build has

$$t_{max} = \begin{cases} 1 & : \quad N_k = 1 \\ 3 \cdot (N_k - 1) & : \quad N_k > 1 \end{cases} \tag{3.3}$$

positive propagators. Figure 3.1 shows some of those topologies at the different loop levels. What kind of, and how many topologies we are exactly faced with will be discussed in Section 3.2. Having

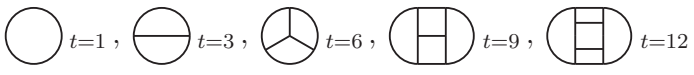

Figure 3.1: Shown are most complicated vacuum topologies at the different loop levels from 1- to 5-loop. By saying most complicated we refer to those topologies with the largest number of propagators with positive powers: t_{max}. Note that not all most complicated topologies (e. g. non-planar ones) are shown.

the auxiliary topologies at hand, we can write down any vacuum integral as a list of its powers of

propagators. So, for instance at 3-loop with auxiliary topology A_6 we have

$$J'(n_0,n_1,n_2,n_3,n_4,n_5,n_6) = \int_{k_1,k_2,k_3}^{(d')} \frac{1}{(k_1^2+1)^{n_1}} \frac{1}{(k_2^2+1)^{n_2}} \frac{1}{(k_2^3+1)^{n_3}} \frac{1}{((k_1-k_2)^2+1)^{n_4}} \times \frac{1}{((k_1-k_3)^2+1)^{n_5}} \frac{1}{((k_2-k_3)^2+1)^{n_6}}\,, \tag{3.4}$$

where the arguments of J' on the left-hand side are, if necessary, written as subscript.

3.2 Topologies, Generalized Recurrence Relations, Sector Relations and Symmetries

We have reviewed the general concept of sector relations and symmetries in Section 2.6.2. Now we adapt the concepts to the vacuum case. In order to prepare the reduction it is necessary to identify the different topologies and choose appropriate representatives. Trivial zeros and antisectors can be, as the name implies, trivially identified and removed from the set of sectors. They are exactly those sectors T_t with $t < N_k$ and $t > t_{max}$. In total there are

$$\sum_{t=0}^{N_k-1} \binom{M}{t} \qquad \text{and} \qquad \sum_{t=t_{max}+1}^{M} \binom{M}{t} \tag{3.5}$$

trivial zeros and antisectors, respectively. Non of those sectors is representing a physical sector.

The next step is to find all linear shift relations (sector relations) among the sectors T_t having the same number of positive propagators t. We end up with sets of sectors sharing the property that their elements are related by certain sector relations. For each set we choose one representative which is, in fact, an arbitrary choice. We choose the one with the greatest identification number. Those which are representing actual graphs are our representatives of the corresponding topology. The remaining sectors, not related by sector relations to the representatives, are the nontrivial antisectors.

Aux Topology	Sectors	triv Zeros	nontriv Zeros	triv Anti	nontriv Anti	Topologies
A_1	2	1	0	0	0	1
A_3	8	4	0	0	0	2
A_6	64	22	4	0	0	5
A_{10}	1024	176	105	1	62	16
A_{15}	32768	1941	3625	121	5030	67

Table 3.2: Summarized are the numbers of sectors belonging to the categories we have introduced in Section 2.6.1. Shown are trivial zeros, nontrivial zeros, trivial antisectors, nontrivial antisectors and the number of topologies. To be more precise, by saying topology we mean the representatives we have chosen.

In Table 3.2 we have summarized the number of trivial zeros, nontrivial zeros, trivial antisectors, nontrivial antisectors and the number of topologies for the auxiliary topologies A_1, A_3, A_6, A_{10} and A_{15}. At this point, we would like to comment on the structure of sector relations. In the vacuum case Eq. (2.66) becomes

$$k_i \longrightarrow k_i' = \sum_{j=1}^{N_k} M_{ij} k_j\,. \tag{3.6}$$

As is turns out, all relevant sector relations used to shift sectors to their physical representatives are those with matrices M having integer matrix elements $M_{ij} \in \mathbb{Z}$. In general, also rational

valued elements $M_{ij} \in \mathbb{Q}$ are allowed as long as the corresponding matrix satisfies $|\det M| \neq 0$. For vacuum tadpoles such matrices start to enter at the 4-loop level.

Let us consider the 4-loop massive tadpole sector T_4 with identification number 537 and binary representation (100011001)

$$J'(n_0,n_1,0,0,0,0,n_6,n_7,0,0,n_{10}) = \int_{k_1,\ldots,k_4}^{(d')} \frac{1}{(k_1^2+1)^{n_1}} \frac{1}{((k_2-k_4)^2+1)^{n_6}} \frac{1}{((k_3-k_4)^2+1)^{n_7}} \times \frac{1}{((k_1-k_2-k_3)^2+1)^{n_{10}}}\,, \tag{3.7}$$

and sector relation

$$k_i^\mu \longrightarrow M_{ij} k_j^\mu \qquad \text{with} \qquad M = \frac{1}{2}\begin{pmatrix} 2 & 0 & 0 & 0 \\ 1 & 1 & -1 & -1 \\ 1 & -1 & 1 & -1 \\ 1 & -1 & -1 & -1 \end{pmatrix}, \tag{3.8}$$

relating sector 537 in Eq. (3.7) to sector 960 (1111000000)

$$J'(n_0,n_1,n_6,n_7,n_{10},0,0,0,0,0,0) = 2^{-d'}\int_{k_1,\ldots,k_4}^{(d')} \frac{1}{(k_1^2+1)^{n_1}} \frac{1}{(k_2^2+1)^{n_6}} \frac{1}{(k_3^2+1)^{n_7}} \frac{1}{(k_4^2+1)^{n_{10}}}\,. \tag{3.9}$$

The factor in front of the integral in Eq. (3.7) comes from the fact that $|\det M| = \frac{1}{2}$. It should be worth mentioning that the restriction to matrices with $M_{ij} = 0, \pm 1$ and $|\det M| \neq 0$ does not lead to a sector relation of sectors 537 and 960. In other words, we would end up with, at least, two T_4 sectors not related by an appropriate sector relation although there exists only one 4-propagator topology, the factorized topology (1-loop)^4. However, sector relations of that type do not occur in the reduction because the corresponding sectors are all subsectors of antisectors which are absent right from the beginning.

As we mentioned before, nontrivial zeros (see Table 3.2) are those sectors which turn out to be zero after performing a suitable momentum shift. For instance, let us consider the 3-loop massive tadpole sector T_3 with identification number 7 (000111). From Eq. (3.4) we immediately have

$$J'(n_0,0,0,0,n_4,n_5,n_6) = \int_{k_1,k_2,k_3}^{(d')} \frac{1}{((k_1-k_2)^2+1)^{n_4}} \frac{1}{((k_1-k_3)^2+1)^{n_5}} \frac{1}{((k_2-k_3)^2+1)^{n_6}}\,, \tag{3.10}$$

which is, at first glance, non-vanishing, but with $k_1 \to k_1+k_2+k_3$ and $k_2 \to k_2+k_3$ we get

$$\begin{aligned} &= \int_{k_1,k_2,k_3}^{(d')} \frac{1}{(k_1^2+1)^{n_4}} \frac{1}{((k_1+k_2)^2+1)^{n_5}} \frac{1}{(k_2^2+1)^{n_6}} \\ &= 0\,, \end{aligned}$$

having no dependence on k_3 in the integrand anymore and therefore vanishes in dimensional regularization. Nontrivial zero (along with trivial zero) sectors are immediately set to zero as soon as they occur in a reduction.

With this in mind, we can easily infer the total number of sector relations necessary to shift the relevant sectors to their representatives. The numbers for auxiliary topology A_1, A_3, A_6, A_{10} and A_{15} are summarized in Table 3.3. In Tables 3.2 and 3.3 we have also listed the number of representatives for each auxiliary topology. There are $1, 2, 5, 16$ and 67 topologies at the different loop levels. More explicitly, the different topologies are diagrammatically shown in Figures 3.3 and A.1. For each topology we have indicated the number of positive propagators and the unique

Aux Topology	Sectors	Sector Relations	Topologies
A_1	2	0	1
A_3	8	2	2
A_6	64	33	5
A_{10}	1024	680	16
A_{15}	32768	22051	67

Table 3.3: The total number of sector relations for auxiliary topology A_1, A_3, A_6, A_{10} and A_{15} necessary to shift all relevant sectors to their representatives.

identification number of its representative as subscript. From the diagrammatic point of view, all graphs with $t < t_{max}$ can be constructed by successively removing propagators (shrinking lines) from those in Figure 3.2. For instance, the 3-loop mercedes topology (identification number of representative: 63) has 6 propagators. It does not matter which propagator is removed, we end up with six T_5 subsectors all representing the v-type topology.

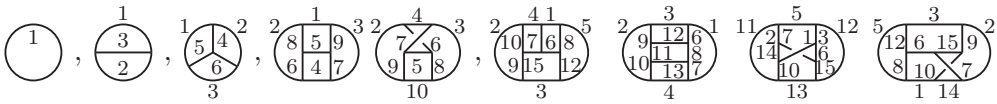

Figure 3.2: Momentum labeling for most complicated vacuum topologies of auxiliary topology A_1, A_3, A_6, A_{10} and A_{15}. By saying most complicated we refer to those topologies with the largest number of propagators with positive powers: t_{max}. The numbering indicates which line in the graph corresponds to which propagator of the auxiliary topology. The ordered sets of propagators for each auxiliary topology are shown in Table 3.1.

As mentioned before, beginning at the 4-loop level, we have more than one most complicated topology. At 4-loop we have two 9-propagator topologies, the planar one with identification number 1022 as well as the non-planar topology 511. At 5-loop it gets even more complicated with exactly four 12-propagator topologies 31740, 32745 and the non-planar ones 30527 and 30699, cf. Figure A.1. One can easily see, each set of topologies consists of generic topologies and factorized topologies build out of topologies from lower loops. There are $1 + 1 + 3 + 10 + 48$ generic topologies and $0 + 1 + 2 + 6 + 19$ factorized ones. Obviously, at 1-loop only a single topology exists and therefore no factorized topologies are present. At 2-loop there are two topologies, the generic topology 7 (sunset topology) and the factorized topology 6, the $(\text{1-loop})^2$. The 3-loop massive tadpole auxiliary topology A_6 consists of three generic topologies (mercedes 63, v-type 62 and basketball topology 51) and two factorized ones, namely topology 60 ($3 + 1$ lines) as well as topology 56, the $(\text{1-loop})^3$. At 4-loop we have ten generic topologies ranging from 9-propagator down to 5-propagator topologies and six factorized ones starting with 7-propagators down to the 4-propagator topology 960, the $(\text{1-loop})^4$. More precisely, we have 7-propagator ($6 + 1$ lines, topology 1012), 6-propagator ($5 + 1$ and $3 + 3$ lines, topology 1008 and 978), 5-propagator ($4 + 1$ and $3 + 1 + 1$ lines, topology 961 and 992) and a single 4-propagator topology ($1+1+1+1$ lines, topology 960). For generic topologies at 4-loop see Figure 3.3. The corresponding subsector trees of auxiliary topology A_3, A_6 and A_{10} are shown in Figures 2.1 and 3.4, respectively. The rather complex subsector tree of auxiliary topology A_{15} is available online [83].

At 5-loop we have 48 generic topologies ranging from 12-propagator down to 6-propagator topologies and 19 factorized ones involving topologies up to 10-propagators:

- $t = 10$: $(9 + 1,\ 32652)$, $(9 + 1,\ 30563)$.
- $t = 9$: $(8 + 1,\ 32608)$, $(8 + 1,\ 32648)$, $(6 + 3,\ 32529)$.

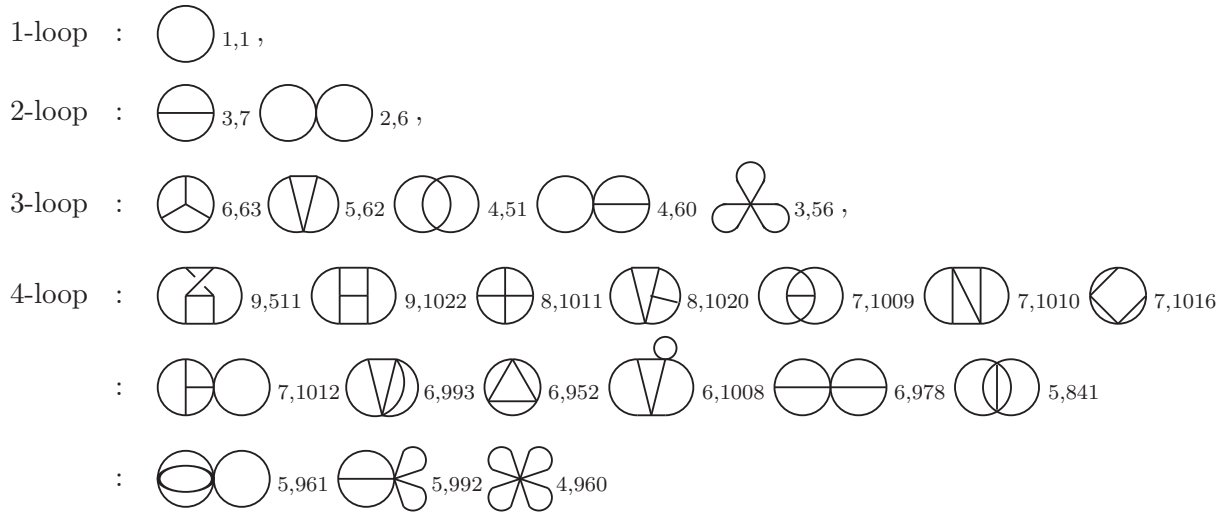

Figure 3.3: The complete set of vacuum topologies up to the 4-loop level is shown. The identification number ID and number of positive propagators t associated to each topology is given as subscript. The set of topologies consists of generic topologies (not factorizing) and those built out of products of topologies from lower loops. We have $1+1+3+10$ generic vacuum topologies and $0+1+2+6$ factorized topologies. Thanks to York Schröder for providing the vacuum topologies [84].

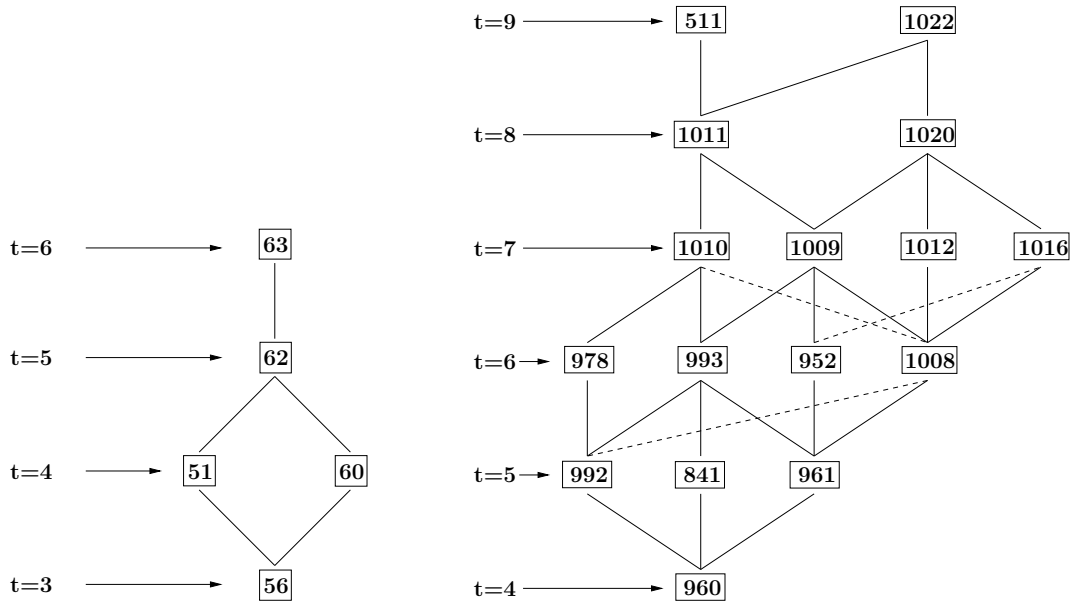

(a) The subsector tree of auxiliary topology A_6.

(b) The subsector tree of auxiliary topology A_{10}.

Figure 3.4: Shown are the subsector trees of auxiliary topology A_6 and A_{10}. Only the representatives of physical subsectors (topologies) are displayed. Starting from the root of the tree ($t = t_{max}$), the topologies connected by solid and dashed lines can be obtained by removing exactly one propagator (shrinking the corresponding line in the graph). For more details see Figure 3.3 and Table A.1.

- $t = 8$: $(7+1,\ 32259)$, $(7+1,\ 32576)$, $(7+1,\ 32640)$, $(6+2,\ 32513)$, $(5+3,\ 32528)$.
- $t = 7$: $(6+1,\ 30872)$, $(6+1,\ 32258)$, $(3+3+1,\ 32288)$, $(5+1+1,\ 32512)$, $(4+3,\ 31745)$.
- $t = 6$: $(5+1,\ 29702)$, $(4+1+1,\ 31746)$, $(3+1+1+1,\ 32256)$.
- $t = 5$: $(1+1+1+1+1,\ 31744)$.

Factorized topologies with more than $t = 10$ propagators are not possible because the most complicated topology at 4-loop has $t_{max} = 9$. For completeness, the representatives including their identification numbers and binary representations are summarized in Tables A.1 and A.2 in Appendix A.1.

After we have specified the representatives, we can move on and discuss the corresponding sector symmetries in more detail. As already mentioned in Section 2.7, a reduction without sector symmetries will, in general, lead to a larger set of master integrals as well as a significantly slower reduction. For example, let us consider the 3-loop massive tadpole sector T_6 with identification number 63 (111111) as shown in Figure 3.3. The underlying symmetry group is that of a regular tetrahedron isomorphic to S_4 with $4! = 24$ symmetries. Consequently, we have 24 symmetry relations for that sector such as

$$J'(n_0, n_1, n_2, n_3, n_4, n_5, n_6) = J'(n_0, n_1, n_3, n_2, n_5, n_4, n_6), \tag{3.11}$$

where propagators $2 \leftrightarrow 3$ and $4 \leftrightarrow 5$ are interchanged. In Eq. (3.11) we have used the representation for auxiliary topology A_6 from Eq. (3.4). As we will see in Section 3.3 the symmetry relations are directly used to symmetrize the expressions obtained from generalized recurrence relations rather than to produce additional identities. Suppose we have an expression like

$$J'(0,1,2,1,2,1,1) + J'(0,1,1,2,1,2,1) \longrightarrow 2J'(0,1,2,1,2,1,1)\,, \tag{3.12}$$

it is immediately simplified to the right-hand side of Eq. (3.12). In Tables A.3 and A.4 we give the numbers of sector symmetries for all representatives.

Let us conclude this section by summarizing the different ingredients we have discussed. Starting from auxiliary topologies A_1, A_3, A_6, A_{10} and A_{15}, all sectors have been divided into several categories. We identified trivial and nontrivial zero sectors, sectors which cannot be associated with graphs (trivial and nontrivial antisectors) and those representing the different topologies (physical subsectors). Sectors being part of the latter are connected by sector relations allowing to choose certain representatives among them. Only the representatives need to be considered in the reduction. Sector symmetries for the representatives have been identified to symmetrize lengthy expressions generated by $N_k(N_k+1)/2+1$ generalized recurrence relations.

3.3 Implementation of the Laporta Algorithm in the Computer Algebra System FORM

The following section describes the implementation of the algorithm in the computer algebra system `FORM`. Although the implementation turns out the be quite general, we always refer to the case of vacuum tadpoles.

3.3.1 Public Implementations and Software: An Overview

For a couple of reasons (as outlined below) we decided to implement our own version of a Laporta algorithm in the algebraic manipulator `FORM` rather than relying on public implementations such

as Reduze [76, 77] (written in C++ using GiNaC library [85]), AIR [86] (written in Maple [87]) or FIRE [88] (written in Mathematica [89]). In addition, there is a large variety of special purpose programs like Mincer [81, 90], Slicer [91] or MATAD [92, 93] for massless 3-loop self-energies and massive 3-loop vacuum diagrams, respectively. They are implemented in the low-level computer algebra systems SCHOONSHIP [42, 94], REDUCE [95] and FORM [20, 21]. In this context, low-level means rather limited built-in mathematical knowledge but efficient and suitable for large computations. The former ones were (SCHOONSHIP) and to some extend are (REDUCE) still being used in particle physics. The development of these computer algebra systems started in early 1960s by particle physicists considering the possibility to automatize Feynman diagram computations which become more and more complicated. The first attempt was made by M. Veltman in 1967 with SCHOONSHIP, which was initially designed for the evaluation of fermion traces. This was followed by A. C. Hearn's algebraic manipulator REDUCE [96] in 1968. Due to the limited computing resources available at that time, they were designed to be compatible as much as possible to the existing computing equipment. After 40 years, the algebraic manipulator REDUCE is still being under development and evolved into a high-level programming language with a lot of build-in features and still, turns out to be much more efficient than the currently available multi-purpose computer algebra systems (CAS).

In the following we want to focus on the algebraic manipulator FORM started being developed in the mid 1980s by J. Vermaseren. It can be seen as a direct descendant of M. Veltman's SCHOONSHIP but has also elements from the programming languages Fortran, C and REDUCE. The program language is, in relation to other computer algebra systems, low level with only very few mathematical functions available. As a consequence, the writing of programs is slightly more involved but the result turns out to be much more efficient than with object oriented computer algebra systems. One may ask, why do we introduce another algebraic manipulator with a complete new programming language while the existing ones are well developed and demonstrated to be effective. For that question we need to understand why people are using computerized algebraic manipulation in the first place. Usually, calculations solely by hand are rather limited due to the increasing complexity. The usage of computer algebra systems pushes the limits significantly beyond what would be possible with paper and pencil.

Let us for example consider a problem which is easily solvable by hand for parameters $l < 3$. Going beyond that level and using computer algebra methods one finds also $l = 3, 4$ are achievable. Let us further assume we need $l = 5$ (which might correspond to a high precision correction from perturbative quantum field theory) but turns turns out to be too big for the implementation. Then one can either wait for more computing resources (i. e. more powerful computers) or try to implement a specialized program for $l = 5$ with the disadvantage of losing generality which might be less convenient. For very complicated problems a tailor made solution is usually the better choice rather than relying on general algorithms [19].

The computer algebra system FORM is primarily designed to handle large computations. The usual problem with computer algebra systems like REDUCE, Mathematica or Maple occurs when the internal representation of some object (e. g. an expression) exceeds a certain limit which is typically of the size of the physical memory. As a consequence, the program becomes either extremely slow, got rejected or even crashes the computer. In FORM the internal representations are far more compact and, which is unique for computer algebra systems, the upper limit for formulae is the available disc space rather than the physical memory. The fact that it can be achieved without having big losses in performance makes FORM the most suitable programming language for our purposes.

Nowadays, the majority of programs is either written in the low-level language FORM or in multi-purpose systems like Mathematica. In the following, we would like to comment on the specific needs for implementing reductions algorithms such as the Laporta algorithm from Section 2.6.4. The performance of the Laporta algorithm depends basically on two important ingredients: an ef-

ficient polynomial greatest common divisor (GCD) algorithm and the possibility to handle a large amount of expressions. For example, the public implementation `Reduze` written in `C++` uses the `sGiNaC` library for symbolic computations. It contains, among other things, GCD and factorization algorithms for multivariate polynomials to simplify algebraic expressions. Alternatively, also specialized polynomial systems like `FERMAT` [97] are used. The management of expressions is done with external key-valued databases (e. g. `Kyoto Cabinet` [98]).

3.3.2 Implementing the Algorithm in FORM

As we already mentioned before, we decided to implement the algorithm in `FORM`. For polynomial algebra we use either the external polynomial system `FERMAT` via the `#external` statement [99] or in the latest version `FORM 4.0` [100] the built-in functionality `polyratfun` which turns out to be fully operational. The management of expressions is done with the built-in `Tablebase` statement.

We have compared the performance of `FERMAT` and `FORM`s built-in polynomial procedures. It turns out, not surprisingly, `FERMAT` is by far more efficient in simplifying the quotients of multivariate polynomials. The larger the number of variables in the polynomials, the bigger is the advantage of using `FERMAT`. However, in order to use external programs one needs to establish a connection which leads to some overhead. This is mainly due to syntax translations and the extraction of the coefficient out of `FORM` expressions. Taking into account the fact that the polynomials we are facing with are rather simple (only one or two[1] variables), we decided to stick to `FORM`s onboard polynomial procedures. However, if desired, it is always possible to switch on the external simplification of polynomials.

In Figure 3.5 we give an overview of the implementation including all programs for the generation of the corresponding sector relations, symmetries and generalized recurrence relations discussed in Sections 2.5, 2.6.2 and more explicitly for vacuum topologies in Section 3.2. These programs are able to generate the necessary ingredients from scratch and, in case appropriate shifts and recurrence relations are provided by external software able to translated it into the notation we are using. In the following we would like to discuss the building blocks and the program flow in Figure 3.5 in more detail.

Once sector relations, symmetries and generalized recurrence relations of auxiliary topology A_x are provided, one can start and generate the corresponding seed integrals for physical sectors (topologies) up to the required r_{max}. The reduction of a sector is started by specifying its identification number ID. As already mentioned, a reduction always starts from the bottom of the subsector tree cf. Fig. 3.4. In other words, if a sector with identification number ID has physical subsectors, they need to be reduced before that sector is reduced. The "Prepare Job" routine takes care that all subsectors are present and ready for substitution as soon as the reduction is started. On top of this, the user can specify the size of a bunch of seed integrals which is delivered in each run by the "Job Center" for processing. If not specified, the algorithm chooses an appropriate bunch size. The "Job Center" calls the "Laporta Main Block" and passes a certain number of seed integrals (as defined in bunch size) for reduction. As indicated, the Laporta algorithm requires proper sector relations to shift physical subsectors to their representatives as well as sector symmetries to symmetrize the corresponding expressions.

In Listing 3.1 we give an example how the symmetrization of expressions is actually implemented. The symmetrization procedures as in Listing 3.1 as well as sector relation procedures are automatically generated for each topology. Since generalized recurrence relations do only relate sectors T_t to subsectors T_{t-1} (cf. Fig. 2.7), we only need to include sector relations and symmetries of physical subsectors with $(t-1)$-propagators for a reduction of t-propagator topologies. The different

[1] In addition to the space-time dimension d from e. g. Eq. (2.77) we introduce an arbitrary power x for exactly one propagator instead of an integer value. This issue is discussed in Section 3.3.3.

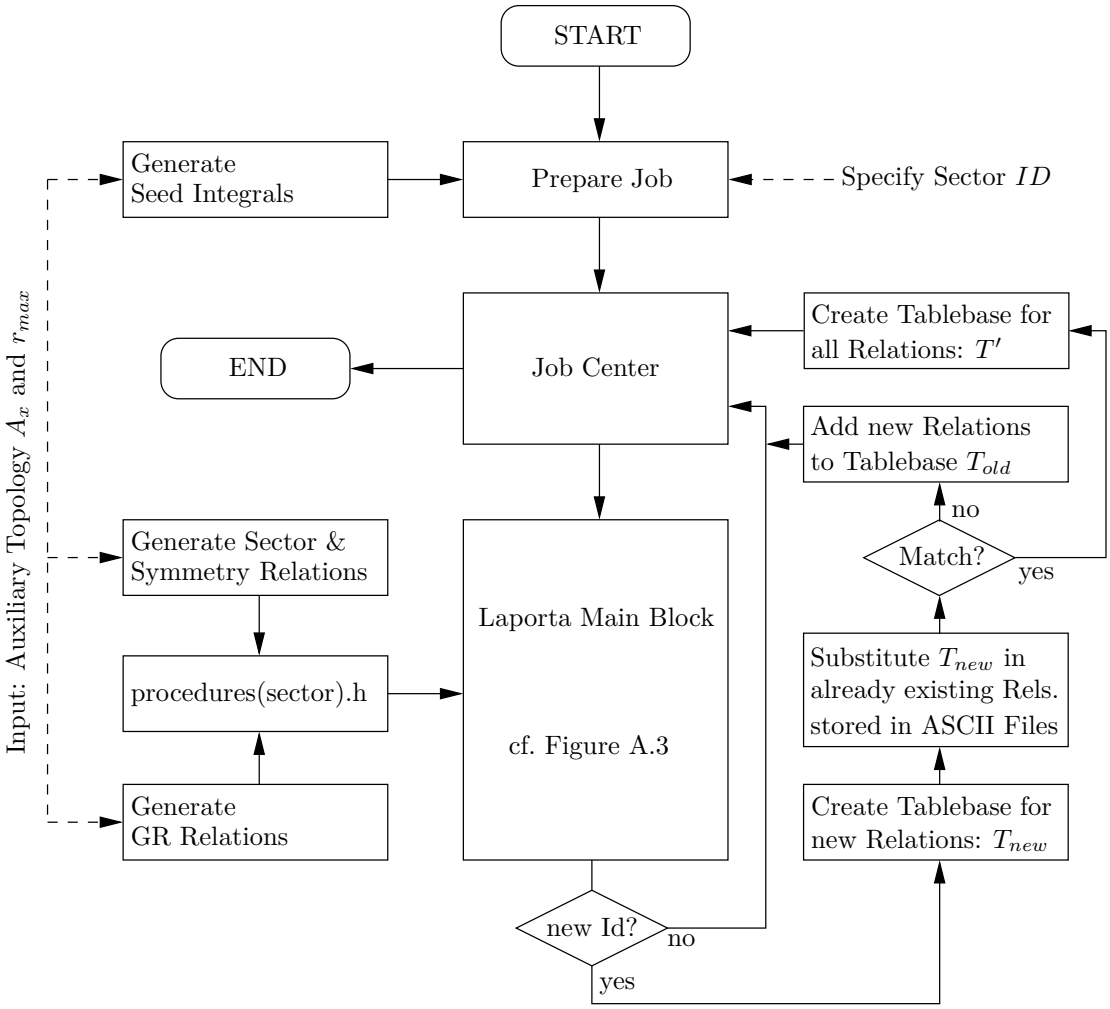

Figure 3.5: The schematic of the implementation including all programs for generation of sector relations, symmetries, generalized recurrence relations (GRR) and seed integrals. Dashed arrows are indicating the input which need to be provided by the user to run the reduction properly.

ingredients in "Laporta Main Block" are the following:

1. Generate generalized recurrence relation for a given seed integral out of set $I_{t,r,D}$.
2. Shift physical subsectors T_{t-1} to their representatives and detect zero sectors.
3. Apply the symmetrization procedure for sector T_t and its physical subsectors.
4. Substitute relations (stored in tablebase T_{old}) of sector T_t already obtained in previous runs.
5. Rewrite expression as left-hand side equals right-hand side. The left-hand side is determined by the ordering given in Section 2.7.
6. Substitute already known recurrence relations for physical subsectors.

In case new relations have been found, denoted in the flow diagram 3.5 by "new Id?", they are not immediately substituted in the relations which are already part of the subsystem. At any time, the subsystem is stored within the tablebase as well as in simple ASCII files for each relation. The

```
id J'(s0?,s1?pos_,s2?pos_,s3?pos_,0,0,0) = fsy(J'(s0,s1,s2,s3,0,0,0),
                                                J'(s0,s1,s3,s2,0,0,0),
                                                J'(s0,s2,s1,s3,0,0,0),
                                                J'(s0,s3,s1,s2,0,0,0),
                                                J'(s0,s2,s3,s1,0,0,0),
                                                J'(s0,s3,s2,s1,0,0,0),
                                                J');
symmetrize fsy; id fsy(?a,J'(?b)) = J'(?b);
```

Listing 3.1: The symmetrization procedure in `FORM` for physical sector 56 (factorized topology 111000, cf. Fig. 3.3) of auxiliary topology A_6. The topology has $3! = 6$ symmetries (all permutations of three elements) as can be seen inside the fsy(...) function on the right-hand side. The procedure works as follows: Once the left-hand side is matched, the integral is replaced by the function fsy(...) containing all possible permutations of propagator powers s_i as dictated by the corresponding sector symmetries. Then the function fsy(...) is uniquely symmetrized (more precisely, the order of arguments is rearranged) by using `FORM`s symmetry statement `symmetrize`. After symmetrization, we take the last argument of fsy(...) as the new integral, cf. Eqs. (3.11) and (3.12). We note that primes as in J' are not allowed and need to be replaced in order to get functional `FORM` code.

substitution is done as follows: A new tablebase T_{new} is created for relations gathered during the last run. That tablebase is then used to substitute those relations in the already existing relations stored in ASCII files. If it turns out that no substitution happened (case differentiation "Match?"), the new relations are simply added to the old tablebase T_{old} using the `tablebase addto` statement. In case some relations were substituted, it is necessary to create a new tablebase directly out of the ASCII files.

The procedure looks, at first glance, rather complicated but turns out to be more efficient than an implementation without tablebases. One can reduce the loss of time caused by creating new tablebases by choosing larger bunch sizes right from the beginning. On the other hand, larger bunch sizes have negative impact on the runtime in the "Laporta Main Block" and, if too large bunch sizes are chosen, memory issues will appear. A typical bunch size value is of about 100 seed integrals. The "Job Center" passes seed integrals $I_{t,r,D}$ until the predefined r_{max} is reached. The order of processing seed integrals is inverse to the order of extracting integrals, see Section 2.6.4.

3.3.3 Adapting the Implementation to Derive Difference Equations

In this section we describe how the implementation discussed in Section 3.3.2 is adapted to derive so-called difference equations. We would like to start extending the notation of Eq. (3.2) by an additional index $X \in [1, M]$ keeping track of an arbitrary power x on propagator D_X

$$J''(\mathbf{n}) = J''(X, n_0, n_1, \ldots, n_M) = \int_{k_1,\ldots,k_{N_k}}^{(d')} \frac{1}{D_1^{n_1} \ldots D_X^{n_X+x} \ldots D_M^{n_M}}, \qquad \mathbf{n} \in \mathbb{Z}^{M+2}, \tag{3.13}$$

with $D_i = q_i^2 + 1$ and $d' = d - 2n_0$, $n_0 \leq 0$. Similar to Eq. (3.2) we neglect the trivial prefactor carrying the mass dependence. In the case $x = 0$ and $n_0 = 0$ we recover the integrals $J'(n_0 = 0, \mathbf{n})$ and $J(\mathbf{n})$ in Eqs. (2.57),(3.2) immediately

$$J(n_1, \ldots, n_M) = J'(n_0 = 0, n_1, \ldots, n_M) = J''(X, n_0 = 0, n_1, \ldots, n_M)\Big|_{x=0}. \tag{3.14}$$

Let us assume we have used the Laporta algorithm successfully and reduced the set $I_{t,r,D}$ for values r_{max}, D_{max} to a small number of master integrals. Those integrals cannot be further simplified

(i. e. expressed through simpler ones) using generalized recurrence relations. They need to be solved by other means. We would like to solve the remaining master integrals by the method of difference equations [18]. For auxiliary topology A_1, A_3, A_6, A_{10} and A_{15} the complete sets of master integrals are given in Section 3.4. The question how to solve these equations will be discussed in great detail in Chapter 4. At this point, only basic concepts and definitions are necessary to proceed with the adaption.

A linear difference equation of order R in variable x is defined as

$$\sum_{j=0}^{R} f_{\mathbf{n},j}(x) J''(X, n_0, n_1, \ldots, n_X + x + j, \ldots, n_M) = G_{\mathbf{n}}(x)\,, \tag{3.15}$$

where $f_{\mathbf{n},j}(x)$ are polynomials in x and space-time dimension d and $G_{\mathbf{n}}(x)$ being known functions. We would like to bring Eq. (3.15) in a different form, by shifting $x \to x - n_X$ we get

$$\sum_{j=0}^{R} p_{\mathbf{n},j}(x) J''(X, n_0, n_1, \ldots, x + j, \ldots, n_M) = F_{\mathbf{n}}(x)\,, \tag{3.16}$$

with $p_{\mathbf{n},j}(x) = f_{\mathbf{n},j}(x - n_X)$ and $F_{\mathbf{n}}(x) = G_{\mathbf{n}}(x - n_X)$. Let us consider a specific $\mathbf{n} = (X = 1, n_0 = 0, 1, \ldots, 1) \in \mathbb{Z}^{M+2}$ corresponding to master integrals of the form

$$B = J''(1, 0, 1, \ldots, 1) = J(x, 1, \ldots, 1)\,, \tag{3.17}$$

and define the quantity

$$U_{D_1}(x) = J(x, 1, \ldots, 1)\,, \tag{3.18}$$

where the subscript D_1 indicates that the first propagator is raised to power x. In case $x = 1$ we recover the master integrals given in Eq. (3.17), the general form of Eq. (3.16) becomes

$$\sum_{j=0}^{R} p_j(x) U_{D_1}(x + j) = F(x)\,. \tag{3.19}$$

The function $F(x)$ on the right-hand side is a linear combination of integrals similar[2] to U_{D_1} but some of the denominators $D_1, D_2, \ldots, D_M$ are missing. In other words, $F(x)$ is composed out of integrals with a smaller number of positive propagators t compared to $U_{D_1}(x)$ which has exactly M positive ones. We can raise any of the M propagators in Eq. (3.17) to power x and in complete analogy to Eq. (3.18) define functions $U_{D_j}(x)$. The corresponding difference equations, each satisfied by one of the U_{D_j} are, in general, all different but coincide in $x = 1$,

$$U_{D_j}(1) = B\,. \tag{3.20}$$

This turns out to be a nontrivial crosscheck of the consistency of the calculation. A more detailed discussion on this and related topics will follow in Chapter 4. For the moment, it is sufficient to know what kind of equations we are looking for. The algorithm discussed in Section 3.3.2 can be modified to derive linear difference equations in a single variable x as defined in Eq. (3.15).

Let us start by recalling the basic assumption made in Laporta's algorithm. We have assumed that all powers of propagators $\mathbf{n} = (n_1, \ldots, n_M)$ are fixed integer values. With an arbitrary power x, the unique ordering given in Section 2.7 does not work but it can be modified to that case without making big changes. We already started in that direction by introducing the notation in Eq. (3.13). Without losing generality, we assume x to be a positive nonzero integer $x \in \mathbb{N}^+ \backslash \{0\}$.

[2]Similar does not mean that the propagator D_1 is necessarily raised to power x.

As a consequence, propagator X always counts as a propagator with positive power independent of the actual value of n_X. For example, let us consider auxiliary topology A_3. We could have the following integrals

$$J''(3,0,1,1,1) \qquad \text{and} \qquad J''(3,0,1,1,0)\,, \tag{3.21}$$

both belonging to the same 3-propagator sector 7 (111) although the latter one seems to be the factorized topology 6 with binary representation (110). From that point of view, the propagator X carrying power $n_X + x$ is distinguished among the others. Therefore we redefine the number of positive propagators t for an integral $J''(X, n_0, n_1, \ldots, n_M)$ as

$$t = \sum_{\substack{i=1 \\ i\neq n_X}}^{M} \theta(n_i - 1) + 1\,. \tag{3.22}$$

In complete analogy to Eqs. (2.58),(2.79) we combine a certain class of integrals together by defining

$$I_{t,r,D,X} \equiv \left\{ J''(X, n_0, n_1, \ldots, n_M) \,|\, \text{with } (r, s = 0) \text{ as usual, } t \text{ via Eq. (3.22)}, n_0 = -D \right\}. \tag{3.23}$$

Since we are interested in deriving appropriate difference equations rather than to perform a reduction, the ordering needs to be adjusted by taking into account the structure of the difference equations in Eq. (3.15). The ordering for extracting integrals is as follows. We take the integral with

1. smallest value n_0. In case of degenerate integrals with the same value n_0 proceed with 2..
2. largest number of different propagators t. If more than one integral has the same value t proceed with 3..
3. largest X. If more than one integral has the same value X proceed with 4..
4. largest value $r' = \sum_{i=1, i\neq n_X}^{M} |n_i|$, the sum of absolute powers of propagators except propagator X. If more than one integral has the same value r' proceed with 5..
5. greatest power n_M. If more than one integral has the same power n_M proceed with the greatest power $n_{M-1}, \ldots$, the greatest n_1.

We start again and give highest priority to integrals with higher dimensions followed by the number of different propagators t according to Eq. (3.22). After that, we are ordering the position of the arbitrary index x by prefering those integrals with larger X which is in fact an arbitrary choice. As a consequence the ordering tends to shuffle the arbitrary index x to smaller values X. Then we take into account that powers of propagators sitting on propagator X should not be treated in the same way as powers of the remaining ones. To be more precise, we are ignoring the value n_X and compute the absolute sum of the remaining propagators as indicated in 4.. This favors a reduction of the remaining indices to smaller values of r' and, to some extent, powers are rerouted to propagator X. Having again a closer look on Eq. (3.15) we realize that this is exactly the behavior we are aiming at. Notice that, if we would have chosen the traditional $r + s$ criterion (see unique ordering in Section 2.7) powers would preferably be shifted to the first few propagators but not to a specific one. We complete the ordering by demanding the same prescription (5.) already used in Section 2.7.

In Table 3.4 an example based on auxiliary topology A_3 (i. e. 2-loop massive tadpoles) is given to show what integral out of a set of integrals is determined to be the most complicated one.

At this point we would like to focus on the implementation. Certain changes need to be done to incorporate this feature in the existing implementation. The most important are discussed with the

Rule	$J''(3,-1,1,1,2)$	$J''(3,-1,1,2,1)$	$J''(3,-1,2,1,1)$	$J''(1,-1,2,1,1)$	$J''(3,0,3,1,1)$
1	-1	-1	-1	-1	0
2	3	3	3	3	3
3	3	3	3	1	3
4	2	3	3	2	4
5	-	$n_2\surd$	n_1	-	-

Table 3.4: Using our choice of an unique ordering to determine the most complicated integral out of a set of five integrals. The integrals $J''(X, n_0, n_1, n_2, n_3)$ are 2-loop massive tadpoles (auxiliary topology A_3) using the notation of Eq. (3.13). We have indicated which integral would be chosen to be the most complicated one.

help of example code. Basically, all procedures implemented for the reduction can also be used for the generation of difference equations. However, they expect integer valued indices and therefore we need to take care what happens with propagator X carrying power $n_X + x$. We are discussing the necessary changes one after another. Let us start and consider the generation of generalized recurrence relations in the case of auxiliary topology A_1 out of the seed integral

$$J''(1,0,1) \longrightarrow I'(0,1+x)\,, \tag{3.24}$$

where we have explicitly written the arbitrary power on propagator 1. Since FORMs pattern matching is not restricted to integer valued function arguments the right-hand side of Eq. (3.24) can be directly replaced by the generalized recurrence relation we already use

$$I'(0,1+x) \longrightarrow 0 = I'(0,1+x) - I'(-1,(1+x)-1)(1+x)\,, \tag{3.25}$$

which is nothing but the D-operator relation of Eq. (2.48). The function I' is temporarily introduced[3] and in the end rewritten back in terms of function J''

$$0 = J''(1,0,1) - (1+x)J''(1,-1,0)\,. \tag{3.26}$$

As we can see from Eq. (3.26), the prefactor contains x and, in general, also the space-time dimension d. The benefit of this rather cumbersome looking procedure is that the existing program routines for generating generalized recurrence relations can be used again. In Listing 3.2 we have outlined the implementation of Eqs.(3.24)-(3.26) in FORM. As it turns out, also the routines for sector relations, symmetries and the identification of zero sectors can be used again. In order to do so, we are temporarily assigning a large positive integer (e. g. let us say 1000) to propagator X i. e. $n_x + x \to n_x + 1000$. After the procedures for sector relations or sector symmetries have been applied to the expression we write the result again in terms of the notation of Eq. (3.13). For example, let us consider auxiliary topology A_6 and the sector symmetrization of sector 56, we could have the following situation

$$J''(3,0,1,2,3,0,0,0) \longrightarrow J'(0,1,2,1003,0,0,0)\,, \tag{3.27}$$

applying the symmetrization procedure given in Listing 3.1 we get

$$J'(0,1,2,1003,0,0,0) \longrightarrow J'(0,1003,2,1,0,0,0)\,. \tag{3.28}$$

As we can see, the sector symmetrization changed the position of the propagator carrying power $n_X + x$ from $X = 3$ to $X = 1$. By looking for the large power we are able to keep track of the index carrying power x. Back in J'' notation the result reads

$$J''(1,0,3,2,1,0,0,0)\,. \tag{3.29}$$

[3]The function I' is similar to J' in Eq. (3.2) but the latter was only used in the context of integer valued arguments.

```
id J''(s00?,s0?,s1?) = I'(s0,x*delta_(1,s00)+s1);
id I'(s0?,s1?) =
                +I'(s0,s1)*polyr(1,1)
                +I'(s0-1,s1+1)*polyr(-s1,1);
id I'(?a,s1?!number_,?b) = J''(nargs_(?a),?a,replace_(x,0)*s1,?b);
```

Listing 3.2: Procedure to generate generalized recurrence relations out of seed integrals J'' in `FORM` for physical sector 1 (cf. Fig. 3.3) of auxiliary topology A_1. The procedure works as follows: The function J'' is rewritten in terms of function I' with propagator power $s1 + x$ similar to Eq. (3.24). For seed integral I' the generalized recurrence relation is generated cf. Eq. (3.25). The function `polyr` contains coefficient functions which are, in general, ratios of multivariate polynomials. As already mentioned, for polynomial simplification `FORM`s build-in functionalities are being used and consequently `polyr` is declared as `polyratfun` [100]. In the end, function I' is expressed in terms of the notation we originally started with.

It must be guaranteed that the value is large enough to avoid wrong identifications of that propagator. In `FORM` the rewriting in terms of J'' is incorporated by subtracting the value initially added to propagator X from all propagator powers $n_1 - 1000, \ldots, n_M - 1000$. The propagator with positive power indicates the position of x. In the end, the value is added again except to propagator X. In Listing 3.3 the procedure is outlined. The rewriting of integrals in Eqs. (3.24)-(3.26) and

```
id J''(s00?,s0?,...,s`M'?) =
   J'(s0,<1000*delta_(1,s00)+s1>,...,<1000*delta_(`M'loop'',s00)+s`M'>);
<--(*)
id J'(s0?,...,s`M'?) = J'(<s0-1000>,...,<s`M'-1000>);
id J'(?a,s1?pos0_,?b) = J''(nargs_(?a),?a,s1,?b);
id J'(s00?,s0?,...,s`M'?) =
   J''(s00,1000+s0,<1000*deltap_(1,s00)+s1>,...,<1000*deltap_(`M',s00)+s`M'>);
```

Listing 3.3: The program code in `FORM` necessary to rewrite notation J'' of Eq. (3.13) in terms of J' in Eq. (3.2) and back again. The program routines of sector symmetries (see Lst. 3.1), relations, and the identification of zeros used for J' are inserted right after the first `id` statement indicated by `(*)`.

Eqs. (3.27)-(3.29) appears trivial and straightforward but it took some time to figure out what would actually be the most reliable way to implement this in `FORM`.

We conclude this section focusing on the generation of seed integrals. Since we are interested in deriving difference equations for the remaining master integrals rather than to perform a reduction, it should be sufficient to consider seed integrals $I_{t,r,D,X}$ with relatively small r_{max}. However, as we will see in Section 3.4.1, we encounter difference equations of order $R = 7$ and presumably even higher ones at the five loop level. In order to obtain such difference equations rather large r_{max} are necessary. We restrict seed integrals to those with $D = 0$ corresponding to integrals with space-time dimensions d. This seems reasonable because we are looking for difference equations having physical space-time dimensions i. e. $d' = d$. On top of this, by introducing index X specifying what propagator is actually raised to power $n_X + x$, we naively enlarge the number of seed integrals by a factor t. This is because each propagator carrying a positive power needs to be treated in the same way. As it turns out, it is not necessary to raise each propagator to power $n_X + x$ separately. We raise only very few propagators to power $n_X + x$ which are determined by the topology under consideration. For example, let us again consider auxiliary topology A_6 and sector 56 with binary

representation (111110). We have exactly two non-equivalent propagators $X = 1, 2$ resulting in two difference equations not related by sector symmetries. In other words, it is sufficient to generate seed integrals where $X = 1$ and $X = 2$ rather than for all possible $X = 1, \ldots, 5$. If we would have generated seed integrals also for $X = 3, 4$ and $X = 5$ ($X = 6$ is not considered because $n_6 = 0$) no additional relations would have been produced because they are all related to the former ones via sector symmetries.

In other words, before seed integrals can be generated one needs to find out the non-equivalent propagators for the corresponding topologies. By doing so, the number of seed integrals is significantly reduced which is especially advantageous in cases where t is large and the number of non-equivalent propagators X rather small. More on this issue will be discussed in Section 3.4.1.

3.4 Reduction: Master Integrals, Bottlenecks, Results

We start this section rediscovering already known results for massive tadpoles up to 4-loop followed by new results at the 5-loop level. This serves as a good check for our implemented algorithms. As we have outlined in great detail in Section 3.3.1, a reduction is performed to reduce massive tadpoles to very few so-called master integrals forming a basis in such a way that all integrals can be expressed in terms of those

$$J'(n_0, n_1, \ldots, n_M) = \sum_{i=1}^{N_M} c_i J'_i \,, \tag{3.30}$$

where the coefficients c_i are ratios of polynomials in space-time dimensions d. In order to find out how many and what kind of master integrals we are faced with, a reduction without subsectors is performed. All subsectors T_{t-1} which are showing up in a reduction of physical sector T_t with identification number ID are immediately set to zero. This renders each reduction of physical sectors T_t independent because subsectors do not have to be substituted in the corresponding subsystems.

The reduction is performed up to $r_{max} = t + 4$ with $D = 0$ where t is the actual number of positive propagators of physical sector T_t as specified in Tables A.1 and A.2. We use generalized recurrence relations as described in Sec. 2.7 and the complete set of sector symmetries for all topologies cf. Tables A.3 and A.4.

In Table 3.5 we have summarized the number of master integrals found in that reduction for auxiliary topology A_1, A_3, A_6, A_{10} and A_{15}. In case of the one-, two-, three-, and four-loop massive tadpole the same number of master integrals, as already known from the literature, is obtained (see e. g. [101]). The number of master integrals at the five-loop level (auxiliary topology A_{15}) has been determined for the first time and turns out to be of the order of twice the number of topologies.

Figure 3.6: In addition to those in Figure 3.3 there are $0 + 0 + 0 + 3$ fully massive master integrals having dots on several propagators. A dot on a line indicates that the corresponding propagator carries an extra power. Lines without dots are representing propagators with power 1.

There is at least a single master integral for each topology which has all positive propagators to power 1, the corner integral. This is especially the case for auxiliary topology A_1, A_3 and A_6

Auxiliary Topology	Master Integrals	Topologies	Runtime
A_1	1	1	< 1 sec
A_3	2	2	< 1 sec
A_6	5	5	~ 2 secs
A_{10}	19	16	~ 2 mins
A_{15}	132	67	~ 5 hrs

Table 3.5: The total number of master integrals in comparison to the number of topologies for auxiliary topology A_1, A_3, A_6, A_{10} and A_{15}. It can be seen that auxiliary topology A_1, A_3 and A_6 corresponding to the one-, two-, and three-loop massive tadpole have exactly the same number of master integrals as topologies. In fact, each topology has exactly one master integral. Starting at 4-loop (auxiliary topology A_{10}) we encounter more master integrals than topologies. At 5-loop (A_{15}) we have roughly a factor two more master integrals than topologies. The runtime given in the last column is the time necessary to process all seed integrals up to $r_{max} = t + 4$ with $D = 0$ using 12 CPUs.

where we have exactly one master integral for each topology. Beyond that level we have additional master integrals having squared and cubed propagators. In Figure 3.6 those master integrals are diagrammatically shown up to 4-loop. The corresponding powers of propagators are given in Table 3.6 using the notation of Eq. (3.1) simplifying to $J(\mathbf{n})$ in case $n_0 = 0$. As a consequence of our

Ad. Master	t	ID	Propagator Powers
1	5	841	$J_{\mathbf{3},1,0,1,0,0,1,0,0,1}$
2	7	1009	$J_{\mathbf{2},1,1,1,1,1,0,0,0,1}$
3	8	1011	$J_{\mathbf{2},1,1,1,1,1,0,0,1,1}$

Table 3.6: In addition to those in Table A.1 there are master integrals with dots on some propagators. In this context, the representatives in Table A.1 denoted as $I_{...}$ are understood as the master integrals $J_{...}$ without dots.

specific choice for the unique ordering in Sec. 3.3.2 we end up with master integrals in physical space-time dimensions i. e. $n_0 = 0$. This means Eq. (3.30) simplifies to

$$J'(n_0, n_1, \ldots, n_M) = \sum_{i=1}^{N_M} c_i J_i \,, \tag{3.31}$$

where N_M is the number of master integrals given in Tab. 3.5. Let us move on and consider the 5-loop case according to auxiliary topology A_{15}. In complete analogy to the one-, two- , three- and four-loop case, each of the 67 topologies has a master integral with all propagators raised to power 1 as well as the 65 additional ones diagrammatically shown in Figure A.2 in Appendix A.1. The master integrals with squared and cubed propagators are again summarized in Table A.6 in Appendix A.1. Consequently, we end up with a total number of master integrals of $67 + 65 = 132$.

An independent reduction has been performed [102] in `Reduze` using integration-by-parts relations and a couple of carefully chosen sector symmetries. The number of master integrals coincides except in 7-propagator topology 30858. In this sector we end up, in addition to the corner integral, with one more master integral with an extra dot, cf. Tables. A.2 and A.6. We double-checked the reduction in this sector and found again two master integrals. From the integration-by-parts reduction [102] one obtains the following relation

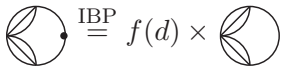

(3.32)

with $f(d) = 1 - d/4$ which is absent in our system of equations. We also performed the reduction with integration-by-parts relations in this sector and found exactly the same relation in a small reduction up to $r_{max} = t + 2$ without using sector symmetries. So, indeed the relation seems to be correct. We do not think this is a conceptional problem of the generalized recurrence relations because in all other sectors we perfectly agree. It might has something to do with the specific choice of the ordering in combination with the symmetrization procedures. For the moment, we stick with the 132 master integrals instead of 131.

We would like to conclude this section with comments on the general reduction. In addition to the reduction outlined above, a full reduction has been performed including substitutions of subsectors. We perform a reduction up to $r_{max} = t + (12 - t) + 1$ with $D = 0$ and $D = 1$ in a reasonable amount of time (few days using 12 CPUs). Even one or two more dots are not a problem at all.

However, as we already know from Eq. (2.78) in Sec. 2.7, each irreducible scalar product less ($s \to s - 1$) increases r by $N_k - 1$. For example, let us consider an integral belonging to sector T_t of auxiliary topology A_{15} having 5 irreducible scalar products i. e. $s = 5$. In the worst case, the T-operator increases r by $5 \cdot (5 - 1) = 20$ and integrals with shifted dimensions $D = 5$ show up. A reduction of this kind of integrals would require a reduction with $r_{max} = t + 20$ and $D = 1, \ldots, 5$ which is simply out of reach.

At the moment, it seems more realistic to perform a reduction using the traditional integration-by-parts relations and a carefully chosen set of sector symmetries rather than rewriting integrals with irreducible scalar products in terms of integrals in higher space-time dimensions. However, by choosing a specific set[4] of sector symmetries we are, in some sense, abandoning the idea of an automated approach which was the idea initially started with cf. Sec. 2.6. It seems that only very few sector symmetries are in fact necessary to reduce the number of master integrals significantly. Unfortunately, it is not known how to identify these sector symmetries in a systematic way. The result presented at this point using a somewhat different approach might be useful for further investigations along these lines.

3.4.1 Difference Equations for Master Integrals

As we have seen in the previous section, the approach we are using does not seem to be the most suitable method to perform a complete reduction. However, for computing difference equations this method is particularly interesting because the master integrals we are faced with do not have irreducible scalar products at all. This means that relatively small r_{max} are sufficient and their value is essentially determined by the actual order R of the difference equations we are looking for. Of course, right from the beginning, we do not know the orders of difference equations but it appears natural to assume that they do not differ very much in the order from those we can find in the literature for the lower loop levels (see e. g. [18]).

Due to the fact that the implementation outlined in Sec. 3.3.3 has not been tested so far we start and derive the already known difference equations up to the 4-loop level before using the implementation for the 5-loop case. In complete analogy to the approach in Sec. 3.4 a reduction without subsectors is performed in order to get an idea what orders of difference equations we are facing. By recalling the definition in Eq. (3.15) we realize that a reduction without subsectors corresponds to the homogeneous part of the difference equation. As mentioned before, it is in general not necessary to generate seed integrals $I_{X,t,r,D}$ for all X because the relations obtained from seed integrals with different X turn out to be related to a large extent by sector symmetries. Only very few so-called non-equivalent propagators, specifying which propagators need to be raised

[4]Remember a reduction without sector symmetries leads to a rather large set of master integrals. On the other hand, one cannot simply include all sector symmetries because of the large number cf. Tables A.3 and A.4.

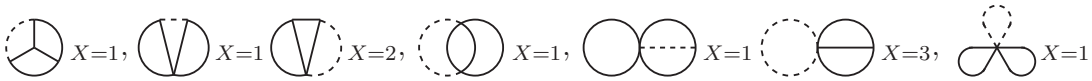

Figure 3.7: Shown are the non-equivalent positions X of the propagator carrying power $n_X + x$ for topologies of auxiliary topology A_6. The propagator raised to power $n_X + x$ is indicated for each topology by dashed lines and in the subscript. The notation of Eq. (3.13) and momentum labeling in Fig. 3.2 is used.

to power $n_X + x$, are necessary to obtain the complete set of difference equations. In Figure 3.7 we give two examples of two non-equivalent propagators on the basis of topology 62 and topology 60 of auxiliary topology A_6. Consequently, at 3-loop we have a total number of 7 difference equations.

In order to find the non-equivalent propagators we generate seed integrals for all X and perform a small reduction with $r_{max} = t$. Those seed integrals producing new relations are determined and the corresponding values of X are specifying the propagators which need to be raised to $n_X + x$. In Table 3.7 we have summarized the orders of the difference equations for auxiliary topology

Topo	t	ID	Propagator X	Order R
1	1	1	1	1

Topo	t	ID	Propagator X	Order R
1	2	6	1	1
2	3	7	1	2

Topo	t	ID	Propagator X	Order R
1	3	56	1	1
2	4	60	1,3	2,1
3	4	51	1	2
4	5	62	1,2	2,2
5	6	63	1	2

Topo	t	ID	Propagator X	Order R
1	4	960	1	1
2	5	992	1,2	2,1
3	5	961	1,4	2,1
4	5	841	1	4
5	6	1008	1,3,4	2,1,2
6	6	993	1,2,4	5,2,2
7	6	978	1	2
8	6	952	1	2
9	7	1016	1,4	2,2
10	7	1012	1,3	2,1
11	7	1010	1,2,5	2,2,2
12	7	1009	1,3,4	3,3,3
13	8	1020	1,3,4,8	2,2,3,2
14	8	1011	1,3	4,3
15	9	1022	1,2	3,2
16	9	511	2	3

Table 3.7: The order R of difference equations for all topologies of auxiliary topology A_1, A_3, A_6 and A_{10}. The last two columns are showing all non-equivalent propagators X and the order R of the difference equation which is associated to that propagator.

A_1, A_3, A_6 and A_{10} obtained from our approach. The orders of difference equations shown in Tab. 3.7 are always the lowest orders found for the corresponding topologies and propagators X. We have observed that a reduction for a particular topology needs to be performed at least up to $r_{max} = R$ in order to find appropriate difference equations. Going beyond that limit additional difference equations of higher orders $R' > R$ will occur. For instance, let us consider topology 1 of auxiliary topology A_1, the corresponding difference equation is of order $R = 1$ and reads

$$J''(1,0,1) + J''(1,0,0)\frac{d-2x}{2x} = 0\,, \tag{3.33}$$

using the notation of Eq. (2.57) and writing power $n_1 + x$ explicitly we get

$$J(1+x) + J(x)\frac{d-2x}{2x} = 0\,, \tag{3.34}$$

which is exactly the recurrence relation we have encountered in Eq. (2.17) for the 1-loop massive tadpole with $m^2 = 1$. The difference equation of topology 1 of order $R = 2$ is

$$J(2+x) - J(x)\frac{d-2x}{2x}\frac{d-2(x+1)}{2(x+1)} = 0\,. \tag{3.35}$$

At this point we would like to point out that Eqs. (3.34) and (3.35) are homogeneous difference equations which are, in fact, exceptional cases. All difference equations discussed in this work[5] are nonhomogeneous difference equations i. e. $G_n(x) \neq 0$ in context of Eq. (3.15).

We do not consider difference equations of higher orders $R' > R$ because, in general, solving these equations gets more and more involved as the order increases. This issue will be discussed in Chapter 4. From Tab. 3.7 we can easily read of the number of difference equations one is facing at the different loop levels. There are $1 + 2 + 7 + 33$ difference equations with orders up to $R = 5$.

In complete analogy to Tab. 3.7, the 5-loop difference equations are summarized in Table A.5 in Appendix A.1. There are in total 234 difference equations for 67 topologies. Even without the subsectors, we were not able to determine the homogeneous part of all of the difference equations which is indicated by the question marks. So far we have found orders of difference equations up to $R = 7$ for two 7-propagator topologies with identification number 30214 and 29703. It is most likely that a large part (presumably all) of the difference equations labeled with questions marks are of orders higher than we can achieve with our implementation at the moment.

t	r_{max}	Runtime
5	8	$\sim$ 1 hr
6	7	$\sim$ 2 hrs
7	6	$\sim$ 10 hrs
8	5-6	$\sim$ 1-2 days
9	4-5	$\sim$ 2-3 days
10	3-4	$\sim$ 2-3 days
11	3-4	$\sim$ 4-5 days
12	3-4	$\sim$ 5-6 days

Table 3.8: Shown are the values of r_{max} we were able to achieve in the reduction without subsectors for auxiliary topology A_{15}. The runtime given in the last column is the time necessary to process all seed integrals $I_{t,r,D,X}$ with $r \leq r_{max}, D = 0$ and X according to Tab. A.5 using up to 12 CPUs.

The reduction of auxiliary topology A_{15} without subsectors has been performed up to the values of r_{max} shown in Table 3.8. At a certain point, we decided to stop the reduction because it took too much time to process and substitute relations generated out of seed integrals with relatively small bunch sizes (typically 20 seed integral).

As mentioned before, the method of generalized recurrence relations is particularly advantageous for small numbers of positive propagators t because we are effectively working with t indices instead of M. With increasing t the advantage gets smaller and we are again faced with large combinatorics. On top of this, also the typical order R of difference equations at the 5-loop level seems to be quite

[5]Except the factorized N_k-propagator topologies $1, 6, 56, 960$ and 31744 of auxiliary topology A_1, A_3, A_6, A_{10} and A_{15}, respectively.

large and therefore reductions up to rather large r are necessary. Based on the values for r_{max} given in Tab. 3.8 we expect the remaining difference equations (cf. Tab. A.5) to be at least of order $R = 7, 6, 5, 4, 4, 4$ for the $7, 8, 9, 10, 11$ and 12-propagator topologies, respectively.

For a given sector T_t one can try and separate the seed integrals with different X and perform independent reductions for each X. This would lead to smaller numbers of seed integrals in each reduction but in the end it does not solve the problem. Eventually, it seems quite difficult to improve the existing implementation to such an extent that all difference equations at 5-loop will be accessible.

Let us now focus on the full reduction including all subsectors. The $1 + 2 + 7 + 33$ difference equations for auxiliary topology A_1, A_3, A_6 and A_{10} corresponding to the 1-, 2- ,3- and 4-loop massive tadpole have been derived without any problems. We used the already known difference equations up to the 4-loop level [103], obtained from an independent calculation, to check our results. They turn out to be in agreement. For example, let us consider topology 7 of auxiliary topology A_3, the corresponding difference equation is a nonhomogeneous difference equation of order $R = 2$ and reads

$$\sum_{j=0}^{R=2} p_j(x) J(x + j, 1, 1) = J(x, 1, 0) \frac{(2 - d)(d - 2x)}{2x} \tag{3.36}$$

with

$$p_0(x) = 2x - d\,, \qquad p_1(x) = 3 + 2x - d\,, \qquad p_2(x) = -3 - 3x\,. \tag{3.37}$$

The right-hand side of Eq. (3.36) represents the nonhomogeneous part $F(x)$ as defined in Eq. (3.16). It contains the factorized topology 6 denoted as $J(x, 1, 0)$ and can be written as a product of two 1-loop massive tadpoles

$$J(x, 1, 0) = J(x)J(1)\,, \tag{3.38}$$

where the function J on the left- and right-hand side are defined according to auxiliary topology A_3 and A_1, respectively. At this point, it is worth mentioning that before a nonhomogeneous difference equation can be solved, the function $F(x)$ needs to be determined. As we will see in Chapter 4, this function is again determined by solving appropriate difference equations.

Let us move on and consider the 5-loop case. Because of the reasons outlined above, we were not able to compute all difference equations. Only very few of those shown in Tab. A.5 are in fact available because many of the corresponding nonhomogeneous parts $F(x)$ are not fully reduced to master integrals. For instance, let us assume a 12-propagator difference equation of order $R = 5$ is given. The nonhomogeneous part $F(x)$ is basically made out of all physical subsectors T_t with $N_k \leq t < 12$ and those subsectors need to be reduced up to $r_{max} = 12 + R$. This is not possible, as can be seen from Tab. 3.8, and therefore a difference equation of that kind is completely out of range even if we were able to compute the homogeneous part in the first place. Of course, such a scenario represents the worst possible case. In practice, although we are rather limited in r_{max}, a considerable number of difference equations is available.

The difference equations we have determined in the full reduction are highlighted in Tab. A.5. Some of the difference equations have been found but are still of higher order (indicated with brackets) compared to what we have found in the reduction without subsectors. For example, the difference equation of topology 32704, $X = 3$ has $R = 2$ but we have got $R = 3$ in the full reduction; indicating that a simpler difference equation is generated later for values $r > r_{max}$. In other words, although we have determined a difference equation of order R it is not excluded that another with $R' < R$ is going to show up later. However, based on our experience it is usually the other way around.

Because of the fact that some of the difference equations are rather lengthy objects we have decided to make them online available [83]. The files contain the complete set of difference equations of auxiliary topology A_1, A_3, A_6, A_{10} as well as those indicated in Table A.5 for A_{15}.

At this point we would like to point out that the 234 difference equations summarized in Tab. A.5 are not sufficient to determine all master integrals. As it can be seen from Tab. A.6, there are in fact 14 master integrals having dots on distinct propagators which are, at first glance, not covered by the difference equation we have derived so far. That is, because we have only considered those where all propagator powers are equal to one, except the propagator which is raised to power $n_X + x$, cf. Eqs. (3.17)-(3.19). In order to solve this problem we can either derive new difference relations for these master integrals by forcing the algorithm to generate difference equations where exactly one of the propagator powers n_i, $i \neq X$ is equal to two, or by trying to find relations which relate the master integrals to those having all propagators to power one $n_i = 1, i \neq X$. We decided to proceed with the latter approach. All of the 14 above mentioned master integrals can be related to those with only one propagator having power $n_i \neq 1$ by using the relations which we derived in the reduction process of Section 3.4, cf. Eq. (3.30). As it turns out, for some masters we need to introduce integrals with more dots compared to the number of dots of the master integral we want to replace. In Figure 3.8b we have shown what integrals need to be considered if the replacement is performed for all of the 14 master integrals. Of course, that specific choice of master integrals is

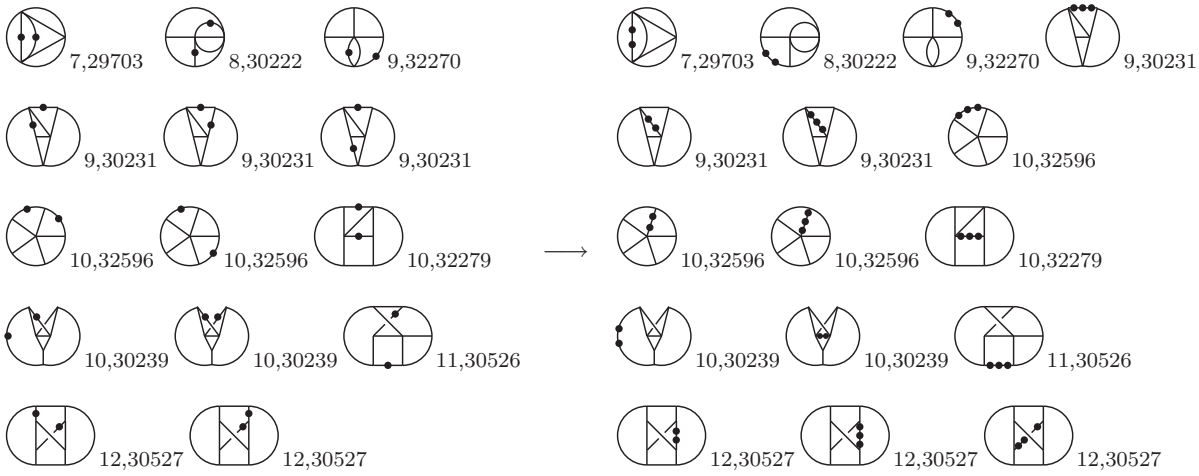

(a) The 14 master integrals which are not covered by the difference equations we have derived and summarized in Table A.5.

(b) The 14 master integrals in (a) can be expressed as a linear combination of those in Figures A.1, A.2 and 16 additional master integrals, all with dots on a single propagator.

Figure 3.8: Basis transformation for fully massive tadpoles at 5-loop with dots sitting on different propagators. The 14 master integrals with dots on different propagators are shown in (a). Our choice of new master integrals is given in (b) where all except one propagator are raised to power one. All new master integrals are covered by the difference equations summarized in Table A.5. In that sense, the new basis in Eq. (3.30) is then formed by the master integral given in Figures A.1 and A.2 where those with dots on different propagators are replaced by the master integrals in (b).

ambiguous. We could have chosen a different set of master integrals because, to a certain extent, we can decide which of the nonequivalent propagators X is raised to a higher power. For example, let us consider topology 30222 which has three non-equivalent propagators $X = 1, 2, 3$. In order to rewrite the corresponding master integral we decided to raise propagator 3 to power 3, but it would also be possible to raise propagator 2 to power 3 or propagator 1 to power 4. The master

Ad. Master	t	ID	Propagator Powers
7	7	29703	$J_{1,1,\mathbf{3},0,1,0,0,0,0,0,0,0,1,1,1}$
15	8	30222	$J_{1,1,\mathbf{3},0,1,1,0,0,0,0,0,1,1,1,0}$
23	9	32270	$J_{1,1,\mathbf{3},1,1,1,0,0,0,0,0,1,1,1,0}$
31	9	30231	$J_{\mathbf{4},1,1,0,1,1,0,0,0,0,1,0,1,1,1}$
32	9	30231	$J_{1,1,1,0,1,1,0,0,0,0,1,0,\mathbf{3},1,1}$
33	9	30231	$J_{1,1,1,0,1,1,0,0,0,0,1,0,\mathbf{4},1,1}$
37	10	32596	$J_{\mathbf{4},1,1,1,1,1,1,0,1,0,1,0,1,0,0}$
38	10	32596	$J_{1,1,1,1,1,\mathbf{3},1,0,1,0,1,0,1,0,0}$
38/1	10	32596	$J_{1,1,1,1,1,\mathbf{4},1,0,1,0,1,0,1,0,0}$
45	10	32279	$J_{\mathbf{4},1,1,1,1,1,0,0,0,0,1,0,1,1,1}$
48	10	30239	$J_{1,1,\mathbf{3},0,1,1,0,0,0,0,0,1,1,1,1,1}$
49	10	30239	$J_{1,1,1,0,1,1,0,0,0,0,0,1,1,1,\mathbf{3},1}$
59	11	30526	$J_{\mathbf{4},1,1,0,1,1,1,0,0,1,1,1,1,1,0}$
63	12	30527	$J_{\mathbf{4},1,1,0,1,1,1,0,0,1,1,1,1,1,1}$
64	12	30527	$J_{1,1,1,0,1,\mathbf{3},1,0,0,1,1,1,1,1,1}$
64/1	12	30527	$J_{1,1,1,0,1,\mathbf{4},1,0,0,1,1,1,1,1,1}$

Table 3.9: The 16 master integrals we have chosen in order to rewrite those with dots on different propagators, cf. Figure 3.8. Combining the master integrals from Tables A.2 and A.6 and replacing the 14 master integrals by those listed above we end up with $67+65+2=134$ master integrals for auxiliary topology A_{15}.

integral of sector 30222 with dots on different propagators, cf. Tab. A.2, can be expressed in terms of those with dots only on single propagators

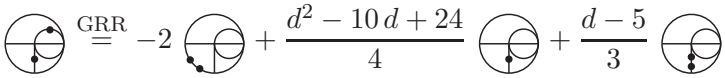

$$\overset{\text{GRR}}{=} -2 + \frac{d^2-10\,d+24}{4} + \frac{d-5}{3} + \text{subsectors}\,, \tag{3.39}$$

which are in turn covered by the difference equations shown in Tab. A.5. There is not always a one-to-one translation[6] especially in the case only a small number of nonequivalent propagators is available. As a consequence, for topology 32596 and 30527 we are left, in each case, with one more master integral and therefore 16 in total. In complete analogy to Tab. A.6, the master integrals diagrammatically shown in Fig. 3.8b are given in Table 3.9 in the usual propagator representation. The master integrals in Fig. 3.8a are, according to the ordering we have used (see Section 2.7) for the reduction, all simpler then those in Fig. 3.8b. However, from the point of solving them by means of difference equations it is exactly the other way around. As we will see in Chapter 4, it simply does not make any difference whether the integral has a propagator to power 1 or 10. The latter case is surprisingly less problematic.

We conclude this section with some addition remarks on the results. A different approach using generalized recurrence relations has been implemented and used to perform a reduction of fully massive tadpoles up to the 5-loop level. For the first time an upper limit on the number of master integrals at 5-loop is given. They are explicitly shown in Tabs. A.2 and A.6. In addition, the algorithm has been adapted to generate difference equations for the remaining master integrals. In order to check the validity of our results we performed cross-checks with already known difference equations up the 4-loop level and found that they perfectly agree. We used the implementation to go one step further and derived difference equations for a large number of physical sectors at the 5-loop level.

[6]The last two integrals in Eq. (3.39) are already master integrals and therefore we replace one master integral in terms of exactly one other.

4 Solving the System of Difference Equations by Means of Factorial Series

In Chapter 3 we have derived difference equations for fully massive tadpoles up to the 5-loop level. Now we would like to discuss how difference equations can be solved in order to get an expression for the remaining master integrals. The theory of linear difference equations [22] is well-developed (G. Boole $\sim$ 1850, N. E. Norlund 1929, L. M. Milne-Thomson 1933) and provides powerful mathematical tools to tackle those problems efficiently. However, as they are not well-known we start this chapter and review the basic concepts and tools for difference equations.

Although the theory of difference equations is known for such a long time the first work on solving actual Feynman integrals was published in 2000 by S. Laporta [18, 104] and a couple of publications [105, 13, 106] using the same method in the following years. Because of the fact that this method offers an almost automatic and independent evaluation of master integrals it became quite popular [14, 15]. The general idea is to solve linear difference equations by means of so-called factorial series. Factorial series turn out to be as important for difference equations as power series for differential equations.

This chapter is organized as follows. In Section 4.1 we introduce the basic definitions. Then in Section 4.2.1 we define the factorial series and summarize important properties. In addition, we introduce Boole's operators [22] to write the solution in terms of factorial series of difference equations in a more convenient way similar to a power series solution of a differential equation. The homogeneous and nonhomogeneous solution of the difference equation are discussed in Section 4.2.2. The general solution is a sum of all homogeneous solutions times some constants as well as a particular solution of the nonhomogeneous system. The determination of these constants will be outlined in Section 4.3 for the Euclidean massive case. Then in Section 4.4 we discuss the numerical evaluation of the factorial series. We conclude this chapter in Section 4.5 by applying the method to fully massive tadpoles up to the 5-loop level.

Although we refer from time to time to massive tadpoles, the following discussion is not restricted to that class of integrals. We try to give a concise review of solving linear difference equations by means of factorial series. The discussion presented here is based on references [18] and [22].

4.1 General Introduction and Definitions

Let us recall the notation introduced in the previous chapter for writing Feynman integrals as lists of integers

$$J''(\mathbf{n}) = J''(X, n_0, n_1, \ldots, n_M) = \int_{k_1,\ldots,k_{N_k}}^{(d')} \frac{1}{D_1^{n_1} \ldots D_X^{n_X+x} \ldots D_M^{n_M}}\,, \qquad \mathbf{n} \in \mathbb{Z}^{M+2}\,, \tag{4.1}$$

with $D_i = q_i^2 + 1$ and $d' = d - 2n_0$, $n_0 \leq 0$. The propagators are defined in an appropriate auxiliary topology such as A_1, A_3, A_6, A_{10} and A_{15} for the vacuum case in Section 3.1. In Section 3.4.1 we have observed that certain functions $J''(\mathbf{n})$ are satisfying so-called linear difference equations of

order R which are defined by (see also Eqs. (3.15)-(3.19) in Sec. 3.3.3)

$$\sum_{j=0}^{R} p_{\mathbf{n},j}(x) J''(X, n_0, n_1, \ldots, x+j, \ldots, n_M) = F_{\mathbf{n}}(x)\,, \tag{4.2}$$

where $p_{\mathbf{n},j}(x)$ are polynomials in x and space-time dimension d and $F_{\mathbf{n}}(x)$ are functions containing integrals similar to J'' but some of the denominators $D_1, D_2, \ldots, D_M$ are canceled. More precisely, if $J''(\mathbf{n})$ belongs to the t-propagator sector T_t, the function $F_{\mathbf{n}}(x)$ on the right-hand side of Eq. (4.2) is in general made out of all t'-propagator subsectors (physical ones) with t' ranging from N_k up to $t-1$. Linear difference equations are belonging to a certain class of functional equations relating functions with integer-shifted arguments. In some sense they can be seen as a discretized form of differential equations [106]. Difference equations such as in Eq. (4.2) are quite similar to the recurrence relations we have derived in Sec. 3.4 but with the difference that they relate integrals with fixed integer valued arguments rather than having an arbitrary index.

One could ask, why do we only consider difference equations in a single variable x and not those in several variables. If we consider difference equations in more than a single variable we would immediately face a system of partial difference equations which is, of course, more difficult to solve than those systems having only a single unknown variable x. Also from the numerical point of view, a system with a large number of variables (let us say a multidimensional integration) is more difficult to solve than a 1-dimensional integration if we ask for a high precision result.

In order to illustrate this let us start with an example of a homogeneous linear difference equation in a single variable [106]. The well-known Fibonacci numbers $1, 1, 2, 3, 5, 8, \ldots$ are defined through the recursive relation

$$I(n+2) = I(n+1) + I(n)\,, \tag{4.3}$$

with seed values

$$I(1) = I(2) = 1\,. \tag{4.4}$$

The recurrence relation in Eq. (4.3) can be understood as a second order linear difference equation with constant coefficients. Let us try to solve the equation by using the ansatz $I(n) = \mu^n$, we get the so-called characteristic equation

$$\mu^2 - \mu - 1 = 0\,, \tag{4.5}$$

which has two solutions

$$\mu_1 = \frac{1+\sqrt{5}}{2}\,, \qquad \mu_2 = \frac{1-\sqrt{5}}{2}\,. \tag{4.6}$$

The general solution is a linear combination of the homogeneous solutions μ_1^n and μ_2^n. The constants can be fixed by using the initial conditions in Eq. (4.4) and yields

$$I(n) = \frac{1}{\sqrt{5}}\mu_1^n - \frac{1}{\sqrt{5}}\mu_2^n\,. \tag{4.7}$$

Let us go ahead and consider another very illustrative example which is the 1-loop massive tadpole of Eq. (2.15) with

$$J(n+1) = -\frac{d-2n}{2nm^2} J(n)\,, \tag{4.8}$$

that is a homogeneous difference equation of first order. The difference equation has been derived in Eq. (2.16) using the corresponding integration-by-parts relation with arbitrary power n or in the general framework of Sec. 3.3.3 in Eq. (3.34) with generalized recurrence relations. We do not solve Eq. (4.8) at this point because we would like to introduce a general formalism first allowing to tackle that kind of problem in a more systematic way.

It is worth mentioning that contrary to what the definition of the linear difference equation in Eq. (4.2) suggests, one could also consider difference equations with respect to the space-time dimensions d' corresponding to $X = 0$. It would be rather simple to adapt the implementation[1] outlined in Sec. 3.3.3 to compute difference equations w.r.t. the space-time dimensions. However, we are not discussing this in the following. For more details see e. g. [107]. A somewhat different approach making use of the analytic properties of the integrals as functions of the space-time dimensions (which is considered to be a complex variable) called the DRA method can be found in [108, 109].

4.2 Solving the Difference Equation via Factorial Series

For reasons of convenience a slightly simplified version of the general definition in Eq. (4.2) is used. In complete analogy to Eqs. (3.17)-(3.19) we pick a specific $\mathbf{n} = (X = 1, n_0 = 0, 1, \ldots, 1) \in \mathbb{Z}^{M+2}$ corresponding to master integrals of the form

$$B = J''(1, 0, 1, \ldots, 1) = J(x, 1, \ldots, 1)\,, \tag{4.9}$$

and define the quantity

$$U(x) = J(x, 1, \ldots, 1)\,. \tag{4.10}$$

In case $x = 1$ we recover the master integrals given in Eq. (4.9), such that the general form of Eq. (4.2) becomes

$$\sum_{j=0}^{R} p_j(x) U(x + j) = F(x)\,, \tag{4.11}$$

where $p_j(x)$ and $F(x)$ are the functions $p_{\mathbf{n},j}(x)$ and $F_{\mathbf{n}}(x)$ in Eq. (4.2) for the $\mathbf{n} \in \mathbb{Z}^{M+2}$ specified above. The general solution of the nonhomogeneous Eq. (4.11) is determined by a particular solution U^{NH} of Eq. (4.11) and the general solution U^{HO} of the homogeneous equation

$$U(x) = U^{HO}(x) + U^{NH}(x)\,, \tag{4.12}$$

where the general solution U^{HO} is given by

$$U^{HO}(x) = \sum_{j=1}^{R} \tilde{\omega}_j(x) U_j^{HO}(x)\,, \tag{4.13}$$

satisfying the homogeneous equation

$$\sum_{j=0}^{R} p_j(x) U^{HO}(x + j) = 0\,. \tag{4.14}$$

The functions $\tilde{\omega}_j(x)$ in Eq. (4.13) are periodic functions of period 1 and the set $\{U_1^{HO}, \ldots, U_R^{HO}\}$ forms a fundamental system of independent solutions of Eq. (4.14). In other words, the full solution of the nonhomogeneous difference equation in Eq. (4.11) reduces to the problem of finding a fundamental system of solutions of the homogeneous equation including the determination of functions $\tilde{\omega}_j(x)$ as well as a particular solution of Eq. (4.11). For more details see Chapter XII in [22].

[1] Actually, the ordering we are using needs to be modified.

4.2.1 The Factorial Series and Boole's Operators

The factorial series of the first kind is defined by

$$\sum_{s=0}^{\infty} \frac{a_s \Gamma(x+1)}{\Gamma(x-K+s+1)} = \frac{\Gamma(x+1)}{\Gamma(x-K+1)} \left(a_0 + \frac{a_1}{x-K+1} + \frac{a_2}{(x-K+1)(x-K+2)} + \ldots \right), \quad (4.15)$$

where a_i are the coefficients of the series and K an arbitrary parameter. It turns out, the series converges in every point on the half-plane limited on the left by $\Re x = \lambda$ where λ is the abscissa of convergence. As we will see later on, the coefficients a_s we are faced with in this work behave as $|a_s| \sim s! s^{\alpha}$ for large s. For a more detailed discussion we refer to [22], Chapter X.

The general idea is to use factorial series as an ansatz for U^{HO} and U^{NH}. At this point, one could ask why to use factorial series and not a simple asymptotic expansion in $1/x$ which is quite similar to factorial series of the first kind. To answer this question, let us consider the following function [106]

$$\Psi'(x) \equiv \frac{d^2}{dn^2} \ln \Gamma(n) \quad (4.16)$$

which satisfies the nonhomogeneous first order difference equation

$$\Psi'(n+1) - \Psi'(n) = -\frac{1}{n^2}. \quad (4.17)$$

We expand Eq. (4.16) in terms of a power series in $1/n$ and obtain the asymptotic series

$$\Psi'(n) = \frac{1}{n} + \frac{1}{2n^2} + \sum_{k=1}^{\infty} \frac{B_{2k}}{n^{2k+1}}, \quad (4.18)$$

where B_{2k} are the Bernoulli numbers behaving for large k as $B_{2k} \approx 2(2k)!/(2\pi)^{2k}$. It is obvious, the expansion in Eq. (4.18) converges only for small n. On the other hand, an expansion in terms of factorial series yields

$$\Psi'(n) = \sum_{s=1}^{\infty} \frac{\Gamma(s)}{s} \frac{\Gamma(n)}{\Gamma(n+s)}, \quad (4.19)$$

being convergent for $n > 0$. Factorial series do have the advantage to be convergent on a large domain. As we will see later on, the factorial series expansions of U^{HO} and U^{NH} are evaluated for relatively large x in order to increase the convergence of the series.

The situation outlined above is quite similar to our problem except the fact that the function $\Psi'(n)$ is not known from the beginning. These functions are the master integrals we are looking for.

Before we discuss how factorial series expansions for the homogeneous and nonhomogeneous solutions U^{HO} and U^{NH} are obtained, it is convenient to introduce a special kind of symbolic operators allowing us to solve the problem in complete analogy to the method of Frobenius for ordinary differential equation. The method has been devised by Boole and therefore the operators are known as Boole's operators. Let us start and define the ρ-operator by

$$\rho^m U(x) = \frac{\Gamma(x+1)}{\Gamma(x-m+1)} U(x-m), \quad (4.20)$$

where m is a positive integer. The operator is distributive and obeys the index law

$$\rho^m \rho^n U(x) = \rho^{m+n} U(x), \quad (4.21)$$

and if the operand be unity we write

$$\rho^m 1 = \rho^m = \frac{\Gamma(x+1)}{\Gamma(x-m+1)}\,. \tag{4.22}$$

The π-operator is defined by

$$\pi U(x) = x\left[U(x) - U(x-1)\right]\,, \tag{4.23}$$

which is clearly distributive and obeys the index law. Some important properties are summarized in the following

$$\begin{aligned} [\pi,\rho]U(x) &= \rho U(x)\,,\\ (\pi+\rho)U(x) &= xU(x)\,,\\ p(\pi)\rho^m U(x) &= \rho^m p(\pi+m)U(x)\,, \end{aligned} \tag{4.24}$$

where $p(\lambda)$ is some polynomial. They can be easily proven by starting right from the operator definitions and using the property of the gamma function $\Gamma(x+1) = x\Gamma(x)$. For more details we refer to [22], Chapter XIV. Having these operators at hand, the factorial series expansion in Eq. (4.15) becomes

$$\sum_{s=0}^{\infty} \frac{a_s \Gamma(x+1)}{\Gamma(x-K+s+1)} = \sum_{s=0}^{\infty} a_s \rho^{K-s} = a_0\rho^K + a_1\rho^{K-1} + \dots\,, \tag{4.25}$$

which is an expansion in powers of ρ^{-1}. Consequently, the treatment is similar to that of a power series approach for ordinary differential equations.

4.2.2 Solution of Homogeneous and Nonhomogeneous Difference Equation

Let us recall the homogeneous difference equation from Sec. 4.2, we have

$$\sum_{j=0}^{R} p_j(x) U^{HO}(x+j) = 0\,, \tag{4.26}$$

by shifting $x \to x - R$ we get

$$\sum_{j=0}^{R} q_j(x) U^{HO}(x-j) = 0\,. \tag{4.27}$$

where $q_i(x)$ are polynomials related to the former ones by $q_j(x) = p_{R-j}(x-R)$. We perform a change of variable $U^{HO}(x) = \mu^x V^{HO}(x)$, Eq. (4.27) becomes

$$\mu^R q_0(x) V^{HO}(x) + \mu^{R-1} q_1(x) V^{HO}(x-1) + \dots + q_R(x) V^{HO}(x-R) = 0\,, \tag{4.28}$$

where μ is an unspecified parameter. We start preparing the equation in such a way that the operators of Sec. 4.2.1 can be used. Let us multiply the equation by $x(x-1)(x-2)\dots(x-R+1)$ having in mind that $xV(x-1) = \rho V(x)$, $x(x-1)V(x-2) = \rho^2 V(x)$, ... holds, we get

$$\left[\phi_0(x,\mu) + \phi_1(x,\mu)\rho + \dots + \phi_R(x,\mu)\rho^R\right] V^{HO}(x) = 0\,, \tag{4.29}$$

where ϕ_i are polynomials in variable x and μ. Because of the fact that a multiplication by x corresponds to the multiplication by $\pi + \rho$ we substitute Eqs. (4.24) as long as possible and arrive at

$$\left[f_0(\pi,\mu) + f_1(\pi,\mu)\rho + f_2(\pi,\mu)\rho^2 + \dots + f_{m+1}(\pi,\mu)\rho^{m+1}\right] V^{HO}(x) = 0\,, \tag{4.30}$$

the so-called first canonical form of the difference equations with polynomials f_i in π and μ. For the difference equations we are considering in this work, the polynomial $f_{m+1}(\pi, \mu)$ turns out to be independent of π. This fact and simple power counting in Eq. (4.30) leads immediately to an algebraic equation in μ

$$f_{m+1}(\mu) = 0\,, \tag{4.31}$$

the so-called characteristic equation. We have already encountered this equation in Eq. (4.5) in the example of Fibonacci's numbers. The characteristic equation has always R solutions different from zero. We denote the λ distinct solutions by $\mu_1, \mu_2, \ldots, \mu_\lambda$ and for each distinct solution $\mu = \mu_i, i = 1, \ldots, \lambda$ the first canonical form in Eq. (4.30) becomes

$$\Big[f_0(\pi) + f_1(\pi)\rho + f_2(\pi)\rho^2 + \cdots + f_m(\pi)\rho^m\Big]\, V^{HO}(x) = 0\,. \tag{4.32}$$

At this point we recall Eq. (4.25) and try to satisfy Eq. (4.32) with a factorial series expansion

$$V^{HO}(x) = \sum_{s=0}^{\infty} \frac{a_s \Gamma(x+1)}{\Gamma(x-K+s+1)} = \sum_{s=0}^{\infty} a_s \rho^{K-s} = a_0\rho^K + a_1\rho^{K-1} + \ldots\,, \tag{4.33}$$

leading to recurrence relations for the coefficients a_s

$$\begin{aligned}
&a_0 f_m(K+m) = 0\,,\\
&a_1 f_m(K+m-1) + a_0 f_{m-1}(K+m-1) = 0\,,\\
&a_2 f_m(K+m-2) + a_1 f_{m-1}(K+m-2) + a_0 f_{m-2}(K+m-2) = 0\,,\\
&\vdots\\
&a_s f_m(K+m-s) + a_{s-1} f_{m-1}(K+m-s) + \cdots + a_{s-m} f_0(K+m-s) = 0\,,
\end{aligned} \tag{4.34}$$

where the last row holds for $s \geq m$. Let us suppose a_0 differs from zero, then from Eq. (4.34) we obtain

$$f_m(K+m) = 0\,, \tag{4.35}$$

the so-called indicial equation having a certain number ν of roots[2], in the following denoted by $K_1, K_2, \ldots, K_\nu$. We further assume that all roots are distinct. In case there are no roots differing just by a positive integer we have

$$f_m(K+m-s) \neq 0\,, \qquad s = 1, 2, 3, \ldots\,, \tag{4.36}$$

and consequently the coefficients a_s can be successively obtained for every s through the recurrence relations in Eq. (4.34). On the other hand, if there are so-called congruent roots i. e. those only differing by a positive integer we will have $f_m(K+m-s_0) = 0$ for some specific s_0 and consequently the term $a_{s_0} f_m(K+m-s_0)$ in Eq. (4.34) is equal to zero. In this situation we are not able to determine a_{s_0} because the remaining part of the recurrence relation always vanishes for the difference equations considered here. The coefficient a_{s_0} keeps undetermined and can be freely chosen, usually we set $a_{s_0} = 0$.

Each series with $\mu_i, i = 1, \ldots, \lambda$ and corresponding solution of the indicial equation $K_{ij}, j = 1, \ldots, \nu_i$,

$$V_{ij}^{HO}(x) = \sum_{s=0}^{\infty} \frac{a_s^{(i,j)} \Gamma(x+1)}{\Gamma(x-K_{ij}+s+1)}\,, \tag{4.37}$$

[2]The number of roots ν coincides with the multiplicity of μ_i.

is a formal solution of the first canonical form given in Eq. (4.30). The coefficients $a_s^{(i,j)}$ are obtained by solving the system of recurrence relations in Eq. (4.34) for (ν_i, K_{ij}). The general solution of the homogeneous difference equation in Eq. (4.26) is a linear combination of all $\sum_{i=1}^{\lambda} \nu_i = R$ solutions

$$U^{HO}(x) = \sum_{i=1}^{\lambda} \sum_{j=1}^{\nu_i} \tilde{\omega}_{ik}(x) \mu_i^x V_{ij}^{HO}(x)\,, \tag{4.38}$$

with periodic functions $\tilde{\omega}_{ij}$ similar to those in Eq. (4.13). As we will see later, in practice, there is usually not more than one solution $U_{ij}^{HO}(x) = \mu_i^x V_{ij}^{HO}(x)$ contributing to the general solution of Eq. (4.38).

Before we proceed and discuss how one can obtain a particular solution of the nonhomogeneous difference equation in Eq. (4.11), we would like to show the concepts introduced above on the basis of the 1-loop massive tadpole [106]. Let us start and recall the difference equation from Eq. (4.8), relabeling n by x and shifting $x \to x - 1$ we get

$$m^2(x-1)J(x) - (x - 1 - d/2)J(x-1) = 0\,, \tag{4.39}$$

which is, as already mentioned, a homogeneous difference equation of first order. Let us try to find a solution in terms of factorial series by substituting $J(x) = \mu^x V(x)$,

$$\mu m^2(x-1)V(x) - (x - 1 - d/2)V(x-1) = 0\,, \tag{4.40}$$

where we have multiplied the equation by μ^{1-x}. That is exactly the form of Eq. (4.28), multiplying by x, using the fact that $xV(x-1) = \rho V(x)$ and keeping in mind that $xV(x) = (\pi + \rho)V(x)$, we obtain the first canonical form

$$\left[f_0(\pi, \mu) + f_1(\pi, \mu)\rho + f_2(\pi, \mu)\rho^2\right] V(x) = 0\,, \tag{4.41}$$

with

$$\begin{aligned} f_0(\pi, \mu) &= \mu m^2 \pi(\pi - 1)\,, \\ f_1(\pi, \mu) &= (2\mu m^2 - 1)(\pi - 1) + d/2\,, \\ f_2(\pi, \mu) &= \mu m^2 - 1\,, \end{aligned} \tag{4.42}$$

where we have used $[\pi, \rho] = \rho$ in order to shift the π-operators to the left. Indeed, f_2 is independent of π, solving the characteristic equation we get $\mu = 1/m^2$. Plugging this value into Eqs. (4.42) and solving the indicial equations $f_{m=1}(\pi = K + 1) = 0$ we obtain $K = -d/2$. Let us determine the recurrence relation for coefficient a_s, from Eq. (4.34) we immediately have

$$a_s f_1(-d/2 + 1 - s) + a_{s-1} f_0(-d/2 + 1 - s) = 0\,, \tag{4.43}$$

and consequently

$$a_s = \frac{1}{s}\left(s + \frac{d}{2}\right)\left(s + \frac{d}{2} - 1\right) a_{s-1}\,. \tag{4.44}$$

It turns out, that the recurrence relation can be solved analytically

$$a_s = \prod_{i=1}^{s} \frac{1}{i}\left(s + \frac{d}{2}\right)\left(i + \frac{d}{2} - 1\right) a_0 = \frac{1}{s!}\frac{\Gamma(d/2 + 1 + s)}{\Gamma(d/2 + 1)}\frac{\Gamma(d/2 + s)}{\Gamma(d/2)} a_0\,, \tag{4.45}$$

which is, in fact, more exception than the rule. All recurrence relations we will encounter in the following are solved numerically. This issue will be discussed in Section 4.4. The coefficient a_0 in

Eq. (4.45) remains undetermined and needs to be calculated by other means. We usually set the coefficients of homogeneous solutions to $a_0 = 1$ such that their value is absorbed in the functions $\tilde{\omega}_{ij}$ in Eq. (4.38). They can be determined by comparing the large-x behaviors of the integral $J(x)$ and its factorial series $V(x)$ as we will outline in Section 4.3. For the moment, it is sufficient to consider the large-x behavior of the 1-loop massive tadpole given in Eq. (2.15),

$$J(x) = (m^2)^{d/2-x} \int_{k_1} \frac{1}{(k_1^2+1)^n} \approx (m^2)^{d/2-x} \pi^{-d/2} \int d^d k_1 e^{-x k_1^2} = (m^2)^{d/2-x} x^{-d/2} \,. \tag{4.46}$$

The factorial series in Eq. (4.33) behaves for large x as $V(x) \approx a_0 x^K$. Plugging the values for μ and K in $U(x) = \mu^x \eta V(x)$, taking the limit to large x and comparing with Eq. (4.46) we immediately find $\eta = (m^2)^{d/2}$. Combining all ingredients, the final result becomes

$$U(x) = (m^2)^{d/2-x} \sum_{s=0}^{\infty} \frac{1}{s!} \frac{\Gamma(x+1)}{\Gamma(x+d/2+s+1)} \frac{\Gamma(d/2+1+s)}{\Gamma(d/2+1)} \frac{\Gamma(d/2+s)}{\Gamma(d/2)} \,, \tag{4.47}$$

which evaluates to the well-known expression

$$J(x) = (m^2)^{d/2-x} \frac{\Gamma(x-d/2)}{\Gamma(x)} \,. \tag{4.48}$$

In this example we performed all steps with an arbitrary mass squared m^2. It was our intention to point out where the dependence on the mass exactly enters. In the case of fully massive tadpoles with auxiliary topology A_1, A_3, A_6, A_{10} and A_{15}, cf. Fig. 3.1, the mass is equal to 1 and will be reconstructed in the end by taking into account the prefactor shown in Eq. (3.2).

Before we focus on the problem how a particular solution for the nonhomogeneous difference equation (4.11) is found, we would like to comment on the convergence of the factorial series obtained for the 1-loop massive tadpole. For large s the term in the factorial series proportional to a_s behaves as

$$\frac{a_s}{\Gamma(x+d/2+s+1)} \approx \frac{s! s^{d-1}}{s! s^{d/2+x}} = s^{d/2-1-x} \,, \tag{4.49}$$

leading to an abscissa of convergence of $x = d/2$. This means that for $x > d/2$ the series converges and the rate of convergence increases with larger values x. On the other hand, Eq. (4.49) tells us that for values $x < d/2$ the series does not converge although the final result in Eq. (4.48) works perfectly for those values. However, in general, neither the recurrence relations for the coefficients a_s nor the summation in Eq. (4.47) can be performed analytically. As we will see later, in practice, the factorial series will be evaluated numerically for values $x' = x + i$ where i is some large integer. This value can be related to the desired one, say $J(x)$, by using recurrence relations such as the relation in Eq. (4.39) recursively $J(x+i-1), J(x+i-2), \ldots, J(x)$. A more detailed discussion on the issue will follow in Section 4.4.

Let us now move on and consider the nonhomogeneous difference equation (4.11) of order R,

$$\sum_{j=0}^{R} p_j(x) U^{NH}(x+j) = F(x) \,, \tag{4.50}$$

where $U^{NH}(x)$ indicates that we are seeking for a particular solution. In complete analogy to the homogeneous case we shift $x \to x - R$ and obtain

$$\sum_{j=0}^{R} q_j(x) U^{NH}(x-j) = F'(x) \,, \tag{4.51}$$

with polynomials $q_j(x) = p_{R-j}(x-R)$ and $F'(x) = F(x-R)$. We assume that the right-hand side is already known in terms of a factorial series expansion $F'(x) = \mu^x T(x)$ with

$$T(x) = c_0\rho^K + c_1\rho^{K-1} + c_2\rho^{K-2} + \dots\,, \tag{4.52}$$

where μ, K are constants and c_i the coefficients of the series. In fact, they are in turn determined by solving appropriate difference equations for the corresponding subsectors. As before, we bring Eq. (4.51) to first canonical form by making the substitution $U^{NH}(x) = \mu'^x V^{NH}(x)$. Using the π- and ρ-operators and Eqs. (4.24) we get

$$\Big[f_0(\pi) + f_1(\pi)\rho + f_2(\pi)\rho^2 + \dots + f_m(\pi)\rho^m\Big]\, V^{NH}(x) = T(x)\,, \tag{4.53}$$

where we have already chosen $\mu' = \mu$ and substituted this value in functions $f_0(\pi), \dots, f_m(\pi)$. Let us assume $V^{NH}(x)$ has an expansion of the form

$$V^{NH}(x) = a_0\rho^{K-m} + a_1\rho^{K-m-1} + a_2\rho^{K-m-2} + \dots\,, \tag{4.54}$$

by substituting $V^{NH}(x)$ in Eq. (4.53) we obtain recurrence relations for the coefficients a_s in the manner as in Eq. (4.34),

$$\begin{aligned}
&a_0 f_m(K) = c_0\,,\\
&a_1 f_m(K-1) + a_0 f_{m-1}(K-1) = c_1\,,\\
&a_2 f_m(K-2) + a_1 f_{m-1}(K-2) + a_0 f_{m-2}(K-2) = c_2\,,\\
&\vdots\\
&a_s f_m(K-s) + a_{s-1} f_{m-1}(K-s) + \dots + a_{s-m} f_0(K-s) = c_s\,,
\end{aligned} \tag{4.55}$$

where the last row holds for $s \geq m$. As before, it can happen that $f_m(K-s_0)$ vanishes for a certain s_0 and consequently we are not able to determine a_{s_0} from Eq. (4.55). In that situation, we are free to choose a value for that coefficient. The assumption we have made regarding the structure of the nonhomogeneous part of the equation $F'(x) = \mu^x T(x)$ is usually not applicable. In fact, we are faced with a structure like

$$F'(x) = \mu^x \sum_{i=0}^{N} p_i(x) T_i(x)\,, \tag{4.56}$$

where N is the number of master integrals the nonhomogeneous part is made of. For each integral, it is necessary to have an appropriate factorial series expansion in order to proceed. With the help of Eqs. (4.24) we replace $p_i(x)$ by $p_i(\pi+\rho)$ and let the operators act on the factorial series expansion T_i. After this procedure, we are again in the situation of having an expansion as in Eq. (4.52) with new coefficients c_i'. If the factorial series $V_{NH}(x)$ converges, we have found a special solution $U^{NH}(x) = \mu^x V^{NH}(x)$ of the nonhomogeneous difference equation (4.11).

4.3 Determine Arbitrary Constants: Large-x Behavior

We have already encountered the problem of determining the function $\tilde{\omega}$ for the 1-loop massive tadpole in Eq. (4.46). In order to discuss this issue more generally let us recall the general solution of the nonhomogeneous difference equation (4.11) given by

$$U(x) = \sum_{j=1}^{R} \eta_j U_j^{HO}(x) + U^{NH}(x)\,. \tag{4.57}$$

where η_j are the constants we need to determine. In Eq. (4.57) we assumed explicitly that x is an integer valued number. In this case, the periodic functions $\tilde{\omega}_j(x)$ from Eq. (4.13) do not depend on x and can be replaced by constants η_j.

The weights η_j of the homogeneous solutions $U_j^{HO}(x)$ can be obtained by comparing the large-x behavior of the integral

$$U(x) = J(x, 1, \ldots, 1)\,, \tag{4.58}$$

and its factorial series in Eq. (4.57). Let us write the integral in Eq. (4.58) as

$$U(x) = \int_{k_1} \frac{1}{(k_1^2+1)^x}\, g(k_1)\,, \tag{4.59}$$

where we have separated the propagator carrying power x from the rest denoted by $g(k_1)$ which is a (N_k-1)-loop two-point function

$$g(k_1) = \int_{k_2,\ldots,k_{N_k}} \frac{1}{D_2 D_3 \ldots D_M}\,, \tag{4.60}$$

and can be understood, from the diagrammatic point of view, as the original diagram where the propagator carrying power x is cut away. In the following we show that the large-x behavior of Eq. (4.58) is determined by the behavior of $g(k_1)$ for small k_1. It should be pointed out, that the derivation only works in the case of massive propagators in Euclidean space-time. Let us start and write the integration in Eq. (4.59) in terms of an angular and radial part

$$U(x) = \frac{1}{\Gamma(d/2)} \int_0^\infty \frac{dk_1^2 (k_1^2)^{d/2-1}}{(k_1^2+1)^x} f(k_1^2)\,, \tag{4.61}$$

where the function f is related to g by

$$f(k_1^2) = \frac{1}{\Omega_d} \int d\Omega_d(\hat{k}_1) g(k_1)\,, \tag{4.62}$$

with $\Omega_d = 2\pi^{d/2}/\Gamma(d/2)$. The key observation is that, in the limit to large x, the denominator $(k_1^2+1)^x$ of Eq. (4.61) gives a strong contribution for values $k_1^2 \approx 0$. Because of the assumptions we have made, the function $f(k_1^2)$ behaves well for values $k_1^2 \geq 0$ which leads to the fact that the large-x behavior is solely determined by $f(k_1^2)$ for small k_1^2. Without going into great detail, it turns out that the leading asymptotic behavior of $U(x)$ is given by

$$U(x) \approx (1)^{d/2-x} x^{-d/2} f(0)\,, \tag{4.63}$$

where the first factor in brackets indicates where the mass dependence would enter in case we would have started with an arbitrary mass squared m_1^2 instead of $m_1^2 = 1$. For more details we refer to the complete derivation in reference [18], Section 5.1. If we compare Eqs. (4.59), (4.63) and (4.46) and keep in mind that $f(0) = g(0)$ we can write

$$\lim_{x\to\infty} U(x) = \int_{k_1} \frac{1}{(k_1^2+1)^x} \times g(0) = x^{-d/2} g(0)\,, \tag{4.64}$$

indicating that in the large-x limit, integral $U(x)$ factorizes into a one-loop massive tadpole having asymptotics $\sim x^{-d/2}$ times $g(0)$ corresponding to an integral with $N_k - 1$ loops. In case the integral $g(0)$ is not known it can be calculated in the same way, which means we generate the corresponding difference equations, solve them by means of factorial series and calculate the arbitrary constants of their solutions by considering the large-x behavior of a function $g'(0)$ having $N_k - 2$ loops. By repeating this procedure we can determine all arbitrary constants η_j for any difference equation.

For example, let us consider topology 51 of auxiliary topology A_6. Let us further assume we have already found the factorial series expansion (μ_i, K_i and coefficients $a_{i,s}$) for

$$U(x) \equiv J(x,1,0,0,1,1) = \quad = \int_{k_1,k_2,k_3} \frac{1}{(k_1^2+1)^x} \frac{1}{k_2^2+1} \frac{1}{(k_1-k_3)^2+1} \frac{1}{(k_2-k_3)^2+1}\,, \tag{4.65}$$

in order to compute the master integral

$$B = U(1) = J(1,1,0,0,1,1) = \quad . \tag{4.66}$$

The remaining task is to determine the weights η_j for the homogeneous solutions in Eq. (4.57). According to Eq. (4.63) they are determined by the function

$$g(0) = \int_{k_2,k_3} \frac{1}{k_2^2+1} \frac{1}{k_3^2+1} \frac{1}{(k_2-k_3)^2+1}\,, \tag{4.67}$$

which turns out to be the sunset integral

$$J(1,1,1) = \quad , \tag{4.68}$$

belonging to topology 7 of auxiliary topology A_3. Again, in case the integral $J(1,1,1)$ has not been determined yet, the corresponding difference equation[3] can be solved by means of a factorial series expansions yielding a certain combination of μ_i, K_i and coefficients $a_{i,s}$. In complete analogy, the weights η_j are determined by comparing the large-x behaviors of

$$J(x,1,1) = \quad = \int_{k_1,k_2} \frac{1}{(k_1^2+1)^x} \frac{1}{k_2^2+1} \frac{1}{(k_1-k_2)^2+1}\,, \tag{4.69}$$

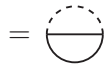

and its factorial series. Taking the limit of large x in Eq. (4.69) we get $g'(0) = J(2)$ which is the 1-loop massive tadpole with squared propagator known in terms of Γ functions; see Eq. (4.48).

4.4 Numerical Evaluation of Factorial Series

In Section 4.2.2 we have outlined how to obtain a solution of a nonhomogeneous difference equation of order R by means of factorial series expansions. The solution requires the determination of R arbitrary constants η_j, the weights of the different homogeneous solutions. They have been determined by comparing the large-x limit of the integral and its factorial series, discussed for the fully massive case in Section 4.3.

As already mentioned, it is usually not possible to solve the system of recurrence relations for coefficients a_s in Eqs. (4.34) and (4.55) analytically. The fact that it was possible for the 1-loop massive tadpole in Eq. (4.45) is only because of its simple structure. Moreover, also the summation of an infinite sum as e. g. in Eq. (4.47) constitutes a severe problem and can, in general, not be done analytically.

We tackle this problem numerically by using truncated expansions in $\epsilon = (4-d)/2$ for all quantities such as the coefficients a_s and a truncated summation of the factorial series up to a large but finite s_{max}. The truncated series are computed up to the first n_ϵ terms. Let us begin and analyze the convergence properties of the factorial series by writing

$$U^{(\alpha)}(x) = \left(\mu^{(\alpha)}\right)^x \sum_{s=0}^{\infty} a_s^{(\alpha)} \frac{\Gamma(x+1)}{\Gamma(x+1-K^{(\alpha)}+s)}\,, \tag{4.70}$$

[3] The difference equation of the massive sunset integral is given in Eqs. (3.36) and (3.37) which is a nonhomogeneous second order difference equation.

where (α) represents either a solution of the homogeneous equation or the particular solution of the nonhomogeneous difference equation. Whether the series converges or not is determined by the abscissa of convergence λ which turns out to be related to the solutions μ_j of the characteristic (4.31) by

$$\begin{array}{lll} \lambda < \infty & : & \text{if none of } \mu_j \text{ satisfies } 0 < |\mu_j/\mu^{(\alpha)} - 1| < 1 \\ \lambda = \infty & : & \text{otherwise} \end{array} , \tag{4.71}$$

where j ranges from $1, \ldots, R$. The proof can be found in [22], Chapter X. An abscissa of convergence $\lambda = \infty$ corresponds to a series which is everywhere divergent. In this case the integral $U^{(\alpha)}(1)$ needs to be calculated by other means. Fortunately, for fully massive tadpoles we have always encountered the former case in Eq. (4.71). The factorial series with $\lambda < \infty$ converges logarithmically, this means the partial sum $S_m(x)$ minus $U^{(\alpha)}(x)$ behaves for large m as

$$|S_m(x) - U^{(\alpha)}(x)| \sim m^{\lambda - x} \,. \tag{4.72}$$

The abscissa of convergence is usually around $\lambda \sim 1$ meaning a direct evaluation of $U^{(\alpha)}(1)$ is not possible. For instance, the abscissa of convergence of the 1-loop massive tadpole in Eq. (4.49) is $\lambda = 2$ in the limit $d \to 4$. From Eq. (4.72) it is easy to see that the rate of convergence increases for larger values of x. Consequently, one chooses a suitable large value x_{max}, computes the corresponding expansion $U^{(\alpha)}(x_{max}+1)$,...,$U^{(\alpha)}(x_{max}+R-1)$ and uses the recurrence relation in Eqs. (4.11) and (4.14) recursively in order to get the expansion for values $U^{(\alpha)}(x_{max}-1), \ldots, U^{(\alpha)}(1)$.

However, one should keep in mind that each iteration of the recurrence relations can result in lowering the number of significant digits E. Let us define the quantity

$$A^{-1} = \min_j |\mu_j/\mu^{(\alpha)}| \,, \tag{4.73}$$

where $j = 1, \ldots, R$. It turns out that the recurrence is unstable in case $A > 1$ inducing an error in each iteration of factor A. In case $A = 1$ and $\mu^{(\alpha)}$ being a root of the characteristic equation (4.31) having multiplicity $\nu > 1$, we observe an error increased by a factor n^{v-1} after n iterations. For more details we refer to [18], Chapter 6.1.

Let us, for example, assume we have solved the characteristic equation and found the roots $\mu_1 = 1$, $\mu_2 = -1/3$ resulting in $A = 3$. Let us further assume the factorial series in Eq. (4.70) needs to be evaluated for $x_{max} = 8$. This would lead to an error of about $3^7 \approx 2000$ or equivalently a loss of 3 significant digits. One can estimate the number of digits C necessary to start with in order to achieve a precision of E significant digits for $U^{(\alpha)}(1)$ by

$$C = E + x_{max} \log_{10} A \,. \tag{4.74}$$

From the point of view of a fixed precision arithmetic (C fixed), it is crucial to choose a value for x_{max} as small as possible but, on the other hand, having in mind that small values x_{max} require very large values of s_{max} to obtain a considerable number of significant digits E. If possible, it is advantageous to work with multiprecision arithmetics where large values for C and x_{max} can be chosen, and rather small values for s_{max} are sufficient to achieve the desired numerical precision. The actual values of C and s_{max} depend on the difference equation and will be discussed in Section 4.5 on the basis of fully massive tadpoles.

Let us conclude this section with some remarks on the truncated series in ϵ. Since all quantities are truncated expansions in ϵ up to the first n_ϵ terms with numerical coefficients, we are basically left with operations like multiplications and divisions of numbers of precision C. With respect to $U^{(\alpha)}(x)$, the dominant operation turns out to be the multiplication of series and therefore one can

estimate that the computing time of $U^{(\alpha)}(x)$ grows quadratically in n_ϵ. However, also divisions of series are involved, for the coefficients a_s in Eqs. (4.34) and (4.55) as well as in each iteration ($x \to x-1$) via the recurrence relation in Eqs. (4.11) and (4.14), but they are by far less frequent than multiplications and therefore negligible in this estimate.

Usually, it is necessary to start with an larger number n_ϵ of terms in the expansion than required in the final answer. That is, because cancellation effects can take place when series are summed, or divided by those starting with a nonvanishing power in ϵ. The number of terms n_ϵ for the expansions are determined case by case, for each difference equations separately. On top of this, it happens that so-called unphysical poles show up. They need to be removed before taking the resulting ϵ expansions as input (coefficients or arbitrary constants) for the next calculation. Unphysical poles are poles whose coefficients are almost zero (for example $< 10^{-30}$). In this case, a cutoff needs to be introduced in order to remove such poles. Otherwise we will lose a considerable amount of significant digits.

4.5 Application to Fully Massive Tadpoles up to 5-loop

In this section we describe how the difference equations obtained in Section 3.4.1 are actually processed in order to get a numerical answer for the remaining master integrals. For this task, we have implemented the procedure outlined in Section 4.2.2 in `FORM`. After the auxiliary topology, sector identification number ID as well as the information which propagator X carries the additional power $n_X + x$ is provided, it performs all the steps necessary to obtain a factorial series expansion for that sector. The program generates files for the specified difference equation containing the parameters μ_i, K_{ij} and coefficients a_s which are then handed to `Mathematica` for numerical evaluation. We decided to perform the numerics in `Mathematica` because it provides a nice balance between speed and programming efforts.

Let us consider a t-propagator difference equation. In general, the nonhomogeneous part $F(x)$ is made out of a large number of physical sectors $T_{t'}$ with $t' < t$ positive propagators. In order to compute a particular solution of the nonhomogeneous difference equation, it is necessary to have factorial series expansions for all subsectors such that the coefficients on the right-hand side of Eq. (4.53) are known. This can be achieved by starting the evaluation from the simplest topologies, that is, the topology with the smallest number of positive propagators, all the way up to the most complicated ones.

Furthermore, as we have pointed out in Section 4.3, the arbitrary constants η_j are determined by integrals having one loop less than the difference equation we are interested in. This means, before one can actually perform the numerical evaluation of a N_k-loop t-propagator difference equation, one should have already performed a similar calculation at $(N_k - 1)$-loop.

Our primary goal is to get first results at the 5-loop level rather than to recalculate the already known master integrals up to the 4-loop level [13, 14, 15]. Consequently, we only compute those integrals at the lower loops levels which are contributing to the 5-loop master integral we are interested in.

The plan of this section is as follows. In order to illustrate the numerics, we show, on the basis of the 1-loop massive tadpole, the general structure of the files generated by our routines and handed to `Mathematica`. We will explicitly show the convergence properties of the factorial series. Then we move on and consider the 2-loop sunset topology (sector 7 of auxiliary topology A_3) where we will show which of the solutions $V_{ij}^{HO}(x)$ and $V^{NH}(x)$ in fact contributes to the full solution $U(x)$ in Eq. (4.12). As we will see, almost all of the homogeneous solutions do not contribute because of wrong asymptotics in the large-x limit. For massive tadpoles, we are usually left with only one out of R homogeneous solutions as well as the particular solution of the nonhomogeneous system.

```
clear[aL1S1R0,aL1S1R1];
(* topology: L1S1 has 1/1 homogeneous solutions *)
L1S1mu1 = 1;
L1S1K1 = -1/2*d;
(* topology: L1S1 has 0 non-homogeneous solution *)
aL1S1R1[1,0] = 1;
aL1S1R1[1,-1] = 0;
aL1S1R1[dummy,1,s_] = Simplify[Solve[{0 == +aL1S1R1[1,1+s]*(-2-2*s)
      +aL1S1R1[1,s]*(2*s+2*s^2+d+2*d*s+1/2*d^2)},aL1S1R1[1,s]][[1,1,2]]];
aL1S1R1[1,s_]:= aL1S1R1[1,s] = aL1S1R1[dummy,1,s] + O[e]^emax; //Simplify
IaL1S1[x_,i_]:= N[Gamma[x+1] * Sum[aL1S1R1[2,s]/Gamma[x-L1S1K1+s+1] * s!,
      {s,i,0,-1}],acc];
(* pushdown relation *)
IaPdL1S1[dummy,X_,b__] = Simplify[Solve[{0 == -polyr[X-1/2*d,1]*
        IaPdL1S1[X,b]+polyr[X,1]*IaPdL1S1[1+X,b]},IaPdL1S1[X,b]][[1,1,2]]];
IaPdL1S1[x_,xmax_,smax_]:= IaPdL1S1[x,xmax,smax] = If[x < xmax,Simplify[
IaPdL1S1[dummy,x,xmax,smax]],IaL1S1[x,smax]];
```

Listing 4.1: The `Mathematica` code for sector 1 of auxiliary topology A_1 generated by the `FORM` routines. The file contains the parameters $\mu = 1$ and $K = -d/2$ indicated by `L1S1mu1` and `L1S1K1`. The parameters are, of course, the same as those we have derived from Eqs. (4.42). The routine finds exactly one homogeneous solution and zero nonhomogeneous solutions. The first coefficient a_1 is set to 1 (`aL1S1R1[1,0] = 1`) which is equivalent to $\eta = 1$ obtained from the large-x expansion in Eq. (4.46). In addition, the recurrence for the coefficients a_s (`aL1S1R1[dummy,1,s_]`) and 'pushdown' ($x \to x - 1$) relation (`IaPdL1S1[dummy,X_,b__]`) are given.

A typical input file for `Mathematica` is shown in Listing 4.1. It contains the parameters μ and K as well as the recurrence for coefficients a_s and the 'pushdown' relation which is repeatedly used in order to relate the $U(x_{max})$ to the desired one, say, $U(1)$. There are exactly four parameters `acc,emax,xmax` and `smax` which need to be specified by the user:

- `acc`: The number of digits used for the numerical evaluation. Corresponds to C in Eq. (4.74).
- `emax`: The number of terms up to ϵ-expansions are performed. Similar to n_ϵ in Section 4.4.
- `xmax`: The value of x where the factorial series $U(x)$ is evaluated. The value is empirically chosen and has typically a value of $x_{max} = 20, \ldots, 50$.
- `smax`: The summation of the factorial series is performed with s_{max} terms. We use values up to $s_{max} \sim 1500$.

Once all the parameter including the space-time dimensions d are specified, one can start and compute ϵ expansions for the coefficients a_s. This is done, for the example in Listing 4.1, by writing `Table[aL1S1R1[2,s] = N[aL1S1R1[1,s]/s!,acc],s,0,smax];` where so-called reduced coefficients $a'_s = a_s/s!$ are computed. That is, from the numerical point of view, necessary because in the limit to large s, the coefficients behave as $|a_s| \sim s! s^\alpha$. After this procedure, the table `aL1S1R1[2,s]` consists of $s_{max} + 1$ coefficients expanded around ϵ up to the n_ϵ-th order with accuracy C. Now, we have all the ingredients in order to start the summation of the truncated factorial series `IaL1S1[x_,i_]`. The summation is started by writing, for example `IaL1S1[10,60]`, which means the series is evaluated at $x = 10$ and truncated at $s_{max} = 60$ terms. We immediately get the ϵ expansion of $U(10)$

$$U(10) \approx 0.013889 + 0.027995\epsilon + 0.029139\epsilon^2 + 0.020779\epsilon^3 + 0.011381\epsilon^4 + \mathcal{O}(\epsilon^5)\,, \tag{4.75}$$

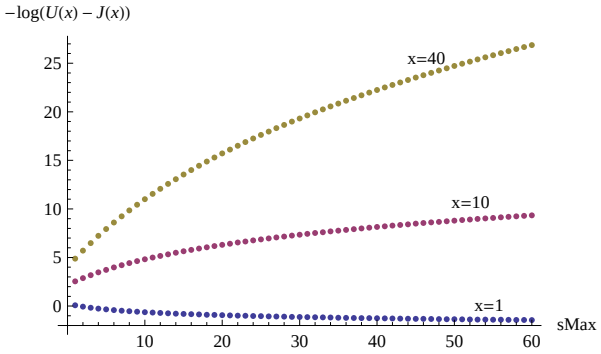

(a) The series converges pretty well for values $x > \lambda = 2$, the abscissa of convergence and, as predicted by Eq. (4.72), the rate of convergence increases for larger values of x.

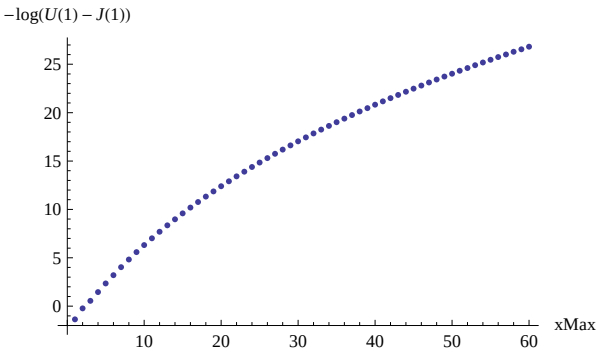

(b) The recurrence relation is repeatedly used to relate $U(x_{max})$ to $U(1)$. In this case we have $A = 1$ indicating that the recurrence relation is stable, cf. Eq. (4.73).

Figure 4.1: Numerical evaluation of fully massive tadpole $J(x)$ and its factorial series $U(x)$ in $d = 4 - 2\epsilon$ dimensions. Plotted is the logarithm of the leading term in ϵ of $J(x) - U(x)$ while varying the values for s_{max} and x_{max}. We have considered two scenarios: In (a) the factorial series is evaluated up to $s = s_{max}$ terms for three different values of $x = 1, 10, 40$. In scenario (b) we truncate the factorial series at $s_{max} = 50$ and compute $U(1)$ via the recurrence relation for values $x_{max} = 1, \ldots, 60$. The calculcation has been performed with a precision of $C = 100$ digits.

where only a 5-digit accuracy is shown. The result agrees up to an error of about 10^{-9} with the exact result $J(10)$ from Eq. (4.48). In Figure 4.1a the error is plotted on a logarithmic scale for three different values of $x = 1, 10, 40$ by varying the number of terms s_{max} included in the factorial series.

As we have already mentioned, the series cannot be evaluated at values $x \leq \lambda$ where λ is the abscissa of convergence (blue dots in Fig. 4.1a). However, these are usually the values we are interested in. In order to get an result for, say $U(1)$, we evaluate the factorial series for some large value $x = x_{max}$ where the series converges pretty well and relate that value to $U(1)$ by using the recurrence relations in Eq. (4.39) repeatedly. This is done by writing `IaPdL1S1[1,30,60]` which means $U(x)$ is evaluated at $x = 30$ with a truncated series of $s_{max} = 60$ terms and then related to $U(1)$ by applying the recurrence relations 29 times $U(29), U(28), \ldots, U(1)$. This is shown in Fig. 4.1b, where the factorial series ($s_{max} = 50$) is evaluated for different values $x = 1, \ldots, 60$ and shifted to $U(1)$ by using the recurrence relation $x_{max} - 1$ times, in case $x_{max} = 60$ we get

$$\frac{U(1)}{\Gamma(1+\epsilon)} \approx -\frac{1}{\epsilon} - 1 - \epsilon - \epsilon^2 - \epsilon^3 - \epsilon^4 + \mathcal{O}(\epsilon^5)\,, \tag{4.76}$$

with an accuracy of about 27-digits. In the case of the 1-loop massive tadpole, the recurrence relations turns out to be stable ($A = 1$) and therefore it is advantageous to choose the value x_{max} as large as possible. However, for all other difference equations we will have an unstable recurrence and therefore the value needs to be chosen carefully.

Let us now move on and consider sector 7 of auxiliary topology A_3. We show on the basis of that example which homogeneous solution is contributing and those who are discarded because of a wrong asymtotic behaviour. Starting from Eq. (4.69), we have

$$J(x,1,1) = \quad = \int_{k_1,k_2} \frac{1}{(k_1^2+1)^x} \frac{1}{k_2^2+1} \frac{1}{(k_1-k_2)^2+1}\,, \tag{4.77}$$

the corresponding difference equation can be found in Section 3.4.1 in Eqs. (3.36) and (3.37). By shifting $x \to x-2$, taking into account that

$$U(x) \equiv J(x,1,1)\,, \qquad J(x-2,1,0) = J(x-2)J(1)\,, \tag{4.78}$$

and making use of the corresponding difference equation (4.8), we can rewrite $J(x-2)$ in terms of $J(x-1)$ and get

$$(x-d)U(x-2) + (2x-d-1)U(x-1) - 3(x-1)U(x) + (d-2)J(x-1)J(1) = 0\,, \tag{4.79}$$

which is a somewhat simpler representation of the difference equation. Of course, the algorithm we have outlined in Section 3.3.3 does not take care of how the polynomials $p_i(x)$ look like. From our point of view, it is not a drawback to work with slightly more complicated polynomials because our approach is highly automated and therefore the advantage is not that big. However, for the following pen and pencil derivation it does.

In complete analogy to the procedure outlined in Section 4.2.2 we start and consider the homogeneous part of difference equation (4.79). Performing the change of variable $U(x) = \mu^x V(x)$, multiplying by $x(x-1)\mu^{2-x}$ and using the properties of the ρ- and π-operator we obtain the first canonical form

$$\left[f_0(\pi,\mu) + f_1(\pi,\mu)\rho + f_2(\pi,\mu)\rho^2 + f_3(\pi,\mu)\rho^3\right] V(x) = 0\,, \tag{4.80}$$

with

$$\begin{aligned}
f_0(\pi,\mu) &= -3\mu^2\pi^3 + 6\mu^2\pi^2 - 3\mu^2\pi\,,\\
f_1(\pi,\mu) &= \left[2\mu - 9\mu^2\right]\pi^2 + \left[21\mu^2 - (3+d)\mu\right]\pi + (d+1)\mu - 12\mu^2\,,\\
f_2(\pi,\mu) &= \left[1 + 4\mu - 9\mu^2\right]\pi - d - (5+d)\mu + 15\mu^2\,,\\
f_3(\pi,\mu) &= 1 + 2\mu - 3\mu^2\,.
\end{aligned} \tag{4.81}$$

Again, we find that f_3 is independent of π and by solving the characteristic equation we obtain $\mu_1 = -1/3$ and $\mu_2 = 1$. The corresponding values of K_i are determined by the indicial equations $f_{m=2}(\pi = K_i + 2m, \mu = \mu_i) = 0$ and give $K_1 = K_2 = 1/2 - d/2$. Before we compute the coefficients a_s via the system of recurrence relations in Eq. (4.34), we focus on the structure of the full solution

$$U(x) = \eta_1 U_1(x) + \eta_2 U_2(x) + U_3(x)\,, \tag{4.82}$$

where HO and NH in the exponent of the homogeneous and nonhomogeneous solutions are suppressed. They are written in terms of factorial series expansions and read

$$U_i(x) = \mu_i^x \sum_{s=0}^{\infty} \frac{a_s^{(i)}\Gamma(x+1)}{\Gamma(x-K_i+s+1)}\,, \qquad j = 1,2,3\,, \tag{4.83}$$

where $a_0^{(1)} = a_0^{(2)} = 1$. The weights η_1 and η_2 are determined by comparing the large-x behaviour of the series

$$\begin{aligned}
U_1(x) &\approx (1)^x x^{1/2-d/2}\,,\\
U_2(x) &\approx (-1/3)^x x^{1/2-d/2}\,,
\end{aligned} \tag{4.84}$$

and $J(x,1,1)$ which is, according to Eqs. (4.64) and (4.69), given by

$$J(x,1,1) \approx x^{-d/2} g(0) = x^{-d/2} J(2)\,, \tag{4.85}$$

which immediately yields $\eta_1 = \eta_2 = 0$. This means, because of the wrong asymptotics in the large-x limit, the homogeneous solutions U_1 and U_2 do not contribute at all. Consequently, we do not need to determine the recurrence relations for coefficients $a_i^{(1)}$ and $a_i^{(2)}$. Going back to Eq. (4.79) and keeping the nonhomogeneous part we get

$$\Big[f_0(\pi) + f_1(\pi)\rho + f_2(\pi)\rho^2\Big]\, V_3(x) = (2-d)(x-1)J(1)\rho V_J(x)\,, \tag{4.86}$$

where $U_3(x) = \mu^x V_3(x)$ and $U_J(x) = \mu^x V_J(x)$ is the factorial series expansion of the 1-loop massive tadpole with coefficients a_s as defined in Eq. (4.44). The values $\mu_3 = \mu, K_3 = K$ of the particular solution $U_3(x)$ are fixed by the factorial series expansion $U_J(x)$ with $\mu = 1$ and $K = -d/2$, cf. Eq. (4.42). Rewriting x on the right-hand side of Eq. (4.86) in terms of operator $\rho + \pi$ and plugging in the factorial series expansion of $V_3(x)$ and $V_J(x)$ we get the recurrence relation for the coefficients $a_s^{(3)}$

$$a_s^{(3)} f_2(\bar{s}) + a_{s-1}^{(3)} f_1(\bar{s}) + a_{s-2}^{(3)} f_0(\bar{s}) = (2-d)J(1)\left[a_s - \left(\frac{d}{2} + s - 1\right) a_{s-1}\right]. \tag{4.87}$$

where $\bar{s} = -d/2 + 2 - s$ and $a_s^{(3)} = 0$ for $s < 0$. We point out again that the coefficients a_s need to be determined before the recurrence relations in Eq. (4.55) can be used. Because of the fact that the homogeneous solutions $U_1(x)$ and $U_2(x)$ do not contribute, the full solution of Eq. (4.82) becomes

$$U(x) = \sum_{s=0}^{\infty} \frac{a_s^{(3)}\Gamma(x+1)}{\Gamma(x+d/2+s+1)}\,, \tag{4.88}$$

with coefficients $a_s^{(3)}$ via the recurrence relation in Eq. (4.87). Now we have everything at hand in order to perform the summation of Eq. (4.88). In analogy to Listing 4.1, a similar program code for the numerical evaluation of sector 7 of auxiliary topology A_3 is generated. For instance, by writing `IaPdL2S7[1,60,600]` and dividing the result by $\Gamma^2(1+\epsilon)$ we get

$$\begin{aligned}\frac{U(1)}{\Gamma^2(1+\epsilon)} \approx -1.5\epsilon^{-2} - 4.5\epsilon^{-1} - 6.984139142 - 18.00878162\epsilon - 27.99422356\epsilon^2 \\ - 72.00378660\epsilon^3 - 111.9974983\epsilon^4 + \mathcal{O}(\epsilon^5)\,,\end{aligned} \tag{4.89}$$

where only the first 10-digits are shown. The result agrees up to an error of 10^{-50} with the analytic result in e. g. [110]. We have used $C = 200$ digits of precision, evaluated the series at $x_{max} = 60$ and truncated the sum at $s_{max} = 600$. Because we are using the recurrence relation in Eq. (4.79) repeatedly, an error of about 3^{60}, equivalent to a loss of approximately 30 digits of precision, is induced[4].

The next step is to evaluate the basketball topology, corresponding to sector 51 of auxiliary topology A_6 we have

$$J(x,1,0,0,1,1) = \quad = \int_{k_1,k_2,k_3} \frac{1}{(k_1^2+1)^x}\frac{1}{k_2^2+1}\frac{1}{(k_1-k_3)^2+1}\frac{1}{(k_2-k_3)^2+1}\,, \tag{4.90}$$

where $U(x) \equiv J(x,1,0,0,1,1)$ satisfies a nonhomogeneous second order difference equation. Solving the corresponding characteristic and indical equations we obtain $\mu_1 = 1, \mu_2 = -1/8$ and $K_1 = -d/2, K_2 = 1-d$. According to Eq. (4.73), the iterative use of the recurrence relation is even more unstable $A = 8$. This suggests that a rather small value x_{max} should be used to evaluate the factorial series $U(x)$. As before, by comparing the large-x behaviour we get $\eta_1 = J(1,1,1)$

[4]Remember, we have $\mu_1 = -1/3$ and $\mu_2 = 1$ and therefore $A = 3$.

and $\eta_2 = 0$ where the 2-loop massive tadpole $J(1,1,1)$ is already evaluted up to high accuracy in Eq. (4.89). The full solution is then given by the homogeneous solution $U_1(x)$ in addition to the particular $U_3(x)$ with $\mu_3 = 1$ and $K_3 = -d/2 - 1$,

$$U(x) = \eta_1 U_1(x) + U_3(x)\,, \tag{4.91}$$

and numerically via `IaPdL3S51[1,40,400]` (only 10-digits are shown)

$$\begin{aligned}\frac{U(1)}{\Gamma^3(1+\epsilon)} \approx{}& -2\cdot 10^{-16}\epsilon^{-4} + 2\epsilon^{-3} + 7.666666667\epsilon^{-2} + 17.5\epsilon^{-1} + 22.91666667 \\ &+ 21.25179105\epsilon - 184.2300051\epsilon^2 - 661.1105862\epsilon^3 - 3685.054779\epsilon^4 + \mathcal{O}(\epsilon^5)\,,\end{aligned} \tag{4.92}$$

where we have performed the summation up to $s_{max} = 400$ terms evaluated at $x_{max} = 40$. The ϵ-expansion in Eq. (4.92) agrees with the result given in the literature e. g. [18]. For the first time, an unphysical pole ϵ^{-4} with small coefficient shows up. The pole is removed by introducing an appropriate cutoff parameter. Let us move on and consider topology 841 of auxiliary topology A_{10}

$$\begin{aligned}J(x,1,0,1,0,0,1,0,0,1) = {}& \quad = \int_{k_1,\ldots,k_4} \frac{1}{(k_1^2+1)^x}\frac{1}{k_2^2+1}\frac{1}{k_4^2+1}\frac{1}{(k_3-k_4)^2+1} \\ &\times \frac{1}{(k_1-k_2-k_3)^2+1}\,,\end{aligned} \tag{4.93}$$

with $U(x) \equiv J(x,1,0,1,0,0,1,0,0,1)$ satisfied by a nonhomogeneous difference equation of fourth order, cf. Tab. 3.7. The corresponding characteristic and indicial equations are solved and yield

$$\begin{aligned}\mu_1 &= 1\,, & K_1 &= 1-d\,,\\ \mu_2 &= 1\,, & K_2 &= -d/2\,,\\ \mu_3 &= -1/3\,, & K_3 &= 3/2 - 3/2d\,,\\ \mu_4 &= -1/15\,, & K_4 &= 3/2 - 3/2d\,,\end{aligned} \tag{4.94}$$

where only the second solution has the correct asymptotics $\eta_1 = \eta_3 = \eta_4 = 0$ and $\eta_2 = J(1,1,0,0,1,1)$ determined by Eq. (4.92). As before, the full solution is only a sum of one homogeneous solution and the particular solution $U_5(x)$ with $\mu_5 = 1$ and $K_5 = -d/2 - 1$,

$$U(x) = \eta_2 U_2(x) + U_5(x)\,. \tag{4.95}$$

One should have in mind, that the iterative use of the corresponding recurrence relation is unstable and due to $A = 15$ only relatively small x_{max} are practical values. The numerical evaluation is executed by `IaPdL4S841[1,20,1000]` and results in

$$\begin{aligned}\frac{U(1)}{\Gamma^4(1+\epsilon)} \approx{}& -2.5\epsilon^{-4} - 11.6666667\epsilon^{-3} - 31.7013889\epsilon^{-2} - 67.5289350\epsilon^{-1} - 140.220544 \\ &- 573.534698\epsilon - 2756.21983\epsilon^2 - 18239.9257\epsilon^3 - 86167.4785\epsilon^4 + \mathcal{O}(\epsilon^5)\,,\end{aligned} \tag{4.96}$$

which agrees in the first 7-digits with the result given in the literature e. g. [13]. The second master integral with two dots corresponding to $U(3)$, cf. Fig. 3.6, reads

$$\begin{aligned}\frac{U(3)}{\Gamma^4(1+\epsilon)} \approx{}& 1.166666667\epsilon^{-3} + 4.479166668\epsilon^{-2} + 10.05208333\epsilon^{-1} + 2.627366651 + 74.67742608\epsilon \\ &- 520.3653331\epsilon^2 + 1324.251969\epsilon^3 - 11776.14198\epsilon^4 + \mathcal{O}(\epsilon^5)\,.\end{aligned} \tag{4.97}$$

Here we have performed the summation up to $s_{max} = 1000$ terms and used the recurrence relation with $x_{max} = 20$. Unphysical poles proportional to $\epsilon^{-7}, \epsilon^{-6}$ and ϵ^{-5} have been removed in case of $U(1)$ by an appropriate cutoff. In case of $U(3)$ we removed poles proportional to $\epsilon^{-6}, \epsilon^{-5}$ and ϵ^{-4}. It should be pointed out that the numerical evaluation was performed with $C = 1150$ digits accuracy and $\epsilon_{max} = 13$.

4.5.1 The 5-loop 6-propagator topology 28686: Massive Sunset Topology

In the previous section we have prepared all the ingredients necessary to evaluate the factorial series of the first nontrivial 5-loop topology 28686

$$J(x,1,1,0,\ldots,0,1,1,1,0) = \quad = \int_{k_1,\ldots,k_5} \frac{1}{(k_1^2+1)^x} \frac{1}{k_2^2+1} \frac{1}{k_3^2+1} \frac{1}{(k_3-k_5)^2+1} \times \frac{1}{(k_4-k_5)^2+1} \frac{1}{(k_1+k_2-k_4)^2+1}\,. \tag{4.98}$$

As before, we define the function $U(x) \equiv J(x,1,1,0,\ldots,0,1,1,1,0)$ and obtain the two master integrals[5] shown in Figs. A.1 and A.2,

$$B_1 = \quad, \qquad B_2 = \quad, \tag{4.99}$$

by evaluating $B_1 = U(1)$ and $B_2 = U(3)$. The function $U(x)$ satisfies the following nonhomogeneous difference equation of fourth order

$$\sum_{j=0}^{R=4} p_j(x) U(x+j) = -15(-2+d)^4(d-2x)J(x)J^4(1) \tag{4.100}$$

with

$$\begin{aligned}
p_0(x) &= x(4-2d+x)(2-d+x)(10-5d+2x)(6-3d+2x)\,,\\
p_1(x) &= 2x(24-17d+3d^2+24x-10dx+4x^2)(120-98d+20d^2+87x-36dx+15x^2)\,,\\
p_2(x) &= 4x(1+x)(1248-932d+196d^2-8d^3+2130x-1180dx+148d^2x+975x^2\\
&\quad -294dx^2+129x^3)\,,\\
p_3(x) &= -128x(1+x)(2+x)(150-83d+11d^2+85x-26dx+11x^2)\,,\\
p_4(x) &= 768x(1+x)(2+x)(3+x)(6-2d+x)\,,
\end{aligned} \tag{4.101}$$

where common factors are canceled in order to simplify the polynomials as much as possible. This and other difference equations at 5-loop can be found in [83]. We can, as in Eq. (4.79), take advantage of the recurrence relation $J(x) = -2x/(d-2x)J(x+1)$ and simplify the polynomials further. Consequently, we can divide the equation in Eq. (4.100) by x and the factor $d-2x$ on the right-hand side cancels. This results in simpler recurrence relations for the coefficients a_s. Solving the characteristic and indicial equation, we get

$$\begin{aligned}
\mu_1 &= 1\,, & K_1 &= -1-d/2\,,\\
\mu_2 &= 1\,, & K_2 &= -d/2\,,\\
\mu_3 &= -1/8\,, & K_3 &= 2-2d\,,\\
\mu_4 &= -1/24\,, & K_4 &= 2-2d\,,
\end{aligned} \tag{4.102}$$

where we have congruent roots K_1 and K_2. For the first time we need to include two homogeneous solutions, those with $\mu_1 = 1$, $K_1 = -1-d/2$ and $\mu_2 = 1$, $K_1 = -d/2$. The corresponding weight η_1 can be fixed by comparing the next-to-leading asymptotic behavior of the factorial series

$$U(x) = \eta_1 U_1(x) + \eta_2 U_2(x) + U_5(x)\,, \tag{4.103}$$

[5]The integral B_1 can be found in the literature [111]. It was evaluated in coordinate space.

and the integral $U(x)$ in Eq. (4.98). Let us therefore recall Eqs. (4.61) and (4.62) from Section 4.3,

$$U(x) = \frac{1}{\Gamma(d/2)} \int_0^\infty \frac{dk_1^2 (k_1^2)^{d/2-1}}{(k_1^2+1)^x} f(k_1^2)\,, \tag{4.104}$$

where

$$f(k_1^2) = \frac{1}{\Omega_d} \int d\Omega_d(\hat{k}_1) g(k_1)\,, \tag{4.105}$$

with $\Omega_d = 2\pi^{d/2}/\Gamma(d/2)$, the d-dimensional solid angle and $g(k_1)$ defined as in Eq. (4.60). As we already know, the large-x behavior of Eq. (4.104) is determined by $f(k_1^2)$ for small values of k_1^2. Performing the change of variable $k_1^2 = \frac{u}{1-u}$, Eq. (4.104) takes the form

$$U(x) = \frac{1}{\Gamma(d/2)} \int_0^1 du\, u^{d/2-1} (1-u)^{x-1-d/2} \bar{f}(u)\,, \qquad \bar{f}(u) = f(u/(1-u))\,. \tag{4.106}$$

We expand the function $\bar{f}(u) = (1-u)^\beta \sum_{s=0}^\infty b_s u^s$ for small u and make use of the beta function in Eq. (1.5), we get

$$U(x) = \mu_0^x \sum_{s=0}^\infty a_s \frac{\Gamma(x+1)}{\Gamma(x+1-K_0+s)} \underset{x\to\infty}{\longrightarrow} a_0 x^{K_0} + a_1 x^{K_0-1} + \dots\,, \tag{4.107}$$

with $\mu_0 = 1$, $K_0 = -d/2$, $\beta = d/2+1$ and $a_s = b_s \Gamma(s+d/2)/\Gamma(d/2)$. The coefficients b_s can be obtained by expanding $f(k_1^2)$ for small k_1^2,

$$f(k_1^2) = \sum_{s=0}^\infty f_s (k_1^2)^s\,, \tag{4.108}$$

and comparing it with $\bar{f}(u) = f(u/(1-u))$ in an expansion for small u. We obtain $b_0 = f_0$ and $b_1 = f_1 + \beta b_0 = f_1 + \beta f_0$. For the 5-loop massive sunset integral in Eq. (4.98), the function $g(k_1)$ is given by

$$g(k_1) = \int_{k_2,\dots,k_5} \frac{1}{(k_2+k_4)^2+1} \frac{1}{k_3^2+1} \frac{1}{(k_3-k_5)^2+1} \frac{1}{(k_4-k_5)^2+1} \frac{1}{(k_1+k_2)^2+1}\,, \tag{4.109}$$

where we have shifted the momentum by $k_2 \to k_2 + k_4$. Expanding $g(k_1)$ to second order yields

$$g(k_1) = g(0) + k_{1\mu} \frac{\partial}{\partial k_{1\mu}} g(k_1)\Big|_{k_1=0} + k_{1\mu} k_{1\nu} \frac{\partial}{\partial k_{1\mu}} \frac{\partial}{\partial k_{1\nu}} g(k_1)\Big|_{k_1=0} + \dots\,, \tag{4.110}$$

where the term proportional to $k_{1\mu}$ vanishes. We take the derivatives with respect to $k_{1\mu}$ and $k_{1\nu}$ and get

$$g(k_1) = g(0) + \int_{k_2,\dots,k_5} \Big[\dots\Big] \left[-2\frac{k_1^2}{(k_2^2+1)^2} + 8\frac{(k_1\cdot k_2)^2}{(k_2^2+1)^3}\right] + \dots\,. \tag{4.111}$$

The bracket $[\dots]$ contains propagators which do not depend on the external momentum k_1, cf. Eq. (4.109). Since the second integral is proportional to k_1^2, we can easily decompose the scalar product

$$g(k_1) = g(0) + k_1^2 \int_{k_2,\dots,k_5} \Big[\dots\Big] \left[-\frac{2}{(k_2^2+1)^2} + \frac{8}{d}\frac{k_2^2+1-1}{(k_2^2+1)^3}\right] + \dots\,, \tag{4.112}$$

and perform the angular integrations to obtain $f(k_1^2)$. According to Eqs. (4.105) and (4.108) we have

$f_0 = f(0) = g(0) =$  , $\quad f_1 = -2$  $+ \frac{8}{d}\Big[$  $-$  $\Big]$. (4.113)

The 4-loop sunset integral with only one dot can be expressed (via the reduction relations obtained in Chapter 3) in terms of the sunset integral without dots

 $= \frac{5-2d}{5}$  , (4.114)

and therefore

$b_0 = f_0 =$  , $\quad b_1 = f_1 + \beta f_0 = \frac{80-42d+13d^2}{10d}$  $- \frac{8}{d}$  . (4.115)

In order to get the weights η_1 and η_2, we compare Eq. (4.107) and the solution in Eq. (4.103) for large x,

$$U(x) \approx a_0 x^{-d/2} + a_1 x^{-d/2-1} + \dots \,, \tag{4.116}$$

with $a_0 = b_0$ and $a_1 = b_1\Gamma(d/2+1)/\Gamma(d/2) = d/2\; b_1$ and consequently $\eta_1 = d/2\; b_1$, $\eta_2 = b_0$. The numerical evaluation for $x = 10$ without using the recurrence relation is done by `IaL5S28686[10,250]` and results in

$$\begin{aligned}\frac{U(10)}{\Gamma^5(1+\epsilon)} \approx {} & -0.0347222222\epsilon^{-4} - 0.255421143\epsilon^{-3} - 0.975147382\epsilon^{-2} - 2.63727153\epsilon^{-1} - 5.85855985 \\ & - 16.6156462\epsilon - 61.4446834\epsilon^2 - 370.873404\epsilon^3 - 1838.14378\epsilon^4 + \mathcal{O}(\epsilon^5)\,, \end{aligned} \tag{4.117}$$

where we performed the summation with a rather small $s_{max} = 250$ and $C = 1150$ digits accuracy. It turns out, the factorial series converges pretty well for $x = 10$. The ϵ-expansion in Eq. (4.117) is given to 9-digit accuracy. We computed the factorial series expansion for different x ranging from $5, \dots, 30$ and compared the leading term with the result obtained by `FIESTA` [112]. We found a perfect agreement. Unfortunately, we are not able to get a suitable result for $x = 1$ nor $x = 3$, yet.

x	$U(x)/\Gamma^5(1+\epsilon)$	`FIESTA`
30	-0.0030788	-0.003079
20	-0.0073099	-0.00731
10	-0.0347222	-0.034722
5	-0.2083345	-0.208331

Table 4.1: Comparison of the coefficient of the leading term $\sim \epsilon^{-4}$ with results obtained by `FIESTA`. The value for $x = 5$ is directly obtained without using the pushdown relation. The rate of convergence is, as expected, quite poor and requires a large $s_{max} = 1300$. In case of $x = 10$, 20 and 30 it is sufficient to sum up $s_{max} = 100$ terms in the truncated factorial series.

The reason is due to a numerical instability of the difference equations in Eq. (4.100) which is used for the pushdown of $U(x_{max})$ down to the desired value $U(x)$ with $x = 1, 3$. Let us therefore inspect the difference equation in more detail. In each pushdown we evaluate $U(x_i+1), \dots, U(x_i+4)$ and solve the recurrence relation for $U(x_i)$. This involves the division by $p_0(x_i)$ which has the following roots

$$x = 0,\; x = 2,\; x = 3,\; x = 4,\; x = 5\,. \tag{4.118}$$

In other words, if we try to evaluate $U(5)$ out of $U(5+1),\ldots,U(5+4)$ we run into a problem. For instance, evaluating the series for $x_{max} = 10$ and using the pushdown relation via `IaPdL5S28686[5,10,1000]` we obtain

$$\frac{U(5)}{\Gamma^5(1+\epsilon)} \approx 4.804061\cdot 10^{-7}\epsilon^{-5} - 0.2083593\epsilon^{-4} - 1.360090\epsilon^{-3} - 4.641037\epsilon^{-2} - 11.35768\epsilon^{-1} + \mathcal{O}(\epsilon^0)\,, \tag{4.119}$$

where the leading term appears because of the instability. The term proportional to ϵ^{-5} should vanish but we need to remove it with an appropriate cutoff. Even with $s_{max} = 1000$ we only achieve 10^{-7} which is rather poor. The same happens for the pushdown of $U(5) \to U(4)$, $U(4) \to U(3)$ and $U(3) \to U(2)$ which completely spoils the numerical evaluation of $U(3)$ and $U(1)$. In case of $x = 3$ with pushdown from $x_{max} = 10$ via `IaPdL5S28686[3,10,1000]` we have

$$\frac{U(3)}{\Gamma^5(1+\epsilon)} \approx 0.00005764873\epsilon^{-7} - 0.002183870\epsilon^{-6} - 0.04013510\epsilon^{-5} - 1.687390\epsilon^{-4} - 8.364475\epsilon^{-3} - 21.58991\epsilon^{-2} + \mathcal{O}(\epsilon^{-1})\,, \tag{4.120}$$

where the first relevant pole is $\sim \epsilon^{-4}$. According to `FIESTA`, its coefficient equals -1.5, we obtain $-1.687...$. Here it is not sufficient to simply increase the number of terms s_{max} in the truncated factorial series. Rather we need to improve our numerics on a deeper level in order to get results for the relevant values $x = 1$ and $x = 3$.

The first cross-check with an independent method shows that the corresponding difference equation is correct. This means, as soon as we have the numerics under control, we can proceed and start to solve the difference equations for higher topologies with $t > 6$ propagators.

5 Summary and Concluding Remarks

For this thesis we studied a certain class of vacuum integrals, the so-called fully massive tadpoles (bubbles). For this purpose, we implemented a Laporta algorithm using the algebraic manipulator FORM. This implementation was used to perform a reduction to master integrals. We have, for the first time, determined the master integrals at the 5-loop level. In addition, the implementation was modified in such a way that we were able to derive difference equations for a large number of these master integrals. Thus we started to solve the system of difference equation at the 5-loop level by means of factorial series expansions.

The Feynman integral reduction of the fully massive tadpoles up to the 5-loop level was performed with a modified Laporta approach. In contrast to the usual integration-by-parts relations we employed generalized recurrence relations based on Tarasov's idea of dimensional recurrence relations. Only the use of those special recurrence relations enabled us to go beyond the 4-loop level and study the reduction problem at 5-loop. The main idea here was to get rid of irreducible scalar products and consequently reduce the effective number of indices (propagators) in the problem of M down to t in case a t-propagator topology is considered. This was especially advantageous for topologies where t is rather small compared to M. Also the complete set of sector symmetries, playing a crucial role in the reduction process, was included. This would have hardly been possible in the traditional approach with integration-by-parts relations. Although our reduction via generalized recurrence relations was successful, we think a complete reduction at 5-loop seems to be more realistic with ordinary integration-by-parts relations and a carefully chosen set of sector symmetries. Our result on the number of master integral can be seen as an upper limit because all the symmetries are included.

Once all master integral were identified, we modified the reduction algorithm in such a way that appropriate difference equations can be derived. We computed difference equations for a considerable number of 5-loop topologies as well as rediscovered the known ones at the lower loop levels. There are 134 master integrals covered by 243 difference equations at the 5-loop level. We determined the full difference equation of 117 and the homogeneous part of 187 difference equations. In case of 56 difference equations we were not able to determine the homogeneous part and therefore even the order of that difference equation is unknown. The difference equations we found have orders up to $R = 7$ and there are, presumably, even higher ones in the set of the 56 unknown. The majority of the difference equations which we fully determined belong to topologies with a rather small number of positive propagators t. This is not very surprising since we ran into computational problems mainly due to large expressions of physical subsectors which are more and more present with increasing t. It should be pointed out that in order to get the nonhomogeneous part of the remaining difference equations, whose homogeneous part is already known, is merely a question of computing time. In the case of the 56 difference equations, where neither the homogeneous nor the nonhomogeneous part is known, we are not complete sure. It is likely, on the one hand, that some are simply of higher order R and we did not found them because of an insufficient depth in the reduction. On the other hand, for some specific topologies e. g. $31246, 32270$ or 31516 where not a single difference equation has been found so far, it seems unlikely that they are, say, all of order $R > 5$. This needs to be investigated in the future.

The master integrals satisfy the difference equations we derived. They can be solved in order to get the ϵ-expansion for the corresponding master integral. We started to solve the system of

difference equation by means of factorial series expansions in the case of the first nontrivial 5-loop topology 28686 (sunset topology). Our factorial series expansion converges but turns out to be, from the numerical point of view, problematic. We performed certain cross-checks and found agreement with the result obtained by `FIESTA`. However, in order to get high precision results for the relevant master integrals we need to improve our numerical evaluation.

In conclusion we point out that the work presented here shows that the 5-loop level is, indeed, doable and accessible with today's methods and resources.

A Appendix

A.1 Additional Figures and Tables

Topo	t	ID	Binary Rep.
1	1	1	I_1

Topo	t	ID	Binary Rep.
1	2	6	$I_{1,1,0}$
2	3	7	$I_{1,1,1}$

Topo	t	ID	Binary Rep.
1	3	56	$I_{1,1,1,0,0,0}$
2	4	60	$I_{1,1,1,1,0,0}$
3	4	51	$I_{1,1,0,0,1,1}$
4	5	62	$I_{1,1,1,1,1,0}$
5	6	63	$I_{1,1,1,1,1,1}$

Topo	t	ID	Binary Rep.
1	4	960	$I_{1,1,1,1,0,0,0,0,0,0}$
2	5	992	$I_{1,1,1,1,1,0,0,0,0,0}$
3	5	961	$I_{1,1,1,1,0,0,0,0,0,1}$
4	5	841	$I_{1,1,0,1,0,0,1,0,0,1}$
5	6	1008	$I_{1,1,1,1,1,1,0,0,0,0}$
6	6	993	$I_{1,1,1,1,1,0,0,0,0,1}$
7	6	978	$I_{1,1,1,1,0,1,0,0,1,0}$
8	6	952	$I_{1,1,1,0,1,1,1,0,0,0}$
9	7	1016	$I_{1,1,1,1,1,1,1,0,0,0}$
10	7	1012	$I_{1,1,1,1,1,1,0,1,0,0}$
11	7	1010	$I_{1,1,1,1,1,1,0,0,1,0}$
12	7	1009	$I_{1,1,1,1,1,1,0,0,0,1}$
13	8	1020	$I_{1,1,1,1,1,1,1,1,0,0}$
14	8	1011	$I_{1,1,1,1,1,1,0,0,1,1}$
15	9	1022	$I_{1,1,1,1,1,1,1,1,1,0}$
16	9	511	$I_{0,1,1,1,1,1,1,1,1,1}$

Table A.1: Our representative(s) of 1,2,5 and 16 physical sector(s) (topologies) of massive tadpoles up to 4-loop. The number of lines t, the unique identification number ID and the corresponding binary representation is shown.

Topo	t	ID	Binary Rep.
1	5	31744	$I_{1,1,1,1,1,0,0,0,0,0,0,0,0,0,0}$
2	6	32256	$I_{1,1,1,1,1,1,0,0,0,0,0,0,0,0,0}$
3	6	31746	$I_{1,1,1,1,1,1,0,0,0,0,0,0,0,0,1,0}$
4	6	29702	$I_{1,1,1,0,1,0,0,0,0,0,0,0,1,1,0}$
5	6	28686	$I_{1,1,1,0,0,0,0,0,0,0,0,1,1,1,0}$
6	7	32512	$I_{1,1,1,1,1,1,1,0,0,0,0,0,0,0,0}$
7	7	32288	$I_{1,1,1,1,1,1,0,0,0,1,0,0,0,0,0}$
8	7	32258	$I_{1,1,1,1,1,1,0,0,0,0,0,0,0,1,0}$
9	7	31754	$I_{1,1,1,1,1,0,0,0,0,0,0,1,0,1,0}$
10	7	30872	$I_{1,1,1,1,0,0,0,1,0,0,1,1,0,0,0}$
11	7	30858	$I_{1,1,1,1,0,0,0,1,0,0,0,1,0,1,0}$
12	7	30214	$I_{1,1,1,0,1,1,0,0,0,0,0,0,1,1,0}$
13	7	29703	$I_{1,1,1,0,1,0,0,0,0,0,0,0,1,1,1}$
14	8	32640	$I_{1,1,1,1,1,1,1,1,0,0,0,0,0,0,0}$
15	8	32576	$I_{1,1,1,1,1,1,1,1,0,1,0,0,0,0,0}$
16	8	32528	$I_{1,1,1,1,1,1,1,1,0,0,0,1,0,0,0}$
17	8	32513	$I_{1,1,1,1,1,1,1,1,0,0,0,0,0,0,1}$
18	8	32386	$I_{1,1,1,1,1,1,1,0,1,0,0,0,0,0,1,0}$
19	8	32274	$I_{1,1,1,1,1,1,1,0,0,0,0,0,1,0,1,0}$
20	8	32266	$I_{1,1,1,1,1,1,1,0,0,0,0,0,0,1,0,1,0}$
21	8	32259	$I_{1,1,1,1,1,1,1,0,0,0,0,0,0,0,1,1}$
22	8	31380	$I_{1,1,1,1,1,0,1,0,1,0,0,1,0,1,0,0}$
23	8	31246	$I_{1,1,1,1,1,0,1,0,0,0,0,0,1,1,1,0}$
24	8	30876	$I_{1,1,1,1,1,0,0,0,1,0,0,1,1,1,0,0}$
25	8	30862	$I_{1,1,1,1,1,0,0,0,1,0,0,0,1,1,1,0}$
26	8	30222	$I_{1,1,1,0,1,1,0,0,0,0,0,1,1,1,1,0}$
27	9	32704	$I_{1,1,1,1,1,1,1,1,1,0,0,0,0,0,0,0}$
28	9	32648	$I_{1,1,1,1,1,1,1,1,0,0,0,1,0,0,0}$
29	9	32608	$I_{1,1,1,1,1,1,1,0,1,1,0,0,0,0,0}$
30	9	32592	$I_{1,1,1,1,1,1,1,0,1,0,1,0,0,0,0}$
31	9	32529	$I_{1,1,1,1,1,1,1,0,0,0,1,0,0,0,1}$
32	9	32518	$I_{1,1,1,1,1,1,1,0,0,0,0,0,0,1,1,0}$
33	9	32394	$I_{1,1,1,1,1,1,0,1,0,0,0,1,0,1,0}$
34	9	32390	$I_{1,1,1,1,1,1,0,1,0,0,0,0,1,1,0}$
35	9	32329	$I_{1,1,1,1,1,1,1,0,0,1,0,0,1,0,0,1}$
36	9	32278	$I_{1,1,1,1,1,1,1,0,0,0,0,0,1,0,1,1,0}$
37	9	32270	$I_{1,1,1,1,1,1,1,0,0,0,0,0,0,1,1,1,0}$
38	9	32267	$I_{1,1,1,1,1,1,1,0,0,0,0,0,0,1,0,1,1}$
39	9	31516	$I_{1,1,1,1,0,1,1,0,0,0,0,1,1,1,0,0}$
40	9	31388	$I_{1,1,1,1,0,1,0,1,0,0,1,1,1,0,0}$
41	9	30231	$I_{1,1,1,0,1,1,0,0,0,0,0,1,0,1,1,1}$
42	10	32736	$I_{1,1,1,1,1,1,1,1,1,1,0,0,0,0,0}$
43	10	32712	$I_{1,1,1,1,1,1,1,1,1,0,0,1,0,0,0}$
44	10	32708	$I_{1,1,1,1,1,1,1,1,1,0,0,0,1,0,0}$
45	10	32674	$I_{1,1,1,1,1,1,1,1,0,1,0,0,0,1,0}$
46	10	32652	$I_{1,1,1,1,1,1,1,1,0,0,0,0,1,1,0,0}$
47	10	32596	$I_{1,1,1,1,1,1,1,0,1,0,1,0,1,0,0}$
48	10	32562	$I_{1,1,1,1,1,1,1,0,0,1,1,0,0,1,0}$
49	10	32534	$I_{1,1,1,1,1,1,1,0,0,0,1,0,1,1,0}$
50	10	32398	$I_{1,1,1,1,1,1,0,1,0,0,0,1,1,1,0}$
51	10	32391	$I_{1,1,1,1,1,1,0,1,0,0,0,0,1,1,1}$
52	10	32279	$I_{1,1,1,1,1,1,0,0,0,0,1,0,1,1,1}$
53	10	31420	$I_{1,1,1,1,0,1,0,1,0,1,1,1,1,0,0}$
54	10	30563	$I_{1,1,1,0,1,1,1,0,1,1,0,0,0,1,1}$
55	10	30239	$I_{1,1,1,0,1,1,0,0,0,0,1,1,1,1,1}$
56	10	29550	$I_{1,1,1,0,0,1,1,0,1,1,0,1,1,1,0}$
57	11	32744	$I_{1,1,1,1,1,1,1,1,1,1,0,1,0,0,0}$
58	11	32737	$I_{1,1,1,1,1,1,1,1,1,1,0,0,0,0,1}$
59	11	32713	$I_{1,1,1,1,1,1,1,1,1,0,0,1,0,0,1}$
60	11	32682	$I_{1,1,1,1,1,1,1,1,0,1,0,1,0,1,0}$
61	11	31736	$I_{1,1,1,1,0,1,1,1,1,1,1,1,0,0,0}$
62	11	30691	$I_{1,1,1,0,1,1,1,1,1,1,0,0,0,1,1}$
63	11	30526	$I_{1,1,1,0,1,1,1,0,0,1,1,1,1,1,0}$
64	12	32745	$I_{1,1,1,1,1,1,1,1,1,1,1,0,1,0,0,1}$
65	12	31740	$I_{1,1,1,1,0,1,1,1,1,1,1,1,1,0,0}$
66	12	30699	$I_{1,1,1,0,1,1,1,1,1,1,1,0,1,0,1,1}$
67	12	30527	$I_{1,1,1,0,1,1,1,0,0,1,1,1,1,1,1}$

Table A.2: Our representatives of all 67 physical sectors (topologies) of massive tadpoles at 5-loop. The number of lines t, the unique identification number ID and the corresponding binary representation is shown.

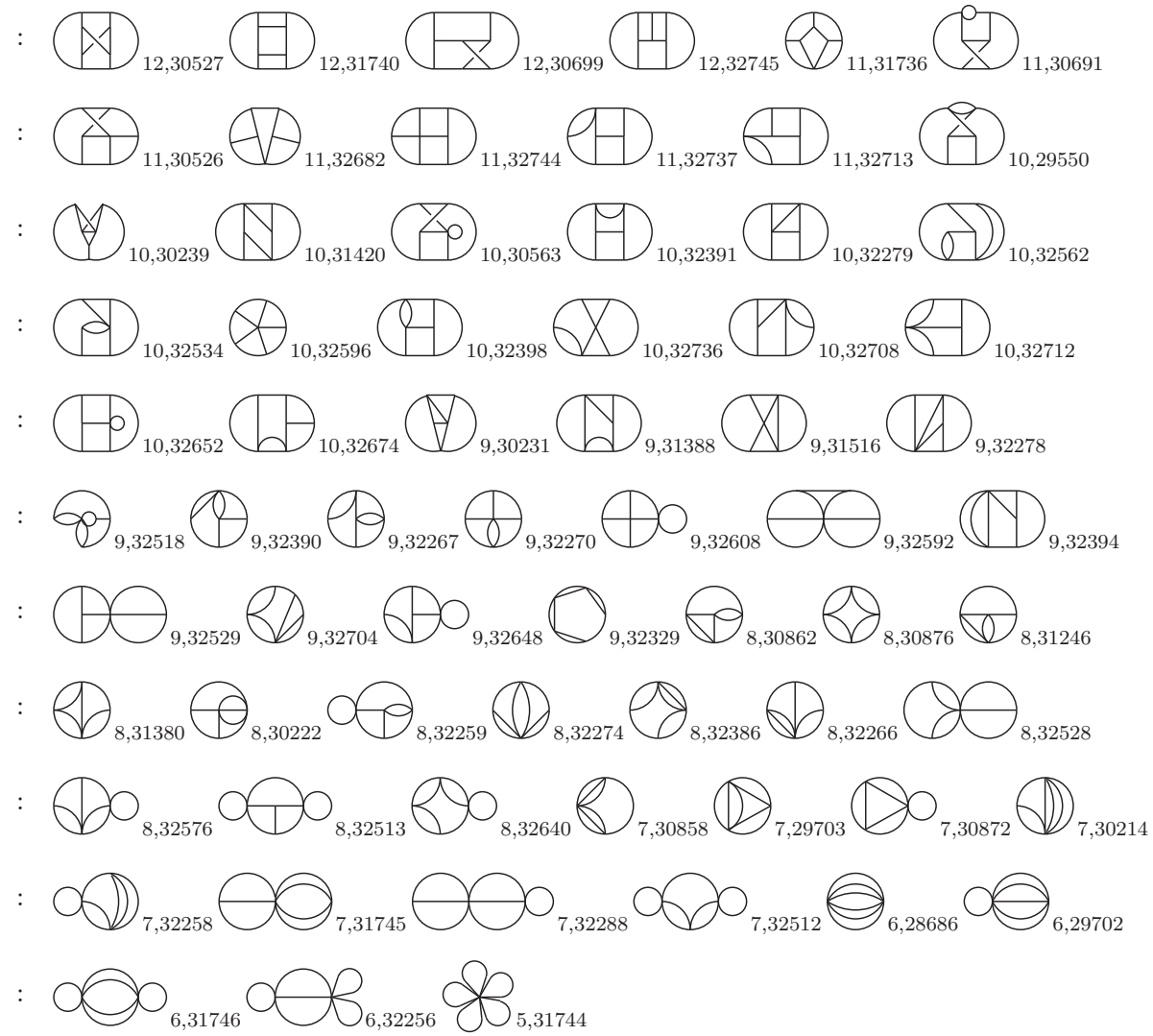

Figure A.1: The complete set of vacuum topologies at the 5-loop level is shown. The identification number ID and number of positive propagators t associated to each topology is given as subcript. The set of topologies consists of generic topologies (not factorizing) and those build out of products of topologies from lower loops. We have 48 generic vacuum topologies and 19 factorized topologies. Thanks to Jannis Schücker for providing the vacuum topologies [113].

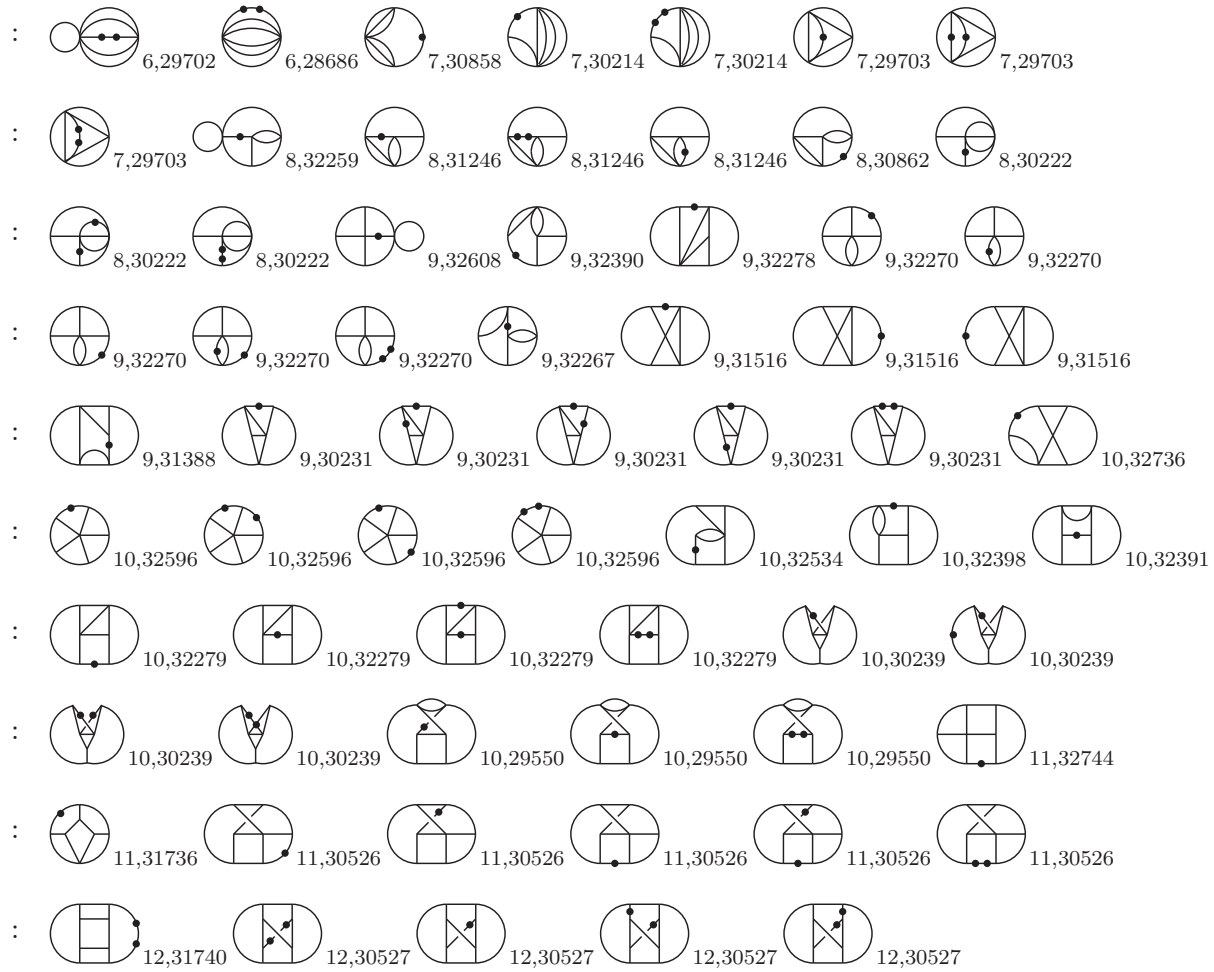

Figure A.2: In addition to those in Figure A.1 there are 65 fully massive 5-loop master integrals with dots on several propagators. A dot on a line indicates that the corresponding propagator carries an extra power. Lines without dots represent propagators with power 1.

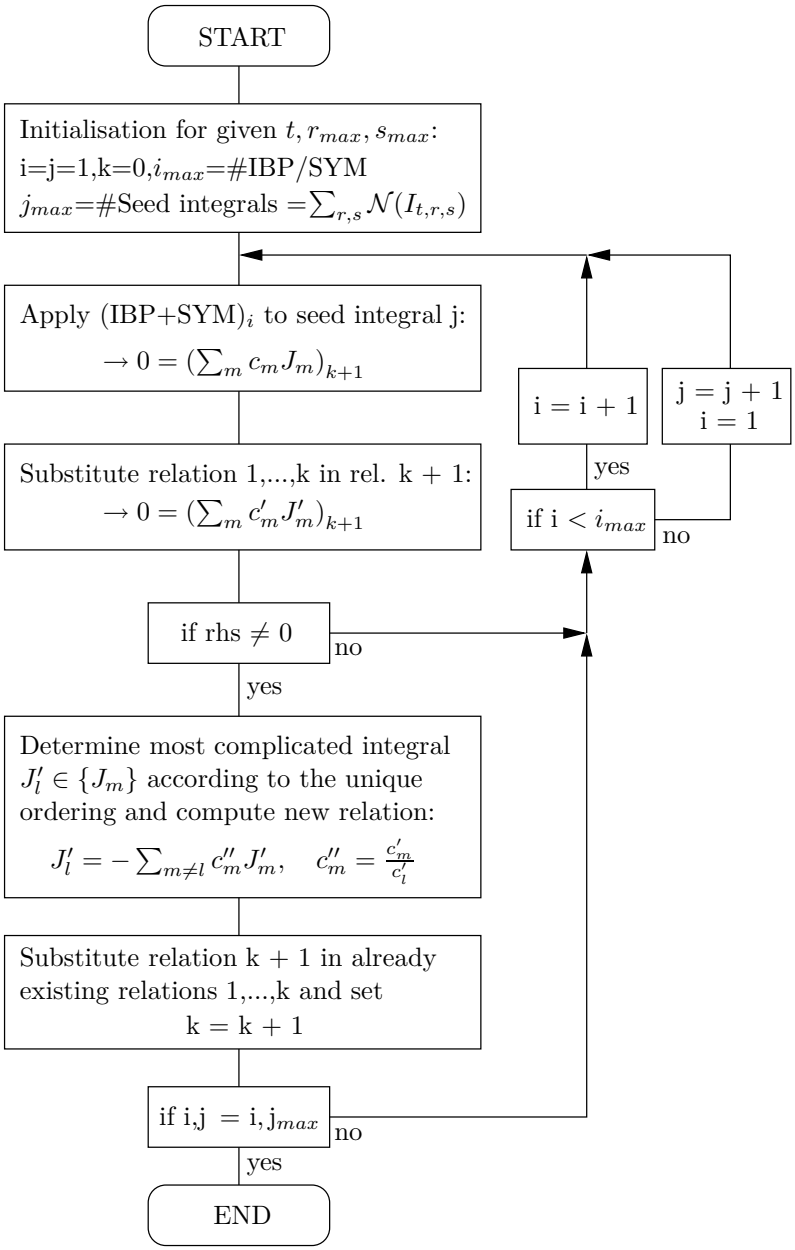

Figure A.3: The schematic of the Laporta algorithm in its basic shape. It is shown how the algorithm can be implemented in computer algebra systems. The algorithm is initialized by specifing the auxiliary topology A_M, the sector T_t (topology) under consideration and upper limits r_{max}, s_{max} for generating and processing the identities.

Topo	t	ID	S(IBP)	S(GRR)
1	1	1	1	1

Topo	t	ID	S(IBP)	S(GRR)
1	2	6	4	2
2	3	7	6	6

Topo	t	ID	S(IBP)	S(GRR)
1	3	56	24	6
2	4	60	12	6
3	4	51	24	24
4	5	62	8	8
5	6	63	24	24

Topo	t	ID	S(IBP)	S(GRR)
1	4	960	192	24
2	5	992	48	12
3	5	961	48	24
4	5	841	120	120
5	6	1008	16	8
6	6	993	12	12
7	6	978	144	72
8	6	952	48	48
9	7	1016	48	48
10	7	1012	48	24
11	7	1010	8	8
12	7	1009	8	8
13	8	1020	8	8
14	8	1011	8	8
15	9	1022	12	12
16	9	511	72	72

Table A.3: The number of sector symmetries for massive tadpoles up to 4-loop. It is shown that the number of sector symmetries in the framework of generalized recurrence relations (GRR) is considerably smaller than in the traditional approach using integration-by-parts (IBP) relations.

Topo	t	ID	S(IBP)	S(GRR)
1	5	31744	1920	120
2	6	32256	288	36
3	6	31746	192	48
4	6	29702	240	120
5	6	28686	720	720
6	7	32512	64	16
7	7	32288	288	72
8	7	32258	24	12
9	7	31754	288	144
10	7	30872	96	48
11	7	30858	72	72
12	7	30214	48	48
13	7	29703	48	48
14	8	32640	96	48
15	8	32576	16	8
16	8	32528	96	48
17	8	32513	192	48
18	8	32386	48	48
19	8	32274	16	16
20	8	32266	12	12
21	8	32259	16	8
22	8	31380	16	16
23	8	31246	8	8
24	8	30876	384	384
25	8	30862	32	32
26	8	30222	24	24
27	9	32704	16	16
28	9	32648	16	8
29	9	32608	16	8
30	9	32592	8	8
31	9	32529	288	144
32	9	32518	48	48
33	9	32394	24	24
34	9	32390	4	4
35	9	32329	384	384
36	9	32278	8	8
37	9	32270	4	4
38	9	32267	16	16
39	9	31516	4	4
40	9	31388	32	32
41	9	30231	12	12
42	10	32736	4	4
43	10	32712	8	8
44	10	32708	8	8
45	10	32674	32	32
46	10	32652	24	12
47	10	32596	10	10
48	10	32562	32	32
49	10	32534	4	4
50	10	32398	4	4
51	10	32391	8	8
52	10	32279	2	2
53	10	31420	32	32
54	10	30563	144	72
55	10	30239	12	12
56	10	29550	16	16
57	11	32744	2	2
58	11	32737	4	4
59	11	32713	8	8
60	11	32682	32	32
61	11	31736	4	4
62	11	30691	16	16
63	11	30526	4	4
64	12	32745	4	4
65	12	31740	48	48
66	12	30699	12	12
67	12	30527	16	16

Table A.4: The number of sector symmetries for massive tadpoles at 5-loop. It is shown that the number of sector symmetries in the framework of generalized recurrence relations (GRR) is considerably smaller than in the traditional approach using integration-by-parts (IBP) relations.

Topo	t	ID	Propag X	Order R
1	5	31744	1	1
2	6	32256	1,2	2,1
3	6	31746	1,3	2,1
4	6	29702	1,3	4,1
5	6	28686	1	4
6	7	32512	1,2,3	2,1,2
7	7	32288	1,5	2,1
8	7	32258	1,2,3,5	5,2,2,1
9	7	31754	1,3	2,2
10	7	30872	1,4	2,1
11	7	30858	1,2	5,2
12	7	30214	1,2,3	7,4,2
13	7	29703	1,3	7,?
14	8	32640	1,2,3	2,1,2
15	8	32576	1,2,5,6	2,2,1,2
16	8	32528	1,2,3	2,2,2
17	8	32513	1,2	2,1
18	8	32386	1,2,3	5,2,2
19	8	32274	1,3,4	5,2,2
20	8	32266	1,2,3,5,6	5,2,2,2,2
21	8	32259	1,2,3,5	3,3,3,1
22	8	31380	1,2,3,8	?,2,2,2
23	8	31246	1,2,4,6	?,?,?,?
24	8	30876	1	2
25	8	30862	1,2	4,3
26	8	30222	1,2,3	?,?,?
27	9	32704	1,2,3,4,6	2,2,2(3),2,2
28	9	32648	1,2,3,4,12	3,1,2,2,2
29	9	32608	1,5,6	4,1,3
30	9	32592	1,3,4,6	2,2,2,2
31	9	32529	1,2	2,2
32	9	32518	1,2	2,2
33	9	32394	1,2,3,12	5,2,2,2
34	9	32390	1,2,3,4,5,8,13	?,3,2,3,3,3,3
35	9	32329	1,3	2,2
36	9	32278	1,2,3,5,14	?,3,2,3,3
37	9	32270	1,2,3,6,12	?,?,?,?,?
38	9	32267	1,2,3,5	3,3,4,2
39	9	31516	1,2,3,6,12	?,?,?,?,?
40	9	31388	1,2,6	3,4,3
41	9	30231	1,13	?,?
42	10	32736	1,2,3,5,6,9	?,4,4,2,3,3
43	10	32712	1,2,5,6,8	3,2,2,2,2
44	10	32708	1,2,3,4,6,13	3,2,2,2,2,2
45	10	32674	1,2,3,4	3,2,2,2
46	10	32652	1,2,3	3,1,2
47	10	32596	1,6	?,?
48	10	32562	1,3,4	3,2,2
49	10	32534	1,2,3,4,11,13	?,4,2,4,3,3
50	10	32398	1,2,3,4,5,6	?,3,2,3,?,2
51	10	32391	1,2,3,6	?,4,3,3
52	10	32279	1,3,4,6,13,14	?,?,?,?,?,?
53	10	31420	1,6	3,3
54	10	30563	1,5	3,1
55	10	30239	1,3,14	?,?,?
56	10	29550	1,6,12	?,?,?
57	11	32744	1,2,5,6,7,8,10	?,4,2,?,3,2,3
58	11	32737	1,2,3,5,6,9,15	3,2,3,2,2,2,3
59	11	32713	1,2,3,4,7	3,2,2,2,2
60	11	32682	1,2,3	2,2,2
61	11	31736	1,3,4,7	?,3,3,?
62	11	30691	1,2,3,5	?,3,3,2
63	11	30526	1,2,3,6,7	?,?,?,?,?
64	12	32745	1,2,3,7,8	3,2,3,2,2
65	12	31740	1	?
66	12	30699	1,2,5	?,3,2
67	12	30527	1,6	?,?

Table A.5: The order R of difference equations for all topologies of auxiliary topology A_{15}. The last two columns show all non-equivalent propagators X and the order R of the difference equation which is associated with that propagator. A question mark indicates that the corresponding difference equation (more precisely the homogeneous part) has not been determined, yet. Those difference equations whose nonhomogeneous part $G_n(x)$ is known are indicated in red.

Ad. Master	t	ID	Propagator Powers
1	6	29702	$J_{\mathbf{3},1,1,0,1,0,0,0,0,0,0,1,1,0}$
2	6	28686	$J_{\mathbf{3},1,1,0,0,0,0,0,0,0,0,1,1,1,0}$
3	7	30858	$J_{\mathbf{2},1,1,1,0,0,0,1,0,0,0,1,0,1,0}$
4	7	30214	$J_{\mathbf{2},1,1,0,1,1,0,0,0,0,0,0,1,1,0}$
5	7	30214	$J_{\mathbf{3},1,1,0,1,1,0,0,0,0,0,0,1,1,0}$
6	7	29703	$J_{\mathbf{2},1,1,0,1,0,0,0,0,0,0,0,1,1,1}$
7	7	29703	$J_{\mathbf{2},\mathbf{2},1,0,1,0,0,0,0,0,0,0,1,1,1}$
8	7	29703	$J_{\mathbf{3},1,1,0,1,0,0,0,0,0,0,0,1,1,1}$
9	8	32259	$J_{\mathbf{2},1,1,1,1,1,0,0,0,0,0,0,0,1,1}$
10	8	31246	$J_{1,\mathbf{2},1,1,0,1,0,0,0,0,0,1,1,1,0}$
11	8	31246	$J_{\mathbf{2},1,1,1,0,1,0,0,0,0,0,1,1,1,0}$
12	8	31246	$J_{\mathbf{3},1,1,1,0,1,0,0,0,0,0,1,1,1,0}$
13	8	30862	$J_{\mathbf{2},1,1,1,0,0,0,1,0,0,0,1,1,1,0}$
14	8	30222	$J_{\mathbf{2},1,1,0,1,1,0,0,0,0,0,1,1,1,0}$
15	8	30222	$J_{\mathbf{2},\mathbf{2},1,0,1,1,0,0,0,0,0,1,1,1,0}$
16	8	30222	$J_{\mathbf{3},1,1,0,1,1,0,0,0,0,0,1,1,1,0}$
17	9	32608	$J_{\mathbf{2},1,1,1,1,1,1,0,1,1,0,0,0,0,0}$
18	9	32390	$J_{\mathbf{2},1,1,1,1,1,1,0,1,0,0,0,0,1,1,0}$
19	9	32278	$J_{\mathbf{2},1,1,1,1,1,1,0,0,0,0,0,1,0,1,1,0}$
20	9	32270	$J_{1,1,\mathbf{2},1,1,1,0,0,0,0,0,1,1,1,0}$
21	9	32270	$J_{1,\mathbf{2},1,1,1,1,0,0,0,0,0,1,1,1,0}$
22	9	32270	$J_{\mathbf{2},1,1,1,1,1,0,0,0,0,0,1,1,1,0}$
23	9	32270	$J_{\mathbf{2},\mathbf{2},1,1,1,1,0,0,0,0,0,1,1,1,0}$
24	9	32270	$J_{\mathbf{3},1,1,1,1,1,0,0,0,0,0,1,1,1,0}$
25	9	32267	$J_{\mathbf{2},1,1,1,1,1,0,0,0,0,0,1,0,1,1}$
26	9	31516	$J_{1,1,\mathbf{2},1,0,1,1,0,0,0,1,1,1,0,0}$
27	9	31516	$J_{1,\mathbf{2},1,1,0,1,1,0,0,0,1,1,1,0,0}$
28	9	31516	$J_{\mathbf{2},1,1,1,0,1,1,0,0,0,1,1,1,0,0}$
29	9	31388	$J_{\mathbf{2},1,1,1,0,1,0,1,0,0,1,1,1,0,0}$
30	9	30231	$J_{\mathbf{2},1,1,0,1,1,0,0,0,0,1,0,1,1,1}$
31	9	30231	$J_{\mathbf{2},1,1,0,1,1,0,0,0,0,\mathbf{2},0,1,1,1}$
32	9	30231	$J_{\mathbf{2},1,\mathbf{2},0,1,1,0,0,0,0,1,0,1,1,1}$
33	9	30231	$J_{\mathbf{2},\mathbf{2},1,0,1,1,0,0,0,0,1,0,1,1,1}$
34	9	30231	$J_{\mathbf{3},1,1,0,1,1,0,0,0,0,1,0,1,1,1}$
35	10	32736	$J_{\mathbf{2},1,1,1,1,1,1,1,1,1,1,0,0,0,0,0}$
36	10	32596	$J_{\mathbf{2},1,1,1,1,1,1,1,0,1,0,1,0,1,0,0}$
37	10	32596	$J_{\mathbf{2},1,\mathbf{2},1,1,1,1,1,0,1,0,1,0,1,0,0}$
38	10	32596	$J_{\mathbf{2},\mathbf{2},1,1,1,1,1,1,0,1,0,1,0,1,0,0}$
39	10	32596	$J_{\mathbf{3},1,1,1,1,1,1,1,0,1,0,1,0,1,0,0}$
40	10	32534	$J_{\mathbf{2},1,1,1,1,1,1,1,0,0,0,1,0,1,1,0}$
41	10	32398	$J_{\mathbf{2},1,1,1,1,1,1,0,1,0,0,0,1,1,1,0}$
42	10	32391	$J_{\mathbf{2},1,1,1,1,1,1,0,1,0,0,0,0,0,1,1,1}$
43	10	32279	$J_{1,1,1,\mathbf{2},1,1,0,0,0,0,1,0,1,1,1}$
44	10	32279	$J_{\mathbf{2},1,1,1,1,1,1,0,0,0,0,1,0,1,1,1}$
45	10	32279	$J_{\mathbf{2},\mathbf{2},1,1,1,1,1,0,0,0,0,1,0,1,1,1}$
46	10	32279	$J_{\mathbf{3},1,1,1,1,1,1,0,0,0,0,1,0,1,1,1}$
47	10	30239	$J_{\mathbf{2},1,1,0,1,1,0,0,0,0,1,1,1,1,1}$
48	10	30239	$J_{\mathbf{2},1,\mathbf{2},0,1,1,0,0,0,0,1,1,1,1,1}$
49	10	30239	$J_{\mathbf{2},\mathbf{2},1,0,1,1,0,0,0,0,1,1,1,1,1}$
50	10	30239	$J_{\mathbf{3},1,1,0,1,1,0,0,0,0,1,1,1,1,1}$
51	10	29550	$J_{1,1,1,0,0,\mathbf{2},1,0,1,1,0,1,1,1,0}$
52	10	29550	$J_{\mathbf{2},1,1,0,0,1,1,0,1,1,0,1,1,1,0}$
53	10	29550	$J_{\mathbf{3},1,1,0,0,1,1,0,1,1,0,1,1,1,0}$
54	11	32744	$J_{\mathbf{2},1,1,1,1,1,1,1,1,1,1,0,1,0,0,0}$
55	11	31736	$J_{\mathbf{2},1,1,1,0,1,1,1,1,1,1,1,0,0,0}$
56	11	30526	$J_{1,1,\mathbf{2},0,1,1,1,0,0,1,1,1,1,1,0}$
57	11	30526	$J_{1,\mathbf{2},1,0,1,1,1,0,0,1,1,1,1,1,0}$
58	11	30526	$J_{\mathbf{2},1,1,0,1,1,1,0,0,1,1,1,1,1,0}$
59	11	30526	$J_{\mathbf{2},\mathbf{2},1,0,1,1,1,0,0,1,1,1,1,1,0}$
60	11	30526	$J_{\mathbf{3},1,1,0,1,1,1,0,0,1,1,1,1,1,0}$
61	12	31740	$J_{\mathbf{3},1,1,1,0,1,1,1,1,1,1,1,1,0,0}$
62	12	30527	$J_{\mathbf{2},1,1,0,1,1,1,0,0,1,1,1,1,1,1}$
63	12	30527	$J_{\mathbf{2},1,\mathbf{2},0,1,1,1,0,0,1,1,1,1,1,1}$
64	12	30527	$J_{\mathbf{2},\mathbf{2},1,0,1,1,1,0,0,1,1,1,1,1,1}$
65	12	30527	$J_{\mathbf{3},1,1,0,1,1,1,0,0,1,1,1,1,1,1}$

Table A.6: In addition to those in Table A.2 there are master integrals with dots on some propagators. In this context, the representatives in Table A.2 denoted as $I_{\ldots}$ are understood as the master integrals $J_{\ldots}$ without dots. Combining both tables we end up with $67 + 65 = 132$ master integrals for auxiliary topology A_{15}.

Bibliography

[1] R.P. Feynman. Space - time approach to quantum electrodynamics. *Phys.Rev.*, 76:769–789, 1949.

[2] Michelangelo L. Mangano and Stephen J. Parke. Multiparton amplitudes in gauge theories. *Phys.Rept.*, 200:301–367, 1991.

[3] Lance J. Dixon. Calculating scattering amplitudes efficiently. 1996.

[4] Gerard 't Hooft. Dimensional regularization and the renormalization group. *Nucl.Phys.*, B61:455–468, 1973.

[5] Mikolaj Misiak and Manfred Munz. Two loop mixing of dimension five flavor changing operators. *Phys.Lett.*, B344:308–318, 1995.

[6] T. van Ritbergen, J.A.M. Vermaseren, and S.A. Larin. The Four loop beta function in quantum chromodynamics. *Phys.Lett.*, B400:379–384, 1997.

[7] K.G. Chetyrkin. Four-loop renormalization of QCD: Full set of renormalization constants and anomalous dimensions. *Nucl.Phys.*, B710:499–510, 2005.

[8] M. Czakon. The Four-loop QCD beta-function and anomalous dimensions. *Nucl.Phys.*, B710:485–498, 2005.

[9] Y. Schroder and M. Steinhauser. Four-loop singlet contribution to the rho parameter. *Phys.Lett.*, B622:124–130, 2005.

[10] R. Boughezal and M. Czakon. Single scale tadpoles and O(G(F m(t)**2 alpha(s)**3)) corrections to the rho parameter. *Nucl.Phys.*, B755:221–238, 2006.

[11] Y. Schröder. Tackling the infrared problem of thermal QCD. *Nucl.Phys.Proc.Suppl.*, 129:572–574, 2004.

[12] K. Kajantie, M. Laine, K. Rummukainen, and Y. Schröder. Four loop vacuum energy density of the SU(N(c)) + adjoint Higgs theory. *JHEP*, 0304:036, 2003.

[13] Stefano Laporta. High precision epsilon expansions of massive four loop vacuum bubbles. *Phys.Lett.*, B549:115–122, 2002.

[14] Y. Schröder and A. Vuorinen. High precision evaluation of four loop vacuum bubbles in three-dimensions. 2003.

[15] Y. Schröder and A. Vuorinen. High-precision epsilon expansions of single-mass-scale four-loop vacuum bubbles. *JHEP*, 0506:051, 2005.

[16] K. G. Chetyrkin and F. V. Tkachov. Integration by Parts: The Algorithm to Calculate beta Functions in 4 Loops. *Nucl. Phys.*, B192:159–204, 1981.

[17] F.V. Tkachov. A Theorem on Analytical Calculability of Four Loop Renormalization Group Functions. *Phys.Lett.*, B100:65–68, 1981.

[18] S. Laporta. High precision calculation of multiloop Feynman integrals by difference equations. *Int.J.Mod.Phys.*, A15:5087–5159, 2000.

[19] J.A.M. Vermaseren. The Symbolic manipulation program FORM. 1992.

[20] J.A.M. Vermaseren. New features of FORM. 2000.

[21] J.A.M. Vermaseren. FORM development. *PoS*, CPP2010:012, 2010.

[22] L. M. Milne-Thomson. *The Calculus of Finite Differences*. Macmillan, London, 1965.

[23] Michael E. Peskin and Daniel V. Schroeder. *An Introduction to Quantum Field Theory*. Westview, 1995.

[24] N.N. Bogoliubov and D.V. Shirkov. *Introduction to the Theory of Quantized Fields*. J. Wiley, New York, 1980.

[25] C. Itzykson and J.-B. Zuber. *Quantum Field Theory*. McGraw-Hill Book Company, 1980.

[26] Chen-Ning Yang and Robert L. Mills. Conservation of Isotopic Spin and Isotopic Gauge Invariance. *Phys.Rev.*, 96:191–195, 1954.

[27] Konstantin G. Chetyrkin, Mikolaj Misiak, and Manfred Munz. Beta functions and anomalous dimensions up to three loops. *Nucl.Phys.*, B518:473–494, 1998.

[28] Thomas Appelquist and Robert D. Pisarski. High-Temperature Yang-Mills Theories and Three-Dimensional Quantum Chromodynamics. *Phys.Rev.*, D23:2305, 1981.

[29] David J. Gross, Robert D. Pisarski, and Laurence G. Yaffe. QCD and Instantons at Finite Temperature. *Rev.Mod.Phys.*, 53:43, 1981.

[30] Andrei D. Linde. Infrared Problem in Thermodynamics of the Yang-Mills Gas. *Phys.Lett.*, B96:289, 1980.

[31] Eric Braaten. Solution to the perturbative infrared catastrophe of hot gauge theories. *Phys.Rev.Lett.*, 74:2164–2167, 1995.

[32] Eric Braaten and Agustin Nieto. Effective field theory approach to high temperature thermodynamics. *Phys.Rev.*, D51:6990–7006, 1995.

[33] W. Pauli and F. Villars. On the Invariant regularization in relativistic quantum theory. *Rev.Mod.Phys.*, 21:434–444, 1949.

[34] Gerard 't Hooft and M.J.G. Veltman. Regularization and Renormalization of Gauge Fields. *Nucl.Phys.*, B44:189–213, 1972.

[35] H. David Politzer. Reliable Perturbative Results for Strong Interactions? *Phys.Rev.Lett.*, 30:1346–1349, 1973.

[36] D.J. Gross and Frank Wilczek. Ultraviolet Behavior of Nonabelian Gauge Theories. *Phys.Rev.Lett.*, 30:1343–1346, 1973.

[37] William E. Caswell. Asymptotic Behavior of Nonabelian Gauge Theories to Two Loop Order. *Phys.Rev.Lett.*, 33:244, 1974.

[38] D.R.T. Jones. Two Loop Diagrams in Yang-Mills Theory. *Nucl.Phys.*, B75:531, 1974.

[39] O.V. Tarasov, A.A. Vladimirov, and A. Yu. Zharkov. The Gell-Mann-Low Function of QCD in the Three Loop Approximation. *Phys.Lett.*, B93:429–432, 1980.

[40] S.A. Larin and J.A.M. Vermaseren. The Three loop QCD Beta function and anomalous dimensions. *Phys.Lett.*, B303:334–336, 1993.

[41] K.G. Chetyrkin and T. Seidensticker. Two loop QCD vertices and three loop MOM beta functions. *Phys.Lett.*, B495:74–80, 2000.

[42] M. Veltman. SCHOONSCHIP. *CERN Preprint*, 1967.

[43] A.A. Vladimirov. Method for Computing Renormalization Group Functions in Dimensional Renormalization Scheme. *Theor.Math.Phys.*, 43:417, 1980.

[44] John C. Collins. Normal Products in Dimensional Regularization. *Nucl.Phys.*, B92:477, 1975.

[45] K.G. Chetyrkin and Vladimir A. Smirnov. R* Operation Corrected. *Phys.Lett.*, B144:419–424, 1984.

[46] L.F. Abbott. The Background Field Method Beyond One Loop. *Nucl.Phys.*, B185:189, 1981.

[47] L. F. Abbott. Introduction to the Background Field Method. *Acta Phys. Polon.*, B13:33, 1982.

[48] M. Laine. *Lecture notes: Quantum Field Theory.* University of Bielefeld, 2005.

[49] J. I. Kapusta and C. Gale. *Finite-Temperature Field Theory Principles and Applications Second Edition.* Cambridge University Press, 2006.

[50] M. Laine. *Lecture notes: Basics of Thermal Field Theory.* University of Bielefeld, 2008.

[51] Paul H. Ginsparg. First Order and Second Order Phase Transitions in Gauge Theories at Finite Temperature. *Nucl.Phys.*, B170:388, 1980.

[52] K. Kajantie, M. Laine, K. Rummukainen, and Mikhail E. Shaposhnikov. Generic rules for high temperature dimensional reduction and their application to the standard model. *Nucl.Phys.*, B458:90–136, 1996.

[53] J. Frenkel, A.V. Saa, and J.C. Taylor. The Pressure in thermal scalar field theory to three loop order. *Phys.Rev.*, D46:3670–3673, 1992.

[54] Rajesh Parwani and Harvendra Singh. The Pressure of hot (g**2 phi**4) theory at order g**5. *Phys.Rev.*, D51:4518–4524, 1995.

[55] A. Gynther, M. Laine, Y. Schröder, C. Torrero, and A. Vuorinen. Four-loop pressure of massless O(N) scalar field theory. *JHEP*, 0704:094, 2007.

[56] Joseph I. Kapusta. Quantum Chromodynamics at High Temperature. *Nucl.Phys.*, B148:461–498, 1979.

[57] T. Toimela. The next term in the thermodynamic potenial of QCD. *Phys.Lett.*, B124:407, 1983.

[58] Peter Brockway Arnold and Cheng-xing Zhai. The Three loop free energy for high temperature QED and QCD with fermions. *Phys.Rev.*, D51:1906–1918, 1995.

[59] Cheng-xing Zhai and Boris M. Kastening. The Free energy of hot gauge theories with fermions through g**5. *Phys.Rev.*, D52:7232–7246, 1995.

[60] Eric Braaten and Agustin Nieto. Free energy of QCD at high temperature. *Phys.Rev.*, D53:3421–3437, 1996.

[61] K. Kajantie, M. Laine, K. Rummukainen, and Y. Schröder. The Pressure of hot QCD up to g6 ln(1/g). *Phys.Rev.*, D67:105008, 2003.

[62] Jan Möller and York Schröder. Dimensionally reduced QCD at high temperature. *Prog.Part.Nucl.Phys.*, 67:168–172, 2012.

[63] M. Laine and Y. Schröder. Two-loop QCD gauge coupling at high temperatures. *JHEP*, 0503:067, 2005.

[64] Jan Möller. Diploma Thesis, University of Bielefeld. 2009.

[65] Jan Möller and York Schröder. in preparation.

[66] Jan Möller and York Schröder. Open problems in hot QCD. *Nucl.Phys.Proc.Suppl.*, 205-206:218–223, 2010.

[67] Scott Chapman. A New dimensionally reduced effective action for QCD at high temperature. *Phys.Rev.*, D50:5308–5313, 1994.

[68] A. Hietanen, K. Kajantie, M. Laine, K. Rummukainen, and Y. Schröder. Plaquette expectation value and gluon condensate in three dimensions. *JHEP*, 0501:013, 2005.

[69] F. Di Renzo, M. Laine, V. Miccio, Y. Schröder, and C. Torrero. The Leading non-perturbative coefficient in the weak-coupling expansion of hot QCD pressure. *JHEP*, 0607:026, 2006.

[70] T. Gehrmann and E. Remiddi. Differential equations for two loop four point functions. *Nucl.Phys.*, B580:485–518, 2000.

[71] Christian Bogner and Stefan Weinzierl. Feynman graph polynomials. *Int.J.Mod.Phys.*, A25:2585–2618, 2010.

[72] O.V. Tarasov. Connection between Feynman integrals having different values of the space-time dimension. *Phys.Rev.*, D54:6479–6490, 1996.

[73] O.V. Tarasov. A New approach to the momentum expansion of multiloop Feynman diagrams. *Nucl.Phys.*, B480:397–412, 1996.

[74] O.V. Tarasov. Generalized recurrence relations for two loop propagator integrals with arbitrary masses. *Nucl.Phys.*, B502:455–482, 1997.

[75] R.N. Lee. Group structure of the integration-by-part identities and its application to the reduction of multiloop integrals. *JHEP*, 0807:031, 2008.

[76] C. Studerus. Reduze-Feynman Integral Reduction in C++. *Comput.Phys.Commun.*, 181:1293–1300, 2010.

[77] A. von Manteuffel and C. Studerus. Reduze 2 - Distributed Feynman Integral Reduction. 2012.

[78] J.A.M. Vermaseren. Axodraw. *Comput.Phys.Commun.*, 83:45–58, 1994.

[79] P.A. Baikov. Explicit solutions of the three loop vacuum integral recurrence relations. *Phys.Lett.*, B385:404–410, 1996.

[80] P.A. Baikov. Explicit solutions of the multiloop integral recurrence relations and its application. *Nucl.Instrum.Meth.*, A389:347–349, 1997.

[81] S.G. Gorishny, S.A. Larin, L.R. Surguladze, and F.V. Tkachov. Mincer: Program for Multiloop Calculations in Quantum Field Theory for the Schoonschip System. *Comput.Phys.Commun.*, 55:381–408, 1989.

[82] A.G. Grozin. Integration by parts: An Introduction. *Int.J.Mod.Phys.*, A26:2807–2854, 2011.

[83] Jan Möller. Difference Equations of Massive Tadpoles up to 5-loop. `http://www.physik.uni-bielefeld.de/~jmoeller`.

[84] K. Kajantie, M. Laine, and Y. Schröder. A Simple way to generate high order vacuum graphs. *Phys.Rev.*, D65:045008, 2002.

[85] Christian Bauer, Alexander Frink, and Richard Kreckel. Introduction to the GiNaC Framework for Symbolic Computation within the C++ Programming Language. *CoRR*, cs.SC/0004015, 2000.

[86] Charalampos Anastasiou and Achilleas Lazopoulos. Automatic integral reduction for higher order perturbative calculations. *JHEP*, 0407:046, 2004.

[87] Maplesoft. Maple 15. `http://www.maplesoft.com/products/maple/`.

[88] A.V. Smirnov. Algorithm FIRE – Feynman Integral REduction. *JHEP*, 0810:107, 2008.

[89] Wolfram Reasearch. Mathematica 8.0. `http://www.wolfram.com/mathematica/`.

[90] J. A. M. Vermaseren S. A. Larin, F. V. Tkachov. *Preprint NIKHEF-H-91-18, Amsterdam*, 1991.

[91] David J. Broadhurst, A.L. Kataev, and O.V. Tarasov. Analytical on-shell QED results: Three loop vacuum polarization, four loop Beta function and the muon anomaly. *Phys.Lett.*, B298:445–452, 1993.

[92] Leo V. Avdeev. Recurrence relations for three loop prototypes of bubble diagrams with a mass. *Comput.Phys.Commun.*, 98:15–19, 1996.

[93] Matthias Steinhauser. MATAD: A Program package for the computation of MAssive TADpoles. *Comput.Phys.Commun.*, 134:335–364, 2001.

[94] H. Strubbe. Manual for Schoonschip: A CDC 6000 / 7000 program for symbolic evaluation of algebraic expressions. *Comput.Phys.Commun.*, 8:1–30, 1974.

[95] A.C. Hearn. REDUCE user's manual Version 3.8. *RAND publication, Santa Monica*, 2004.

[96] A.C. Hearn. REDUCE: A user-oriented interactive system for algebraic simplification. *Interactive Systems for Experimental Applied Mathematics*, pages 69–70, 1968.

[97] Robert H. Lewis. Fermat Users Guide for Linux and Mac OSX 32 bit and 64 bit versions, July 25, 2011. `http://www.home.bway.net/lewis/`.

[98] Kyoto Cabinet: A Straightforward Implementation of DBM. `http://www.fallabs.com/kyotocabinet/`.

[99] M. Tentyukov and J. A. M. Vermaseren. Extension of the functionality of the symbolic program FORM by external software. *Comput. Phys. Commun.*, 176:385–405, 2007.

[100] J. Kuipers, T. Ueda, J.A.M. Vermaseren, and J. Vollinga. FORM version 4.0. 2012.

[101] Y. Schröder. Automatic reduction of four loop bubbles. *Nucl.Phys.Proc.Suppl.*, 116:402–406, 2003.

[102] Cedric Studerus. Notes on 5-loop Massive Tadpoles. *Not published*, 2011.

[103] York Schröder. Private Notes on Difference Equations of Massive Tadpoles up to 4-loop. *Not published*.

[104] S. Laporta. Calculation of master integrals by difference equations. *Phys.Lett.*, B504:188–194, 2001.

[105] S. Laporta. High precision epsilon expansions of three loop master integrals contributing to the electron g-2 in QED. *Phys.Lett.*, B523:95–101, 2001.

[106] S. Laporta. Calculation of Feynman integrals by difference equations. *Acta Phys.Polon.*, B34:5323–5334, 2003.

[107] O.V. Tarasov. Application and explicit solution of recurrence relations with respect to space-time dimension. *Nucl.Phys.Proc.Suppl.*, 89:237–245, 2000.

[108] R.N. Lee. Space-time dimensionality D as complex variable: Calculating loop integrals using dimensional recurrence relation and analytical properties with respect to D. *Nucl.Phys.*, B830:474–492, 2010.

[109] Roman N. Lee. DRA method: Powerful tool for the calculation of the loop integrals. 2012. 6 pages, contribution to ACAT2011 proceedings, Uxbridge, London, September 5-9, 2011.

[110] Andrei I. Davydychev and J.B. Tausk. Two loop selfenergy diagrams with different masses and the momentum expansion. *Nucl.Phys.*, B397:123–142, 1993.

[111] S. Groote, J.G. Korner, and A.A. Pivovarov. On the evaluation of a certain class of Feynman diagrams in x-space: Sunrise-type topologies at any loop order. *Annals Phys.*, 322:2374–2445, 2007.

[112] A.V. Smirnov and M.N. Tentyukov. Feynman Integral Evaluation by a Sector decomposiTion Approach (FIESTA). *Comput.Phys.Commun.*, 180:735–746, 2009.

[113] Jannis Schücker. Templates for 5-loop Vacuum Diagrams in Axodraw. *Not published*.

Acknowledgements

Ich möchte mich auf diesem Wege zunächst bei Prof. Dr. York Schröder für die ausgezeichnete Betreuung während meiner Zeit als Doktorand bedanken. Darüberhinaus danke ich Dr. Markos Maniatis fuer ein allerzeit offenes Ohr und die Bereitschaft diese Arbeit zu begutachten. Auch gebührt mein Dank Dr. Cedric Studerus für das Korrekturlesen der hier vorliegenden Arbeit.

Ich möchte mich bei allen Mitgliedern der Arbeitsgruppe E6/D6 der theoretischen Physik der Universität Bielefeld bedanken. Erst diese Menschen trugen zu der auf der einen Seite professionellen aber auch freundschaftlichen Atmosphäre entscheidend bei. Auf diese Zeit werde ich rückblickend immer positive zurückschauen.

Ein besonderer Dank gebührt auch Frau Gudrun Eickmeyer und Frau Susi Reder für ihre hervorragenden organistorischen Leistungen und die menschliche Bereicherung der Arbeitsgruppe.

Ich möchte mich bei allen Freunden insbesondere Florian Kühnel und Yannis Burnier für eine tolle Zeit bedanken. Mein Dank gebührt auch meiner Familie die mich durchweg bei meinen Wünschen und Zielen unterstützt haben. Ohne euch wäre ich nicht da wo ich jetzt bin.

Zu guter Letzt danke ich Daniela für eine unvergessliche Zeit. Ich liebe dich.

Eigenständigkeitserklärung

Zur Dissertation mit dem Titel

Fully Massive Tadpoles at 5-loop: Reduction and Difference Equations

Hiermit erkläre ich die vorliegende Arbeit selbstständig und ohne fremde Hilfe verfasst und nur die angegebene Literatur und Hilfsmittel verwendet zu haben.

Bielefeld, 11.06.2012

Jan Möller